University of Washington
Department of Civil and Environmental Engineering

EFFECTS OF PLANFORM GEOMETRY ON TIDAL FLUSHING AND MIXING IN MARINAS

Ronld E. Nece
Eugene P. Richey
Joonpyo Rhee
H. Norman Smith

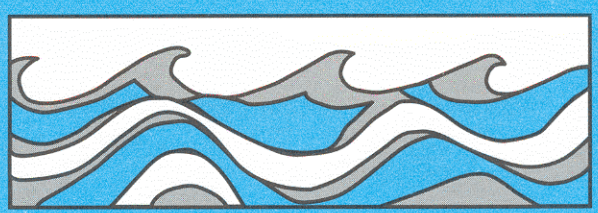

Water Resources Series
Technical Report No. 62
December 1979

Seattle, Washington
98195

Department of Civil Engineering
University of Washington
Seattle, Washington 98195

EFFECTS OF PLANFORM GEOMETRY ON TIDAL FLUSHING AND MIXING IN MARINAS

Ronld E. Nece
Eugene P. Richey
Joonpyo Rhee
H. Norman Smith

Water Resources Series
Technical Report No. 62

December 1979

Charles W. Harris Hydraulics Laboratory

Department of Civil Engineering

University of Washington

Seattle, Washington 98195

EFFECTS OF PLANFORM GEOMETRY ON TIDAL FLUSHING AND MIXING IN MARINAS

by

Ronald E. Nece, Eugene P. Richey, Joonpyo Rhee

and H. Norman Smith

December 1979

Technical Report No. 62

CONTENTS

Acknowledgment ii
Abstract iii
Figures iv
Tables vi
List of Abbreviations and Symbols vii

1. Introduction 1

2. Background 2
   Modeling of Small Harbors 2
   Examples of Site-Specific Studies 5
   Effects of Marina Geometry on Tidal Flushing and Circulation 6
   Hydraulic Model Approach to Present Study 7

3. Experimental Procedures 9
   Data Sought 9
   Model Basin Tide Tank 10
   Model Construction and Installation 10
   Photo Densitometer 11
   Operating Sequence 13
   Experimental Precautions 14

4. Data Reduction Procedures 16
   Densitometer Readings 16
   Determination of Exchange Coefficient 17
   Spatial Distribution of Net Water Exchange 18

5. Experimental Results 19
   Configurations Tested 19
   Average (Gross) Exchange Coefficients 20
   Effect of Planform Geometry on Uniformity of Mixing 23
   Example Investigation of Cycle-to-Cycle Flushing Repetition 25

6. Conclusions 26

References 31

ACKNOWLEDGMENT

The work reported here was sponsored by the Corvallis Environmental Research Laboratory, Office of Research and Development, United States Environmental Protection Agency, Corvallis, Oregon. The work was carried out under Grant No. R806146-01-1. Mr. R. J. Callaway, Marine Division, Corvallis Environmental Research Laboratory, was the project officer. In accordance with the grant agreement, this document has been submitted for publication as a research report of the Office of Research and Development, U. S. Environmental Protection Agency.

The experimental program described was conducted in the Charles W. Harris Hydraulics Laboratory of the Department of Civil Engineering, University of Washington. The project was carried out under the supervision of Professor Ronald E. Nece (Principal Investigator) and Professor Eugene P. Richey (Co-Investigator). The bulk of the experimentation and data analysis was performed by Mr. Joonpyo Rhee, Research Assistant. Details of the experimental apparatus and procedures were developed by Mr. H. Norman Smith, Research Engineer. Mr. Sum Kay Lau, graduate student, assisted in the experimental program.

ABSTRACT

Physical hydraulic models of small-boat basins (marinas) possessing a rectangular planform were tested to determine the effects of various geometry parameters on tidal flushing and internal circulation in small harbors. The schematic model marinas were scaled to have surface areas, water depths, and tide ranges comparable to 'prototype' marinas in the Pacific Northwest. The geometry parameters investigated, to varying degrees, were:

1. Planform geometry aspect ratio.
2. Ratio of entrance cross-sectional area to basin planform area.
3. Effect of rounding of corners in the basin interior.
4. Orientation and location of single entrances.
5. Effect of two entrances versus a single entrance.

Results are presented in terms of average tidal flushing (exchange) coefficients for each configuration tested, and by contour drawings of equal local per-cycle exchange coefficients for a number of configurations, all at the same tide range, in order to compare the spatial variabilities in local exchange obtained for different planform geometries. Emphasis is placed on those variables - planform geometry and aspect ratio - over which designers may have most latitude in designing a marina for a specific site.

It is concluded that for rectangular planform basins optimum exchange, both overall and in terms of spatial uniformity, is achieved when the aspect ratio (basin length to width ratio) lies between 1/2 and 2.0, the interior corners are rounded, and the single entrance is centrally located in the breakwater, or enclosure, on the seaward side of the harbor. Rounding of interior corners has little effect on average flushing but does increase the uniformity of local exchange throughout the basin. Effects of basin length : width ratio are delineated for basins with typical single asymmetric entrances.

Results were obtained by a photographic technique incorporating the use of a photodensitometer. This procedure provided quantitative verification of some conclusions which had been reached previously by strictly visual or non-quantitative photographic observations used in conjunction with fluorescent dye measurements.

This report was submitted in fulfillment of Grant No. R806146-01-1 by the University of Washington, Department of Civil Engineering, under the sponsorship of the U.S. Environmental Protection Agency. The report covers the period October 1, 1978 to September 30, 1979, and the work was completed as of November 5, 1979.

FIGURES

Number		Page
1	Details of Laboratory Tide Tank	33
2	Definition and Notation Diagram	34
3	Data Plot Symbol Identification	35
4	Average Exchange Coefficients, Single Asymmetric Entrance, H = 3 feet	36
5	Average Exchange Coefficients, Single Asymmetric Entrance H = 6 feet	37
6	Average Exchange Coefficients, Single Asymmetric Entrance, H = 12 feet	38
7	Average Exchange Coefficients, Single Asymmetric Entrance, Summary Plot	39
8	Comparison of Average Exchange Coefficients, Single Asymmetric Entrance, Square Corners vs. Rounded Corners; H = 6 feet	40
9	Comparison of Average Exchange Coefficients, Square-Corner Basin, Asymmetric Entrance vs. Center Entrance; H = 6 feet	40
10	Comparison of Average Exchange Coefficients, Rectangular Basin, Single 250-foot Entrance vs. Two Entrances; H = 6 feet	41
11	Comparison of Average Exchange Coefficients, Rectangular Basin, Single 500-foot Entrance vs. Two Entrances; H = 6 feet	41
12	Comparison of Average Exchange Coefficients, Single Asymmetric Entrance, Fluorescent Dye Method (1976) vs. Photodensitometer Method (1979), H = 12 feet	42
13	Comparison of Average Exchange Coefficients, Single Asymmetric Entrance, Fluorescent Dye Method (1976) vs. Photodensitometer Method (1979)	43
14	Square Corners, Single Entrance, H = 6 feet, w = 125 feet, L/B = 0.21	44
15	Square Corners, Single Entrance, H = 6 feet, w = 125 feet, L/B = 0.30	45

FIGURES
(continued)

Number		Page
16	Square Corners, Single Entrance, H = 6 feet, w = 125 feet, L/B = 0.53	46
17	Square Corners, Single Entrance, H = 6 feet, w = 125 feet, L/B = 0.83	47
18	Square Corners, Single Entrance, H = 6 feet, w = 125 feet, L/B = 1.20	48
19	Square Corners, Single Entrance, H = 6 feet, w = 125 feet, L/B = 1.88	49
20	Square Corners, Single Entrance, H = 6 feet, w = 125 feet, L/B = 3.33	50
21	Square Corners, Single Entrance, H = 6 feet, w = 125 feet, L/B = 4.80	51
22	Square Corners, Single Entrance, H = 6 feet, w = 250 feet, L/B = 1.88	52
23	Square Corners, Single Entrance, H = 6 feet, w = 250 feet, L/B = 3.33	53
24	Rounded Corners, Single Entrance, H = 6 feet, w = 125 feet, L/B = 0.30	54
25	Rounded Corners, Single Entrance, H = 6 feet, w = 125 feet, L/B = 0.53	55
26	Rounded Corners, Single Entrance, H = 6 feet, w = 125 feet, L/B = 0.83	56
27	Rounded Corners, Single Entrance, H = 6 feet, w = 125 feet, L/B = 1.20	57
28	Rounded Corners, Single Entrance, H = 6 feet, w = 125 feet, L/B = 1.88	58
29	Rounded Corners, Single Entrance, H = 6 feet, w = 125 feet, L/B = 3.33	59
30	Square Corners, Center Entrance, H = 6 feet, w = 125 feet, L/B = 0.53	60
31	Square Corners, Center Entrance, H = 6 feet, w = 125 feet, L/B = 0.83	61

FIGURES
(continued)

Number		Page
32	Square Corners, Center Entrance, H = 6 feet, w = 125 feet, L/B = 1.20	62
33	Square Corners, Center Entrance, H = 6 feet, w = 125 feet, L/B = 1.88	63
34	Square Corners, Double Entrance, H = 6 feet, w = 125, 125, L/B = 1.88	64
35	Square Corners, Double Entrance, H = 6 feet, w = 125, 250, L/B = 1.88	65
36	Square Corners, Double Entrance, H = 6 feet, w = 250, 250, L/B = 1.88	66
37	Square Corners, Double Entrance, H = 6 feet, w = 125, 125, L/B = 3.33	67
38	Square Corners, Double Entrance, H = 6 feet, w = 125, 250, L/B = 3.33	68
39	Square Corners, Double Entrance, H = 6 feet, w = 250, 250, L/B = 3.33	69
40	C/C_o vs. Number of Tidal Cycles, Square Corners, Single Entrance, H = 6 feet, w = 125 feet, L/B = 1.88	70
41	C/C_o in Sub-Areas (2,2) and (4,3) vs. Number of Tidal Cycles, H = 6 feet, w = 125 feet, L/B = 1.88	71

TABLES

Number		Page
1	Metric Equivalents	72
2	Data Summary	73

LIST OF ABBREVIATIONS AND SYMBOLS

ABBREVIATIONS

L/B	-- aspect ratio, marina basin length : width ratio
MLLW	-- mean lower low water (tidal datum)
TPR	-- tidal prism ratio (Eq. 3.3)

SYMBOLS

A	-- marina basin planform area
A_r	-- model : prototype area ratio
a	-- cross-sectional area of entrance channel
B	-- marina basin width, normal to beach line
C	-- concentration of tracer water
C_i	-- concentration in the i - th area element
C_M	-- spatial average concentration under artificially mixed conditions
C_n	-- concentration after n cycles
C_o	-- initial concentration
d	-- water depth at mean tide elevation
$\underline{E}$	-- local per-cycle exchange coefficient
$\overline{E}$	-- spatial average per-cycle exchange coefficient
E_i	-- local exchange coefficient in the i - th area element
H	-- tidal range
i	-- (subscript), indicating conditions at low water
L	-- marina basin length, parallel to beach line
L	-- (subscript), indicating conditions at low water
L_r	-- model : prototype horizontal length ratio
N	-- number of grid points or area segments
n	-- number of complete tidal cycles
$\underline{R}$	-- local per-cycle retention coefficient
$\overline{R}$	-- spatial average retention coefficient
R_i	-- local retention coefficient in the i - th area element
S	-- standard deviation
T_r	-- model : prototype time ratio
V_r	-- model : prototype velocity ratio
w	-- width of entrance channel
Z_r	-- model : prototype vertical length ratio

SECTION 1

INTRODUCTION

Physical hydraulic model tests of various site-specific salt-water small-boat basin (marina) designs, and some rather limited tests on generalized basin geometries, have provided qualitative understanding of tidal flushing characteristics of such harbors. Tidal flushing, or its corresponding "exchange time", is a dominant factor in the quality of water within such basins relative to that of ambient waters with which they connect. Trends in overall (gross) water exchange by tidal flushing have been documented previously, but quantitative methods still must be expanded so that designs of proposed marinas can be evaluated adequately to predict spatial variability in local water exchange rates within the basins, e.g., are these local "hot spots" of poor exchange which could lead to fish kills, etc. This type of information is needed by regulatory and permit-granting agencies when evaluating design proposals to determine if proposed facilities may be constructed or if the designs must be modified.

In the absence of readily available economical computer models linking velocity fields and diffusion (mixing) in such basins, laboratory models continue to provide information needed now for decision purposes and for use in developing mathematical models which might ultimately remove the need for site-specific model studies.

This report presents details of a laboratory study designed to develop such information.

Effects of particular geometry parameters upon the gross exchange and the spatial variability in local exchange due to tidal flushing action were examined. The geometry parameters investigated, to varying degrees, were:

1. Planform geometry aspect ratio.
2. Ratio of entrance cross-sectional areas to basin planform area.
3. Effect of rounding of corners in the basin interior.
4. Orientation and location of single entrances.
5. Effect of two entrances versus a single entrance.

Emphasis in this study is on spatial variability of exchange. Data on gross flushing rates are also presented, and are correlated with previous results. The experimental results were obtained by a photodensitometric technique; this experimental method allows local per-cycle water exchanges to be determined at any desired number of locations within the basin being examined without interfering with or stopping the tidal flow as was the case with previously used fluorescent dye techniques.

The schematic "model" marinas studied by conventional Froudelaw scaling relationships were built using the 10:1 vertical distortion ratio common for tidal models. Scale ratios relating laboratory basins to equivalent "prototype" harbors were 1:500 horizontal and 1:50 vertical. The horizontal (level) bottom basins tested had surface areas, mean water depths, and tide ranges comparable to "prototype" tidal marinas in the Pacific Northwest.

Ideally, the results of this study would be expressed in dimensionless form for design and evaluation purposes when applied to specific projects. Pertinent, or critical, length dimensions include the tide range, basin length and width, entrance width, water depth, and the distance from the entrance to the innermost point in the basin. Critical areas are the harbor planform areas and the cross-sectional area of the entrance. Geometry parameters include the number and orientation of entrances, and the aspect ratio (length:width ratio) of the basin planform. Any formal dimensional analysis procedure would yield a large number of dimensionless ratios which would characterize the physical configurations of a marina. However, the number of variables that can be varied readily by a designer is relatively small. The entrance width and the water depth in the harbor are generally fixed by navigation requirements; the tide range is given at a particular site; the planform area of the basin is determined by economic considerations, i.e., the number of moorages required if the project is to be economically feasible. Therefore, the number of dimensionless ratios which can be varied by a designer is not large, and these in turn relate to planform geometry. Consequently, planform geometry variations indicated in the above list were investigated.

SECTION 2

BACKGROUND

MODELING OF SMALL HARBORS

Models of relatively small, partially enclosed basins in tidal waters can be considered to form a sub-set of estuary models. Physical models have been used for years in engineering studies of particular estuaries. Recently there has been a continued development in mathematical modeling of estuaries. Hinwood and Wallis (1975) reviewed approximately 100 mathematical models of water and waste movement in tidal bays and estuaries, with the basic objective of determining criteria for selecting a model, or models, for a specific task. The authors noted that, inevitably, some models may have been missed in their summary; also, in the intervening years, new models have been developed.

The development of mathematical models which can provide adequate details of the highly complex, unsteady flows in small tidal harbors is still an ongoing process. One-dimensional approaches have been used by Brandsma et. al. (1973) for marinas in which the individual segments or sub-basins are regular and canal-like in planform. Tide-induced mass transport in long canal-type lagoons open to the sea at both ends has been calculated with one-dimensional shallow water wave equations by Van de Kreeke and Dean (1975). Neither procedure is valid for the relatively small embayments of concern here, where unsteady angular momentum effects associated with flows having pronounced separation due to tidal inflows through relatively small entrances are dominant in establishing the flow field in the basin.

Tidal flow models (mathematical) for bays and estuaries are traditionally two-dimensional, and many now do not include the transverse shear stress term needed to account properly for flows at a surface of separation (e.g., tidal inflow through an opening in a breakwater) and for the resulting circulation cells or gyres established within a harbor as a consequence of flow separation at the harbor entrance. Fischer (1976a) has pointed out that the only way for a two-dimensional numerical model to reproduce such phenomena would be for the model to incorporate a transverse shear term whose magnitude was chosen to make the model match prototype results; therefore, predictive modeling for proposed geometries would not be possible. The problem of handling the unsteady flow-separation problem is crucial to the numerical modeling of the flows considered in the present study. Abbot

(1977), as reviewed by Askren (1979), numerically simulated the flow interaction between a rectangular basin and a channel with an oscillating tidal flow. It was found that proper simulation of basin entrance effects required the momentum diffusion coefficients in the vertically-averaged equations of motion used to be higher near the basin entrance than in the interior. The finite difference scheme employed used a uniform spatial grid throughout the entire planform area considered; an alternative would be to use finer grid scales near the basin entrance.

Askren (1979) simulated circulation patterns in rectangular marina basins, where the circulation was induced by steady (non-tidal) flow past the mouth of the entrance. The problem of flow separation did not have to be handled because of the particular geometry investigated.

Objectives of the above studies were to determine the hydrodynamic characteristics of basin circulation, i.e., the determination of local depth-averaged velocities for either the steady or unsteady flows examined. Exchange per se of ambient and interior waters was not considered; diffusion and mixing between the ambient and interior waters were not incorporated into any transport model built upon the results of the hydrodynamic circulation calculations. Such calculations would require that appropriate diffusion and coefficient values would be included.

Because of the problems outlined above, physical hydraulic models are still common in many studies of small basins; use of physical models was also the choice for this study.

Limitations of distorted physical models for determining diffusion and mixing in tidal flows are well acknowledged. Fischer and Holley (1971), in reviewing the performance of such models in constant density portions of estuaries, conclude that dispersive effects of transverse gradients may be magnified, diminished, or correctly modeled, depending on the prototype dimensionless (dispersion) time scale. In narrow estuaries (perhaps more appropriate to the present study) dispersion due to transverse gradients may be modeled properly but dispersion in the model is usually caused primarily by vertical gradients and the overall result is magnified. In short, in distorted models, turbulent mixing (diffusion) coefficients do not scale properly. Fischer (1976b) concludes that while there is no total agreement on how well physical hydraulic models simulate mixing, such models constitute a useful engineering tool for problems involving three-dimensionality and complex boundaries. Few other (existing) tools are adequate.

EXAMPLES OF SITE-SPECIFIC MODEL STUDIES

Some physical model studies designed to determine the tidal exchange (flushing) performance of various marinas are examined in the following discussion. All models were of the single-fluid type, simulating fully-mixed (unstratified) conditions in the prototype.

Model study results yielding predicted average tidal flushing characteristics of a number of existing and proposed marinas on Puget Sound, Washington, were summarized by Nece and Richey (1975). The tests were made in the same tide tank used in the present study. Flushing performance was determined from measurements of relative concentrations of fluorescent dye in the model basin over a number of tidal cycles. A more recent report by Nece and Richey (1979) updated and added to the prior list of flushing characteristics of site-specific projects. The more recent tests used the photographic techniques employed in the present study, so that information on spatial variations in local flushing within the basins was obtained. In none of the cases cited was there a special attempt to precisely simulate longshore currents past the mouth of the marina because it was determined from field observations that, in these cases, currents were not significant and thus it was not necessary to model them closely. However, models were properly located in the tide tank so that prevailing or reversing currents past the marina entrance were in the correct direction with respect to the tide phase. The tides in all cases were repetitive and sinusoidal.

A model study of a Pacific Northwest small-boat basin in which typical mixed tides and selective sampling of fluorescent dye concentrations on consecutive tidal cycles at specific points in the marina basin was reported by Brogdon (1975).

Two other specific studies are noted in which the marina was located on the side of a tidal river where the "longshore" currents are indeed strong and can have considerable influence on the circulation and flushing within the marina. Both studies concerned installations on the Pacific Ocean coast, in Oregon.

The first, by Richey and Skjelbreia (1978), used the photographic technique, thus obtaining information on local flushing rates. Field studies of tidal flushing in the same marina (Yaquina) were subsequently conducted by personnel of the U.S. Environmental Protection Agency. Dye concentrations at each of the four designated stations within the basin in the laboratory model study were measured in the field over four tidal cycles. For two stations the time-histories of dye concentration in the model and in the field were in good agreement; for the two stations farthest from the entrance, the model indicated greater exchange than was noted in the field, although the trends with time were the same in both the model and field (R. J. Callaway, personal communication). The second, by Schluchter and Slotta (1978), utilized the fluorescent dye methods. The latter laboratory model study was followed by field tests where prototype flushing characteristics were obtained from dye studies conducted in the

field. A 90 percent flushing time was defined as the time in tidal cycles required to remove 90 percent of the water which was in the basin at a particular time, say at high water slack. For comparable river discharges and tide ranges, this time in the model was 5.7 cycles, compared to 6.9 cycles calculated on the basis of spot data in the prototype. The model in this case then slightly over-estimated the flushing capability of the prototype. There was density stratification in the prototype, so that current patterns in the model did depart from those observed in the field.

EFFECTS OF MARINA GEOMETRY ON TIDAL FLUSHING AND CIRCULATION

Previous studies have dealt with various aspects of effects of planform geometry upon the flushing and circulation characteristics of the marina.

Vollmers (1976) made physical model studies to improve circulation in the Delfzijl Harbor, Netherlands. The harbor, which is extremely elongated, has two entrances. Entrance conditions were modified so that a through flow current adequate to flush the harbor was obtained. The use of multiple entrances for harbors such as this, situated parallel to a tidal river, can be advantageous.

Askren (1979) performed numerical simulation of the circulation patterns within rectangular marina basins. Only steady state conditions were examined. There was no tidal flow into or out of the basin, which was situated on the edge of a steadily flowing river. Circulation patterns within the basin were shear-induced by river velocities past the zero-length (normal to river flow) entrance. Solutions considered effects of varying basin length, basin width, entrance width, entrance placement, number of entrances, and the boundary (river) velocity at entrance. It was concluded that the shear-driven circulation may be enhanced by increasing the relative width, and that a square plan view with a single entrance centrally located in the breakwater produces both maximum basin-averaged circulation and maximum sedimentation within the basin. Planform geometries were comparable to those in the current study, but the driving mechanism for circulation was entirely different and there was no flushing.

Yanagi (1976) conducted tide tank tests of a rectangular basin with a single asymmetric entrance and reported the residual single-gyre circulation within the nearly square basin. Trends noted in the laboratory results were also observed in field tests in a rectangular bay of 1000 x 800 meter planform, with an 80-meter entrance width.

Slotta and Noble (1977) attempted to relate the water quality of Oregon coastal marinas to harbor geometry through the use of sediment chemistry. Thirteen marinas were studied. Conclusions about water quality were based on benthic samples obtained from one to three sampling stations within each marina; benthic samples from ambient waters were not taken.

Sediment quality was used as an index of flushing. Five dimensionless basin parameters were assigned limiting values which were considered optimum for obtaining adequate flushing. In particular, recommendations were presented concerning relative sizes of planform and entrance cross-section areas. A nonogram and some criteria were developed for use in the design of new marinas. These recommendations were to improve the design process; since this is also the objective of the current study, these results must be (and are) compared with present findings. Parenthetically it should be noted that the Slotta and Noble approach of linking hydraulics and water quality is that which must be taken ultimately.

Nece et. al. (1976) conducted laboratory tests which actually constitute an earlier, limited version of this study. The same tide tank was used; planform geometries and tide ranges were comparable to those investigated most thoroughly in the present studies. Conclusions apply for simple small rectangular harbors with single asymmetric entrances where wind, stratification, and longshore current effects are negligible. Best tidal flushing occurred when the basin aspect (length:width) ratio was kept between the limits of 1:3 and 3:1; for basin planforms outside this range multiple circulation cells existed within the harbor and the basin-average tidal flushing was reduced. It was found that rounding the interior corners of the harbor did not improve the gross flushing, although mixing throughout the basin appeared to be more uniform. Since only gross exchanges were determined with the fluorescent dye technique, the latter observation was not quantified. Concern about local exchange performance is shared by fisheries agencies, particularly in the Puget Sound area of Washington where juvenile migrant salmon pass through or reside temporarily in small-boat basins of the size tested.

HYDRAULIC MODEL APPROACH TO PRESENT STUDY

The choice of using a physical model approach in the present study was pragmatic, based on the lack of a tested numerical model adequate for the problem, prior experience in the use and interpretation of physical models, and the continued availability of a small laboratory basin suited to the study.

The Schluchter and Slotta (1978) tidal exchange calculations are based on samples withdrawn, at integer cycle times, at the bottom and at the water surface at only five corresponding stations in the prototype and model. It is difficult to assess the significance of the difference noted in flushing times because there was stratification in the field tests and the dye used in the model was evidently not fully neutrally buoyant. The overall discrepancy between model and prototype, when converted into percentage differences in model and prototype per cycle exchange and retention coefficients (defined in Section 3) are only about 14 and 6 percent, respectively.

Current measurements using drogues were made by Nece and Richey (1972) in the model and prototype of a marina in which density stratification was not present. Model and field pathlines at comparable times on the tidal cycle showed good agreement, indicating that the distorted model satisfactorily reproduced the complex circulation patterns within the basin.

Vertical distortion, and also low Reynolds numbers in the model, rule out equivalence of local diffusion characteristics in the model and prototype. Transport in the water bodies studied here is convection dominated. As the models do reproduce the tide-induced currents of the prototype basins, it is felt that water exchange is also adequately reproduced. For the present study in particular, where relative performance is to be linked to basin geometry, the relative flushing values obtained from the laboratory tests for different geometries certainly should be sufficiently accurate to define trends and to use in water quality models which may be developed in the future.

It is emphasized that the present results apply only to basins where wind effects are negligible and where an unstratified, fully mixed condition exists. This is not a severe limitation in many areas where the fully mixed condition does occur in the shallower water at the edges of tidal water bodies.

SECTION 3

EXPERIMENTAL PROCEDURES

DATA SOUGHT

The specific information to be determined and quantified in this study was the relative exchange of water within a marina basin with ambient water due to tidal flushing of the basin. This information can be expressed in terms of an "exchange coefficient".

The average per-cycle exchange coefficient, which indicates that fraction of water in a basin or a segment of the basin which is removed (flushed out) and replaced with ambient water during each tidal cycle (in this report the tidal cycle length is defined as the tidal period from high water to following high water), is represented by the equations

$$E = 1 - R \tag{3.1}$$

and

$$R = \left(\frac{C_n}{C_o}\right)^{1/n} \tag{3.2}$$

where

E = average, per cycle, exchange coefficient
R = average, per cycle, retention coefficient
C_o = initial spatial average concentration, for the volume considered
C_n = spatial average concentration for the same volume after n cycles, or periods, where n is an integer

In this report, the local value of exchange coefficient for a particular segment of the basin is designated by E, while the spatial average coefficient applicable to the entire basin is designated as $\bar{E}$.

These relationships assume identical, repetitive tides, with actual velocity fields and mixing patterns being reproduced from one cycle to the next. Although $\bar{E}$ and $\bar{R}$ could be defined using any starting time on the tidal cycle, it is most convenient to utilize either high water or low water

slack as the condition for which they apply. In this study, low water slack was used; most prior results have used high water slack values, e.g., Nece and Rickey (1975), Nece et al. (1976), Schlucter and Slotta (1978). The low water definition was selected because at this position on the tidal cycle the residual currents caused during the flood portion, very much in evidence at high water in the typical marinas examined in schematic fashion here, have diminished during the subsequent ebb flow. This condition poses two advantages: first, from an experimental standpoint, conditions are indeed much more likely to be repeated in more detail from one cycle to the next; second, the spatial distribution of relative concentrations within the basin should be more indicative of the effective mixing within the basin over an entire tidal cycle.

A predicted exchange ratio $\bar{E}$ can be calculated by the tidal prism method. This method assumes that water in the basin at low water is thoroughly mixed with ambient water on the flood tide. The ratio is defined as

$$\text{Tidal Prism Ratio (TPR)} = \frac{\text{(Basin Vol. at High Tide) - Basin Vol. at Low Tide}}{\text{Basin Volume at High Tide}} \qquad (3.3)$$

where the numerator is known as the "tidal prism." Use of the simple tidal prism ratio, despite its acknowledged shortcomings in estuary calculations, is considered rational for comparing flushing of small marine harbors which communicate directly with ambient waters and are not subject to freshwater inflows.

MODEL BASIN TIDE TANK

The tests were conducted in a laboratory basin having a nominal overall plan size of 8 feet by 12 feet, with an 18-inch working depth. The constant amplitude, constant period tides were produced by a tide generator which was a variable-elevation waste weir, driven through appropriate gear reducers, and a Scotch yoke mechanism to obtain harmonic motion, and fed by a constant rate water supply entering the tank through a perforated manifold. Baffles separated the inflow section from the working area of the tank. Tide ranges and water levels could be adjusted by cams and threaded rods, respectively, on the weir drive mechanism; the variable speed gear box provided the capability for changing tidal periods. Schematic details of the tank are shown in Figure 1.

MODEL CONSTRUCTION AND INSTALLATION

The laboratory studies were treated as model studies of idealized marina basin shapes. The distorted laboratory model had a horizontal length ratio L_r = 1:500 and a vertical scale ration Z_r = 1:50. The corresponding area, velocity and time ratios, using Froude law scaling relationships, were:

$$A_r = L_r^2 = 1 : 250{,}000 \tag{3.4}$$

$$V_r = Z_r^{\frac{1}{2}} = 1 : 7.07 \tag{3.5}$$

$$T_r = \frac{L_r}{V_r} = \frac{L_r}{Z_r^{\frac{1}{2}}} = 1 : 70.7 \tag{3.6}$$

The repetitive, sinusoidal 12.42-hour, semi-diurnal tides assumed for the prototype were then simulated in the model tests by tides of constant period equal to 10.54 minutes.

For simplicity, the models were constructed with vertical walls and were placed on a horizontal, raised platform in the tide tank. Water depths were uniform throughout the entire model. The 1/2-inch plywood, 6¼-inch high, vertical walls were fastened to pieces of painted steel angles which provided weight for positioning as well as vertical alignment for the outer walls of basin. The walls were not permanently attached to the platform, so that platform geometries could be changed. Bottom and corner joints were scaled with white tape for each test. The walls and platform were painted white. Black-painted wood strips of 2-inch width were attached to the tops of the walls, with inner edges aligned with the inner faces of the marina walls, to provide contrast for photographing the basins from above.

Semi-circular jetties were used at the entrance(s) to insure that tidal flow into the basin on the flood occupied the entire cross-section of the entrance. The rounded ends of the jetties were formed using half-sections of 3.5-inch O.D. PVC pipe. The corner rounding in the marina basin used in some tests was obtained by using sheet-metal, bent to a 6-inch radius.

Roughness strips, vertical 1/2-inch wide metal strips fastened to the basin bottom platform, were situated just outside the jetty noses in order to induce turbulence in the flow entering the basin.

The basin planforms and notation employed are shown in Figure 2.

PHOTO DENSITOMETER

The use of photography to measure dye concentrations in hydraulic laboratory experiments is not new; on the other hand, it does not appear to be common. Procedures involving the use of automated, expensive equipment providing more fine-graned detail than was obtained in the present study were described by Ward (1973). The manual procedures using relatively inexpensive equipment, as in the current work, represent extensions of earlier versions described by Richey and Smith (1977a,b). The basin principles are the same. The photographic technique tracked the change in tracer dye concentration with time at selected grid points in the basin by measuring dye density at these points at specified times on sequent tidal cycles.

Dye density values were measured directly from 35-mm black-and-white negatives, using a Tobias Associates Model TBX photodensitometer. This device is a portable, manually-operated unit with a digital readout of opacity (or optical density). The readout range is from 0.01 to 3.00, where the density reading is expressed as a logarithm (to the base 10) of the opacity. Aperture selections (1, 2 and 3 mm) allow variations in spatial resolution. The densitometer was operated in this study by placing the 35 mm negative over the aperture; correct placement of the negative was obtained through alignment with a corresponding x-y grid. The sensor probe was then placed in contact with the negative and a density reading taken; the operation was repeated for the number of points desired from the negative.

Photos were taken by a camera mounted approximately 7 feet above the center of the marina basin. Lighting was provided by four photoflood lamps (General Electric EBW No. 82) mounted about the same distance above the basin and located to minimize shadows and give uniform lighting of the water surface in the marina. The film used was Kodak Plus-X pan (ASA 125); the camera setting was f 2 at an exposure time of 1/15 second. A red filter was used.

Film negatives were processed so that the density range corresponded, as closely as possible, to the linear portion of the film characteristic curve. The film (positive) density at any point is proportional to the average concentration of dye within the water column at that point. Ideal and typical response curves (calibration curves) for the negatives are shown in the sketch below; the range of optical density readings is typical of the dye concentrations used. Mother Stewart's bluing was the dye used in all tests.

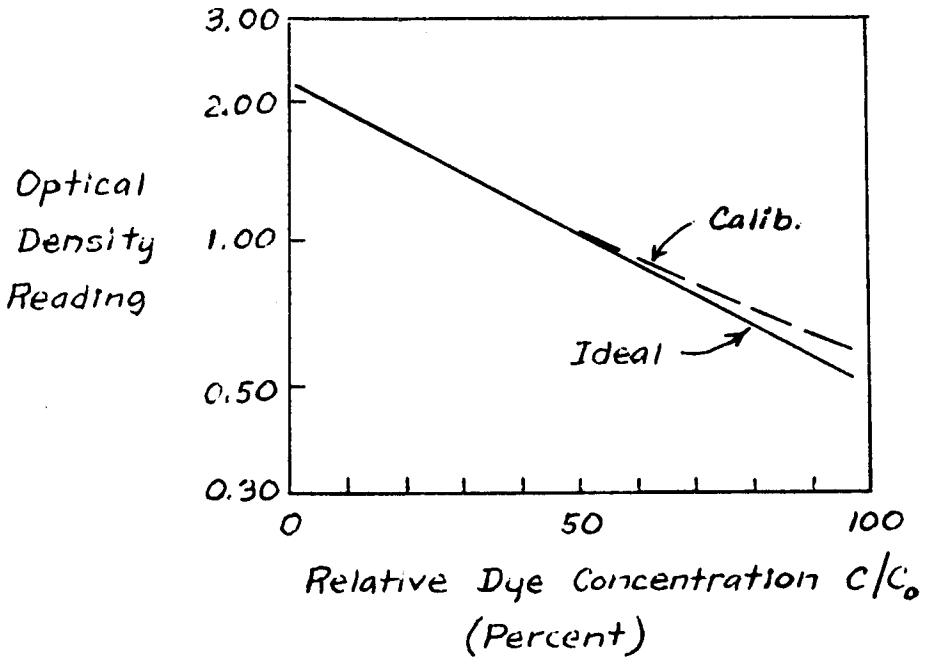

OPERATING SEQUENCE

The camera was automated to take a photo at each quarter-point in a tidal cycle; an automated "clock," located within the field of view, indicated the cycle number and position on the cycle for each photo. The photoflood lamps were controlled by the same circuit and illuminated only long enough for the picture to be taken before they were extinguished; one objective in this operation was to minimize surface heating of the water by the lamps and thus minimize introduction of stratification effects which could upset the single fluid, unstratified conditions desired.

The following procedural steps were used in a single laboratory test:

1. With water level in the tide tank at low water slack (low tide) elevation, insert a temporary barrier dam across the entrance, separating basin and ambient waters.

2. Photograph the model when filled with clear water at low tide level to establish a background light level, at C = zero percent. Standard black and white control strips are placed in the camera field of vision for control purposes.

3. The basin is dosed with the amount of dye required to produce a concentration, C = 25 percent of C_o. Mix the dye thoroughly into the basin, allow the water to become quiescent, and photograph the basin; this provides the C/C_o = 0.25 calibration conditions.

4. Add equal increments of dye, following the above procedures, to obtain the C/C_o = 0.50, 0.75, and 1.00 values.

5. Raise the water level in the tide tank and in the marina basin to high tide elevation, add the calculated amount of dye (proportional to the tidal prism) to bring the concentration to C_o, mix the dye in the basin and take a photograph when the basin waters are quiescent.

6. Remove the barrier dam and simultaneously start the tide generator.

7. Take photographs at quarter-cycle points until the desired number (4) of complete cycles is completed. Conditions at the first low tide level after the generator was started give the C_o values (no ambient water has entered the basin); four cycles later, readings at low water give the C_n values (n = 4).

8. At low water slack corresponding to n = 4, stop the tide generator and simultaneously replace the barrier dam. Thoroughly mix the waters in the basin, allow to become quiescent, and take a final photograph which indicates the spatially averaged dye concentration in the basin.

9. Develop the roll of film to insure that the negatives are adequate.

Step five was not essential, but it minimized errors associated with "start up" time, when the marina waters are brought from the (artificial) quiescent condition to normal tidalconditions. The choice of four tidal cycles was based partly on experience with prior tests using fluorescent dye methods. In either case, after too large a number of tests, the precision with which R can be calculated decreases. Also, with more than four tests, dye concentrations drop to where the densitometer calibration curves tend to become more non-linear.

The negatives constitute an easily-stored permanent data record. A reader board located within the camera field of view contained necessary particulars for each test; data, planform geometry details, tidal range, and camera settings.

EXPERIMENTAL PRECAUTIONS

The experiments described were intended to simulate turbulent flow conditions in unstratified waters. Two major problems in matching these requirements were encountered during the course of the experiments.

One major difficulty was stratification, which usually resulted because the temperature of the marina water was higher than that of the ambient water. This condition was primarily the result of heat transfer from the air in the laboratory. The usual consequence was that the color, denser ambient waters would underrun the marina water, upwell to some degree along the back walls of the marina, and displace larger volumes of marina water than would be the case for unstratified conditions. The end result was an artificially high value of $\bar{E}$, the gross, or overall, exchange coefficient. Water used in the tests was drawn from city domestic supply mains, and warmed as the tests proceeded from winter to summer, reducing the likelihood of stratification. If stratification was noted, the test was either aborted or the fact was noted in the data log for use in interpretation of final results. The laboratory tests were designed to give conservation flushing results compatible with unstratified conditions. It has been observed in actual marinas, e.g., Richey and Smith (1977a) and R.J. Callaway (personal communication) that where density stratification occurs the colder, denser ambient water underruns the warmer surface water and causes an accelerated flushing of the surface layer water.

The range in temperatures of water drawn from the city mains was approximately 20¼F, resulting in an approximate 30-40 percent variation in kinematic viscosity over the period of the study. Reynolds numbers were obviously low; the maximum tidal range and minimum entrance width combination, with the warmest water used in the tests, would provide a peak, instantaneous Reynolds number of about 3,000 for flow through the basin entrance. At such low Reynolds numbers, variations in the Reynolds numbers do indeed cause variations in flow structure. Although these were minimized

by the roughness strips at the model entrance, qualitative observations from photos taken on repeat runs with large water temperature differences do indicate some differences in flow patterns in the basin. Typically, these differences show up in the appearance of the front of the ambient water which enters the basin on the flood die; there are some consequent differences in details of the mixing patterns.

Where repeat runs were made for particular planform geometry - tide combinations, the following pragmatic choice was made in selecting the data which are tabulated and plotted in this report. The test selected was that giving the smallest value of $\bar{E}$.

SECTION 4

DATA REDUCTION PROCEDURES

DENSITOMETER READINGS

Lighting was not completely uniform over the basin, and light reflected from the basin floor also had to travel different distances through the water column en route to the camera lens. Consequently, uniformly mixed dye concentrations in the uniform depth water body produced slightly different densitometer readings at different coordinates in the basin. To overcome this problem, a family of 12 calibration curves was determined for each basin, with the calibration values read using the 3-mm eye centered in one of 12 equally sized rectangles in either a 3 x 4 or a 2 x 6 grid, whichever best fit the planform configuration.

For all configurations reported, concentrations were read at the same 12 locations, using the 3-mm diameter eye. For the test combinations in which a more detailed description of spatial distribution of exchange was sought, 120 readings were taken using the 1-mm eye. The area of the basin planform on the 35-mm film negative was approximately 220 mm^2. The percentages of basin area covered by the densitometer readings for the 3-mm and 1-mm eyes were approximately 38 and 43, respectively, considered adequate for averaging as well as for local sampling.

Plotted calibration curves could be read for the 12-point data reduction, but the process was too time-consuming for the 120-point reductions. Since all of the concentration curves were relatively straight from $C/C_0 = 0$ to $C/C_0 = 0.75$, and since dye concentrations at the end of the fourth cycle were within this range, a program assuming straight lines between each of the points on the calibration curve was developed. Using the above, with the assumption that the calibration curves in a family were parallel, it was easy to extract concentration values using only the initial condition, the final condition, and one typical set of points representing the curve. Values obtained from this program differed from those read directly from the plotted calibration curves by a maximum of 2 percent, this latter when the calibration curves in reality tended to be more non-linear.

DETERMINATION OF EXCHANGE COEFFICIENT

The exchange coefficients plotted on figures in this report are all based on the assumption that conditions were indeed repetitive over the four tidal cycles of each test.

Values of the local exchange coefficient, E, were based on local values of low tide concentrations at the initial conditions and at the end of the fourth cycle. The local coefficients R_i and E_i were then determined at each (i = th) grid point:

$$R_i = \left(\frac{C_{4,L}}{C_{1,L,i}}\right)^{\frac{1}{4}}, \quad E_i = 1 - R_i \tag{4.1}$$

Consequently, the spatial average, or gross, exchange coefficient for the entire basin was calculated as follows, for the 12-point and 120-point reductions, respectively:

$$\bar{E} = \frac{\sum_{i=1}^{12} E_i}{12} \tag{4.2}$$

and

$$\bar{E} = \frac{\sum_{i=1}^{120} E_i}{120} \tag{4.3}$$

The third determination of $\bar{E}$ plotted in the report uses the artificially, fully mixed condition produced by step number 8 outlined in the operating sequence. Identifying this condition by $C_{M,L}$,

$$\bar{R} = \left(\frac{C_{M,L}}{C_{o,L}}\right)^{\frac{1}{4}}, \quad \bar{E} = 1 - \bar{R} \tag{4.5}$$

$$E_i = 1 - R_i, \text{ etc.} \tag{4.6}$$

Values of $\bar{E}$ found in this way are referred to in tables as "average R_i" values. The values are not plotted, but are discussed. This determination does not require any assumptions about repetitiveness. The results for the four individual cycles at a grid point provide an index of how really repetitive was the cycle-to-cycle behavior.

SPATIAL DISTRIBUTION OF NET WATER EXCHANGE

This determination was made for 26 basin planform-tide range combinations, using the 120-point grid results. Data presentation is in two parts.

First, the local E values were entered at the corresponding points in a planform drawing of the basin, and isopleths of E values (at even 0.05-step increments) were plotted on the drawings. These contour plots provide visual indication of the spatial variation in effective water exchange.

A visual measure of the uniformity of local exchange within the basin is provided by histograms showing the number of occurrences for each E_i, to the nearest 0.01, for each test. A statistical measure of the uniformity of mixing is given by the standard deviation S, calculated by

$$S = \sqrt{\frac{\sum_{i=1}^{N} (E_i - \bar{E})^2}{N - 1}} \qquad (4.7)$$

where N = 120.

SECTION 5

EXPERIMENTAL RESULTS

CONFIGURATIONS TESTED

All experiments were conducted on marina basins of the same planform area and same uniform depth at mean tide. The variables were the tide range, entrance width, entrance location(s), and the rounding of interior corners of the rectangular basin. All dimensions listed are equivalent "prototype" values.

The planform area A was 1.25×10^6 square feet (28.7 acres).* This is larger than the area of most Pacific Northwest marinas, but is exceeded by some (Slotta and Noble, 1977). On the basis of limited boat density values given by Nece et al. (1976), the "prototype" of the present tests could accomodate approximately 1,000 boats.

The mean depth, d, within the basin was 16 feet, taken at mean water level. The three tide ranges, H, used were: neap, 3 feet; mean, 6 feet; spring, 12 feet. These values are representative of marinas in the Pacific Northwest and in Puget Sound in particular. At H = 12 feet and d = 16 feet, the depth of water in the basin at low tide is 10 feet; this is a representative value where dredged depths in regional marinas tend to be about 10 feet below MLLW.

The range of aspect ration L/B used in the tests varied from 0.21 to 4.80, more than spanning the usual range found in small-boat basins with single entrances aligned with one side wall. The discrete values of L/B, expressed as rations, were: 5/24, 6/20, 8/15, 10/12, 12/10, 15/8, 20/6, and 24/5. The values were chosen so that a grid of 120 equal-sized squares could be obtained for use in densitometer readings to obtain the data on spatial distribution of the local exchange coefficient, E.

As indicated on Figure 2, a single 250-foot radius was selected to investigate effects of rounding the interior corners of the rectangular basin. The reduction in planform area was 3.2 percent, small enough so that the same physical L and B distances could be used for the regular square-corner tests and the rounded-corner tests.

The three entrance widths w were 125, 250, and 500 feet. The first is most representative of field dimensions, which often result as a compromise

---

*Foot units are used in this report because of their retained use in tide tables, United States engineering design, etc. A listing of metric equivalents is given in Table 1.

between wave protection and navigation clearance requirements and was emphasized in the tests.

Emphasis was placed on the behavior of marinas with a single asymmetric entrance aligned with one side wall. A limited number of tests were run with a single 125-foot entrance located in the center of the 'breakwater' separating the marina from the exterior 'sea'. A limited number of two entrance tests were run, with each of the entrances aligned with a side wall and leaving an isolated breakwater on the seaward edge of the basin. Because there was no net longshore current in the model basin, there was no 'upstream' or downstream' connotation placed on the entrance locations. The rounded corner, center entrance, and tide was considered most representative for comparing the flushing and circulation characteristics of the various planform configurations.

AVERAGE (GROSS) EXCHANGE COEFFICIENTS

This section presents the results for the spatially average exchange coefficient $\overline{E}$. The experimentally obtained values are listed in Table 2; identification of symbols used for plotting the test results is given in Figure 3, and results are plotted in Figures 4-13.

Results for the basic square-corner, rectangular basin with a single asymmetric entrance are given in Figures 4-7. Individual data points for tide ranges H of 3, 6, and 12 feet are shown on Figures 4, 5, and 6, respectively; summary curves are shown on Figure 7. It should be noted that each curve of w = constant actually is a curve of a/A = constant, where a is the cross-sectional area of the entrance; this latter can be defined either at mean sea level (independent of tide range) or at low water (dependent on H). Some general conclusions can be drawn; these are essentially confirmations of the earlier findings in the comparable study by Nece et al. (1976).

For the narrow entrance (w = 125 feet) there is relatively little variation in $\overline{E}$ for a given tide range H over the range of L/B from 1/2 to 2; the overall flushing falls off markedly for L/B less than 1/3 and greater than 3. Defining a flushing 'efficiency' as the ratio $\overline{E}$/TPR, it can be noted that the efficiency generally increases as the tide range H decreases. Efficiency values of greater than unity have been noted at low tide ranges in previous model studies of specific marinas. For the intermediate width (w = 250 feet) best overall flushing occurs when the L/B ration is either less or greater than unity, that ratio which might be anticipated to be an optimum value. The limited results for the widest entrance (w = 500 feet) indicate that the flushing is generally better when L/B is greater than unity, i.e., when the long axis of the marina parallels the seaward side breakwater.

Effects of L/B and w noted above are linked to the angular momentum (about some centrally located vertical axis) of the complex flow within the harbor. The preservation of this angular momentum, associated with the deflection of flood tide flows through the entrance, is especially important to the internal circulation and, hence, harbor blushing. Circulation cells, or gyres, which are created on the flood flow by moments of effective stresses associated

with flow separation at the entrance grow in both circulation strength and size until they occupy a significant part of the basin. Further, these cells may persist well into the ebb phase of the tidal cycle. As a consequence of the angular momentum established within the basin, even in the absence of external longshore currents the ebb flows are often skewed instead of leaving the basin in a direction parallel to the entrance axis. Higher velocities on the flood and part of the ebb occur near the basin perimeter; lower velocities occur near its center. The angular momentum allows the inflowing ambient water to sweep past a major portion of the basin's interior boundaries without losing its identity through diffusion. Thus, it might be expected that factors which contribute to increased angular momentum would improve overall flushing.

The above discussion may be over-simplified. The time-location history of the 'front' of the flood tide jet is important; for simplicity here it is considered in the absence of diffusion or mixing. Consider ambient water which enters the harbor as a two-dimensional jet able to circumnavigate the basin. Water which so completes the circuit has a velocity component along the breakwater side of the basin as it approaches the entrance from within (say, clockwise in the upper left-hand diagram in Figure 2). If this not fully-mixed stream of ambient water reaches the entrance at about high water slack, some will be deflected back into the basin on the ebb and some will leave the basin and thus not accomplish any effective exchange. The dips in the $\overline{E}$ curves near L/B = 1.0 for the w = 250 feet case could reflect this phenomenon. However, at low tide ranges the stream may not move around the entire perimeter, but rather simply move un-mixed basin water into a position where it leaves the harbor on the ebb tide. This situation produces an $\overline{E}$ which is greater than that predicted by assuming full mixing on the flood portion of the tidal cycle, i.e., $\overline{E} > TPR$, the condition noted on the data plots.

When L/B is less than 1/3 or greater than 3, multiple circulation cells exist within the basin. The cells toward the rear of the basin do not participate fully in the exchange process, and as a result the overall flushing is reduced.

The two narrower entrance widths (w = 125, 250) seem to lend themselves fairly well to the reasoning outlined above. For the 500-foot width, tested over the full L/B range at the 6-foot tide only, at the smallest L/B, the entrance width w was equal to L, and for the Largest L/B was equal to B, so in neither case do the angular momentum considerations apply.

Figure 8 shows there is little difference in gross flushing performance between the rectangular and rounded-corner basins of equal aspect ratio.

Figure 9 indicates that the gross flushing is better for a centrally located than for an asymmetric entrance. As for the rounded-corner tests, experiments were restricted to one tide range and to the narrowest entrance. It is interesting that these results parallel the findings of Askren (1979) for nontidal circulation induced by longshore currents, with no flow through the entrance. The results are reasonable in light of the angular momentum-flood

flow jet discussion above. Nece et al. (1976) defined a penetration distance as the distance travelled along its pathline by a particle of water from the time it enters the basin at the time of mean sea level crossing until high water slack. Assuming that steady flow jet relations can be applied to the water particle (so that jet diffusion is indeed incorporated in the analysis), the jet penetration distance for A and d held constant, is proportional to $H^{2/3}$ and inversely proportional to $w^{1/3}$. For H = 6 feet and w = 125 feet, the penetration distance estimated for the tested geometry is 2300 feet. Taking for example the aspect ratio L/B = 15/8 = 1.88, L ≈ 1500 feet and B ≈ 800 feet. For the single asymmetric entrance, if the jet were to behave according to this very crude analysis and if it were to follow the basin perimeter, a particle of water entering at maximum flood current velocity would be at the opposite rear corner of the basin at high water slack; assuming symmetrical behavior in the two halves of the basin for the central entrance case, the same assumptions show that the comparable water particle would traverse three of the four sides of the half-basin, so that the gyres in the center entrance case would be relatively stronger.

The results can be compared with model results obtained by Schlucter and Slotta (1978). Using dimensions scaled from figures in their paper, the marina tested was rectangular with a surface area A = 59,000 square meters, a nearly "central" entrance of width w = 196 meters, tide range H = 1.83 meters (given), depth not specified, a low net longshore current past the mouth, and L/B = 0.43. The 90 percent exchange time of 5.7 tidal cycles in the model corresponds to an $\bar{E}$ = 0.33, a value in close agreement with present results.

Results from the double entrance tests are shown in Figures 10 and 11. In each case the solid line applies for the single asymmetric entrance. Only two L/B configurations were tested, 1.88 and 3.31, as this entrance arrangement is logical only for basins with the long axis oriented parallel to the shoreline. Equal entrance areas were obtained with two 125-foot entrances and a single 250-foot entrance, etc. The two entrances appear to improve overall flushing at large L/B ratios (again reasonable from momentum - jet penetration considerations), but do not improve conditions at smaller L/B ratios where the two inflows are more apt to interfere with each other.

A limited comparison of results of the present study with data from comparable tests using flourescent dye techniques on the same laboratory apparatus (Nece et al., 1976). Direct comparison for H = 12 feet, w = 125 feet, is possible; the A and d values were the same in both studies. Figure 12 shows data points (not specifically presented, although used) in the earlier study, and the present study curve plotted from Figure 6. Agreement is reasonably good. Figure 13 shows curves of $\bar{E}$ vs. H for three sets of comparable L/B ratios, again for 2 = 125 feet. Again, in all but one set of values, agreement is reasonable. There is no reason why the two sets of results should agree, because the $\bar{E}$ values in the earlier tests were based on high tide -- high tide cycles, while the present studies used low tide -- low tide cycles. Nevertheless, the comparison indicates indirectly a reasonable agreement between experimental techniques. More important is the apparent conclusion that either low water or high water conditions can be used for adequate determination of the gross exchange coefficient.

EFFECT OF PLANFORM GEOMETRY ON UNIFORMITY OF MIXING

These results, based on the 120-point readings, are shown in Figures 14-39 which follow sequentially the corresponding entries in Table 2. In the table, the entry $S/\overline{E}$ provides an index of uniformity of mixing; the smaller the value, the more uniform the exchange. Numerical values of local E in the figures are expressed in percent. On the contour plots, each E value represents the value assumed to be the average over a square area 102 feet on a side (120 x 102 x 102 = 1.25 x 10^6 ft^2). All results apply for the 6-foot tide range. Each basic planform configuration will be discussed in turn.

The local E values plotted apply from low water to low water. At low water, as discussed previously, residual motions resulting from tide-induced circulation in the basin are at a minimum, but some interpretation of the motions which have occurred in the basin during the complete tidal cycle can be determined from the local E values. Generally, high E values indicate presence of ambient (external) water. An area of low E surrounded by higher E values indicates a residual gyre where the exchange/mixing has been lower in the center of the cell. Low E values in a corner region indicate a typical cell in a corner driven by the primary flow which has separated from the wall upstream from the corner.

Results for the square-corner basin with the single asymmetric entrance, w = 125 feet, are on Figures 14-21.

Predictably, the greatest non-uniformity of mixing, or exchange, occurs in the extreme cases, L/B = 0.21 (5/24) and 4.80 (24/5), particularly the latter for which $\overline{E}$ is also low. In both cases the local E values are lowest at the innermost part of the basin, where residual weak circulation cells are visible. These secondary cells possess a counterclockwise circulation.

Exchange is surprisingly uniform over the entire basin for the next most extreme aspect ratios, L/B = 0.30 (6/20) and 3.33 (20/6), although the evidence of separate counterclockwise gyres in the inner end of the basin is again present in each case. Indeed, for L/B = 3.33, the net exchange is better at the rear of the basin than it is near the mouth.

Proceeding from L/B = 0.53 (8/15) to L/B = 1.88 (15/8), as shown on Figures 16 through 19, there is evidence of a single large clockwise gyre. This is especially true for L/B = 1.20 (Figure 18), where the exchange coefficient isopleths outline very clearly the essentially circular cell. For L/B = 1.20 and 1.88, the poorest net exchange occurs in the central region of the basin.

Use of a wider entrance, w = 250 feet, is shown to a limited extent on Figures 22 and 23 for the aspect ratios L/B = 1.88 and 3.33, respectively. Relative performances are essentially reversed from those for the same L/B values with w = 125 feet. Although $\overline{E}$ is about the same for the two entrance widths when L/B = 3.33 ($\overline{E}$ = o.25 for w = 125 feet, 0.24 for w = 250 feet), in the latter case the mixing is far less uniform and the lowest exchange occurs at the inner end of the basin.

Results for the rounded-corner basin, w = 125 feet, are on Figures 24-29, which may be compared with Figures 15-20, respectively, for the square-corner basin. It has already been noted that changing from square to rounded interior corners had little effect on the average exchange coefficient. The $S/\overline{E}$ ratio is also essentially the same for all aspect ratios except L/B = 1.20 and 1.88, where this ratio is much lower for the rounded-corner case. For the rounded-corner basin, the marked depression in exchange noted in the central region of the basin with square corners no longer occurs. Also, for these two L/B configurations, minimum local E values are much higher for the rounded-corner basins. For the L/B < 1 cases, the low exchange (separation cell) areas in the lower right-hand corner (in the drawings) which exist in the square-corner basins have been eliminated by the rounding of the interior corners. The contour plots of local E values do provide quantitative evidence that eliminating sharp corners along interior boundaries does indeed result in more uniform mixing throughout the basin.

Results for the single, centrally located (w = 125 feet) entrance are shown on Figures 30 through 33, for the four tested L/B ratios ranging from 0.53 to 1.88. Ideally, the exchange coefficient isopleths would be symmetrical about an axis drawn through the center of the entrance; in neither field nor laboratory, however, would such ideal conditions be anticipated. The plots do indicate residual cells on either side of the central axis; these cells, in the photographs, appear superficially to be symmetrical.

Figure 9, and the entries in Table 2, indicate that $\overline{E}$ is improved when the asymmetric entrance is moved to a central location, and this result has been discussed from a momentum-jet penetration standpoint. For the two cases of L/B < 1, the uniformity $S/\overline{E}$ is about the same for the two entrance locations, although minimum local E values are correspondingly higher for the center entrance. For L/B > 1, uniformity is markedly increased by moving the entrance to the center. If as a first approximation the effect of the central location for the entrance is viewed as dividing the original basin into two basins each of L/B equal to one half the original, then the trend in mixing performance is consistent with the behavior of the basin with a signle, asymmetric entrance.

Double entrance data are shown in Figures 34 through 39. Again, symmetry which ideally would exist for two equal-width entrances at the opposite corners of the basin is not apparent; the asymmetry in mixing patterns is more noticeable for the case of two 250-foot entrances than for the case of the two 125-foot entrances. The experimental asymmetry does not appear to be connected to any consistent peculiarity of the model tank. In a field situation it would be extremely difficult to avoid asymmetry.

The two 125-foot entrance configuration has the most uniform distribution of exchange, and the two 250-foot entrance case has the poorest uniformity as well as the largest number of low local E values. The latter configuration is also apparently most sensitive to any disturbances or irregularities which might be associated with the external conditions. Again, the narrow entrance layout has more momentum in the flood flow streams into the basin, a situation tending toward a more stable circulation pattern. For the 125/250-foot entrances, however, both the smaller gyre and lower average exchange occur in the end of the basin containing the narrower of the two entrances.

EXAMPLE INVESTIGATION OF CYCLE-TO-CYCLE FLUSHING REPETITION

All results for gross tidal exchange coefficients $\bar{E}$ and local exchange coefficients E are presented under the assumption that conditions are repetitive from one cycle to the next. The values cited have been based on this assumption, with numerical values based on measured C/C_0 values at the end of four cycles. An investigation into the applicability of the procedure is shown in Figures 40 and 41.

The figures apply to the configuration of L/B = 1.88, square-corner basin, w = 125 feet and H = 6 feet; this was an arbitrary choice. Figure 40 shows the average C/C_0 at the end of each complete tidal cycle (at low water) based on an average of the 12-point readings, and also the corresponding C/C_0 values calculated at each low water on the basis of $\bar{E}$ = 0.24 (the value obtained by the artificial mixing of the basin waters after n = 4 cycles). The two C/C_0 values at n = 4 do not agree because of slight differences in $\bar{E}$ determined by the different methods for the test. The two curves are essentially the same, indicating that on an overall basis the basin did exchange nearly the same proportion of its water on each cycle. Repetitive overall behavior was obtained within 4 cycles.

The sub-areas having coordinates (2,2) and (4,3) whose exchange histories are shown in Figure 41 are located in Figure 40. The former lies within the central region of the single gyre (Figure 19), and the latter is at the corner of the basin farthest from the entrance. In each case the local E values from the 3-mm eye densitometer readings apply to about 38 percent of the area of the segment, centrally located in the sub-area. The local curves of C/C_0 versus or demonstrate variability in exchange from cycle to cycle. The element (2,2) responds more quickly in the testing program, while the element (4,3) experiences little exchange during the first cycle; the curves of measured C/C_0 values indicate that about three cycles are necessary before the basin reaches repetitive conditions in the laboratory tests. At n = 4, however, the behavior does appear to be more repetitive. (Values of measured and calculated C/C_0 agree at n = 4, because the local E value was determined from the measured C/C_0 at n = 4.)

The essentially quasi-steady state conditions for repetitive tides described by the numbers cited in this report do not describe the full dynamics of the tidal flushing process. Of equal interest might be the variation of local C with time over the period of a tidal cycle. All results presented apply for low-water conditions. Conditions for each 1/4 cycle are recorded on the films constituting the project data files, but they have not been shown because complete calibrations (concentration vs. densitometer reading) were performed only at low-water conditions.

SECTION 6

CONCLUSIONS

Conclusions are presented sequentially concerning the effects of the five particular geometry parameters listed in Section 1. The conclusions apply only to the hydraulic performance of the marina, i.e., to overall and uniformity of tidal flushing. Tidal exchange in itself is not an index of water quality, although in general as the exchange improves the quality of the water within the basin approaches that of the ambient waters. In judging the water quality of a marina, relative rather than absolute standards should be employed because quality of water in the marina cannot exceed that of the exterior water with which it exchanges.

Comparisons presented here of effects of different planform geometries are based on results for the 6-foot tide range. Again, from a design standpoint, this particular value was chosen because it is typical of mean ranges in the Pacific Northwest.

1. Planform geometry aspect ratio. The study confirmed the earlier conclusions (Nece et al., 1976) that for $L/B < 1/3$ and for $L/B > 3$, multiple circulation cells (gyres) exist within rectangular basins with single asymmetric entrances. Variations in local exchange associated with the cells was quantified. When multiple cells exist the gross exchange decreases and spatial variability of local exchange increases.

The exchange contour drawings also show that when only a single gyre exists, the exchange is lower in the center of the basin than it is near much of the perimeter, due to the residual circulation when the gyre is established. This may be a positive result from a fisheries standpoint, as juvenile migrant salmon which reside temporarily in marinas tend to remain in the relatively shallower water near the basin perimeter where local exchanges may be greater than the gross exchange for the basin.

A comment is in order concerning the oval-shaped marina with an asymmetric entrance that has become popular in the Pacific Northwest. This design produces a single-gyre circulation pattern and good overall flushing performance. Since this study indicates the exchange would tend to be greater than average around the perimeter, such oval basins should be favorable from a fish-protection standpoint. The test configurations closest to these oval shapes were the rounded-corner basins with L/B values from 0.53 to 1.88 (figures 25-28); the exchange contour

plots show that the lower E regions in the center of the single gyre are not large and do not have E values which are significantly lower than $\bar{E}$.

2. Ratio of entrance cross-sectional area, a, to basin planform area, A. As noted previously, each curve for w = constant on Figures 4-7 represents a curve of a/A = constant and for H = constant also represents conditions of equal momentum flux input to the basin. The range of discrete entrance widths w from 125 feet to 500 feet provides a fourfold variation in a/A, but for a constant H (as shown in the summary plot Figure 7) the differences in $\bar{E}$ are no large between the various curves of w = constant than they are between various L/B ratios for the same w. Indeed, it is interesting to note that, for H = constant, near L/B = 1.0 the values of $\bar{E}$ for the various w = constant curves (H = constant) are very comparable. Also, for a particular a/A, large variations in uniformity as well as average exchange exist over ranges of L/B; this is particularly true for L/B < 1/3 and L/B > 3, as noted above. This behavior is linked to the effective penetration distance of the inflow jet. Because such wide variations in performance do occur for a/A and H constant as planform geometry varies (including effects of rounded corners and other than single, corner-located asymmetric entrances), it is concluded that the a/A ratio is not a governing factor.

These conclusions should be tested against the criteria proposed by Slotta and Noble (1977). One of the conclusions expressed in that publication was that the ratios A/a and $A/a^{1/2}w$ should be kept below 400 and 100, respectively, to obtain optimal basin configuration for flushing. (The entrance cross sectional area a is that existing at low tide.) For H = 6 feet, the corresponding values of the dimensionless area ratios are listed below for the basins tested in the present study.

w-ft	A/a	$A/a^{1/2}w$
125	769	248
250	385	88
500	192	31

The w - 125 feet case does not satisfy the proposed criteria. However, for a number of planform geometries the overall exchange coefficient $\bar{E}$ was close to the tidal prism ratio, and local exchange showed quite good uniformity throughout the basin. From a purely hydraulic standpoint, the marina flushing would be considered satisfactory. Therefore, it is suggested that the Slotta and Noble criteria should not be treated as rigid design standards.

3. Effect of rounding of corners in the basin interior. Rounding of interior corners apparently has little effect on overall flushing, but it has been quantified that the rounding of corners does indeed produce greater uniformity in local exchange throughout the basin. "Hot spots" of poor local exchange are mostly eliminated.

4. Orientation and location of single entrances. On the basis of the limited experiments performed, it appears that a single center entrance produces better flushing behavior than does a single corner-located asymmetric entrance. This result was obtained for rectangular, square-corner basins only; presumably, the same result would hold for basins with rounded corners. As discussed in Section 5, this result can be attributed partially to the fact that the jet entering the basin on the flood tide is able to circumnavigate a greater length of basin perimeter than it could in a basin with an asymmetric entrance, all other geometry parameters being the same.

One precautionary statement must be made. In the experimental program, the entrance was designed so that the flood tide inflow entered as a uniform flow in a direction normal to the other face of the marina. In a more typical field situation the entrance would more likely be a gap in a breakwater. Consequently, the presence of longshore currents the inflow would enter the basin with some momentum parallel to the shoreline and, as a consequence, the flow pattern in the basin would not possess the symmetry sought in the laboratory tests. However, the results of the theoretical study of Askren (1979) for circulation induced in basins by a steady, non-tidal longshore current past entrances in frontal breakwaters indicated that a central location was the optimum site for a single entrance. Thus, the two sets of results, obtained for different boundary conditions, lead to the same conclusion.

The experimental data, in particular the exchange contours, show that for an elongated basin with a single asymmetric entrance the uniformity of flushing and in particular the exchange in the innermost part of the basin is better when $L/B < 1$ than it is when $L/B > 1$. Again, this behavior can be linked to the penetration distance of the inflow jet. The recommendation, with respect to design criteria, is that when a basin is elongated (say, with aspect ratio exceeding an absolute value of 2.0) and a single asymmetric entrance is used, the entrance should be aligned so that the inflow direction is parallel to the long asix of the basin.

No conclusions can be presented for entrances where the flood tide inflow is deliberately directed at some angle other than the one used in the tests.

5. Effect of two entrances versus a single entrance. Results are quite limited. In general, two-entrance basins would be very sensitive to effects of persistent longshore currents which were deliberately avoided in the laboratory experiments. Short-circuiting could exist if the longshore currents are primarily uni-directional. Generalizations are dangerous for multi-entrance basins, because the interior circulation patterns are sensitive to local head levels which result from the physical configurations of the entrances, near shore, and details of the longshore current patterns. However, on the basis of the limited results, it appears that more uniform flushing is obtained when the entrances are of equal, or at least comparable, width.

On the basis of the results presented, although the particular configuration was not tested, the best design for a rectangular basin for optimum tidal flushing would incorporate an aspect ratio L/B between 0.5 and 2.0, rounded corners, and a center entrance. Asymmetric entrance basins within the same L/B range also possessed satisfactory flushing action, particularly those with rounded corners. As noted, these results would indicate that basins with oval planform and asymmetric entrance such as have been built and/or proposed at a limited number of sites in the Pacific Northwest should possess satisfactory exchange characteristics.

Each project is subject to site-specific limitations imposed by shoreline topography, suitability and size of the area available for dredge/fill operations, and property line locations. To illustrate application of results from this study, the following situation is hypothesized where site constraints can be relaxed and a rectangular basin, center-entrance design can be adopted. The hypothetical project has the following conditions:

Surface area = 20 acres (8.1 hectares), required to accommodate between 650 and 700 small boats (primarily pleasure craft, few commercial vessels).

Entrance width = 150 feet (45.8 m), fixed by navigation requirements

Mean tide level = 7.0 feet (2.1 m), MLLW

Mean tide range = 7.0 feet (2.1 m), MLLW

Bottom elevation in dredged entrance and most of basin = -12.0 feet (-3.7 m), MLLW

An allowable L/B ratio is 0.5. Using this, then L = 660 feet and B = 1320 feet. The ratio A/a, using low water at the entrance, is 375. The tidal prism ratio is TPR = 0.31.

From Figure 9, for a single center entrance of w = 125 feet (A/a = 769) and H = 6 feet, at L/B = 0.5, $\bar{E}$ is estimated to be 0.34. Using the curve for w = 250 feet (A/a = 385) on Figure 5 and assuming a comparable increase in $\bar{E}$ of 0.33 to 0.35, which is greater than the tidal prism ratio.

It is evident that this study will provide guided estimates, but not precise values, of gross flushing coefficients for various harbor planforms having entrance orientations comparable to those tested. Center entrances not normal to the outer face of the marina still should be investigated because they would produce at least two non-equal gyres within the basin.

It still remains to link the tidal exchange coefficients to a quantitative comparison of the quality of water within the marina to that of the ambient water. This information, based on actual field sampling, is needed before designs can be evaluated properly and predicted water quality is compared against local water quality standards. Therefore, correlation with

field measurements of water quality parameters is absolutely necessary from a pragmatic approach to determine how significant hydraulic behavior really is to marina water quality.

The photodensitometer technique employed in this study does provide a way to quantify details of tidal exchange in the type of harbor investigated. Therefore, if such details continue to be important in the evaluation of proposed marinas, and pending the further development of mathematical models adapted to the problem, the photographic technique appears to be a good interim tool for use in the design of small harbors to achieve satisfactory hydraulic conditions.

From a fluid mechanics standpoint this study has followed a purely experimental approach, in which determination of percentages or fractions of actual water exchange has been the objective. A rationale advanced for the method is that convective transport dominates in both model and prototype, so that scale effects on mixing processes in the distorted scale physical models are not significant in the overall results. On the other hand, the numerical of results of Askren (1979) and Abbott (1977), and in particular extensions of the latter's methods to predictions of tide-induced motions in enclosed harbors carried out at Oregon State University (1977), have as their aim the calculation of the convective currents. A joint use of the photodensitometer technique with these essentially two-dimensional numerical techniques would seem to point toward a better understanding of the effects of diffusion in the tidal flushing process. This joint-use procedure is suggested as a logical way of testing the mathematical models as they are developed further, and is recommended as a course of future research.

REFERENCES

Abbott, M.B. 1977. Marina Flushing and Circulation Tests. Danish Hydraulic Institute, Hoersholm, Denmark. 22 pp.

Askren, D.R. 1979. Numerical Simulation of Sedimentation and Circulation in Rectangular Marina Basins. NOAA Technical Report NOS 77. U.S. Department of Commerce, National Oceanic and Atmospheric Administration, Rockville, Maryland. 114 pp.

Brandsma, M.G., J-J Lee and F.R. Bowerman. 1973. Marina del Ray: Computer Simulation of Pollutant Transport in Semi-Enclosed Water Body. Sea Grant Publication No. USC-SG-1-73. University of Southern California, Los Angeles, California. 113 pp.

Brogdon, N.J., Jr. 1975. Westport Small-Boat Basin Revision Study: Hydraulic Model Investigation. Miscellaneous Paper H-75-8. U.S. Army Engineer Waterways Experiment Station, Vicksburg, Missippi.

Fischer, H.B. and E.R. Holley. 1971. Analysis of the Use of Distorted Hydraulic Models for Dispersion Studies. Water Resources Research, Vol. 7, No. 1, February. 46-51.

Fischer, H.B. 1976a. Some Remarks on Computer Modeling of Coastal Flows. Proceedings ASCE, Vol. 102, No. WW4, November. 395-406.

Fischer, H.B. 1976b. Mixing and Dispersion in Estuaries Annual Review of Fluid Mechanics. Annual Reviews, Inc., Palo Alto, California. 107-133.

Hinwood, J.B. and I.G. Wallis. 1975. Review of Models of Tidal Waters. Proceedings ASCE, Vol. 101, No. HY 11, November. 1405-1421.

Nece, R.E. and E.P. Richey. 1972. Flushing Characteristics of Small-Boat Marinas. Proceedings 13th Coastal Engineering Conference. ASCE. Vancouver, Canada. 2499-2512.

Nece, R.E. and E.P. Richey. 1975. Application of Physical Tidal Models in Harbor and Marina Design. Proceedings Symposium on Modeling Techniques. ASCE. San Francisco, California. 783-801.

Nece, R.E., R.A. Falconer and T. Tsutsumi. 1976. Planform Influence on Flushing and Circulation in Small Harbors. Proceedings 15th Coastal Engineering Conference. ASCE. Honolulu, Hawaii. 3471 - 3486.

Nece, R.E. and E.P. Richey. 1979. Tidal Flushing in Flounder Bay. Charles W. Harris Hydraulics Laboratory Technical Report No. 61. University of Washington, Seattle, Washington. 21 pp.

Oregon State University. 1977. Marina Flushing and Circulation Tests. (In collaboration with the Danish Hydraulic Institute). Corvallis, Oregon.

Richey, E.P. and H.N. Smith. 1977a. Birch Bay Marina: Hydraulics of Proposed Expansion. Charles W. Harris Hydraulics Laboratory Technical Report No. 53. University of Washington, Seattle, Washington. 38 pp.

Richey, E.P. and H.N. Smith. 1977b. Squalicum Small Boat Basin: Flushing Characteristics by Hydraulic Model. Charles W. Harris Hydraulics Laboratory Technical Report No. 55. University of Washington, Seattle, Washington.

Richey, E.P. and N.K. Skjelbreia. 1978. Yaquina Bay Marina: Circulation and Exchange Characteristics. Charles W. Harris Hydraulics Laboratory Technical Report No. 56. University of Washington, Seattle, Washington. 25 pp.

Schluchter, S.S. and L. Slotta. 1978. Flushing Studies of Marinas. Coastal Zone '78 Proceedings Symposium on Technical, Environmental, Socioeconomic and Regulatory Aspects of Coastal Zone Management. ASCE. San Francisco, California. 1878-1896.

Slotta, L. and S.M. Noble. 1977. Use of Benthic Sediments as Indicators of Marina Flushing. Sea Grant Publication No. ORESU-T-77-007. Oregon State University, Corvallis, Oregon. 56 pp.

Van de Kreeke, J. and R.G. Dean. 1975. Tide-Induced Mass Transport in Lagoons. Proceedings ASCE, Vol. 101, No. WW4, November. 393-403.

Vollmers H. 1976. Harbour Inlets on Tidal Estuaries. Proceedings 15th Coastal Engineering Conference. ASCE. Honolulu, Hawaii. 1854-1867.

Ward, P.R.B. 1973. Measurement of Dye Concentrations by Photography. Proceedings ASCE, Vol. 99, NO. EE3, June. 165-175.

Yanagi, T. 1976. Fundamental Study on the Tidal Residual Circulation - I. Journal of the Oceanographical Society of Japan, Vol. 32. 199-208.

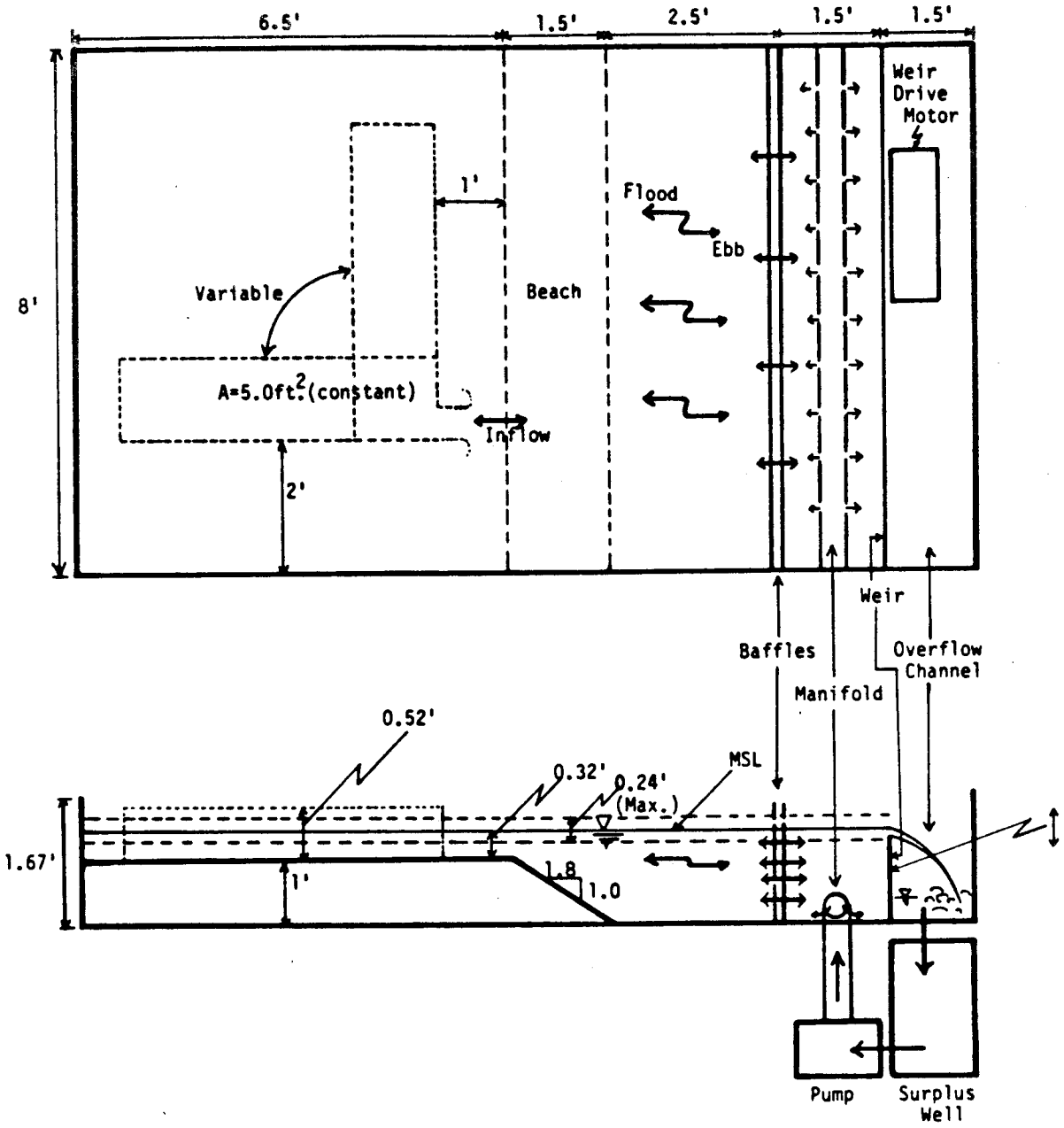

Figure 1. Details of Laboratory Tide Tank

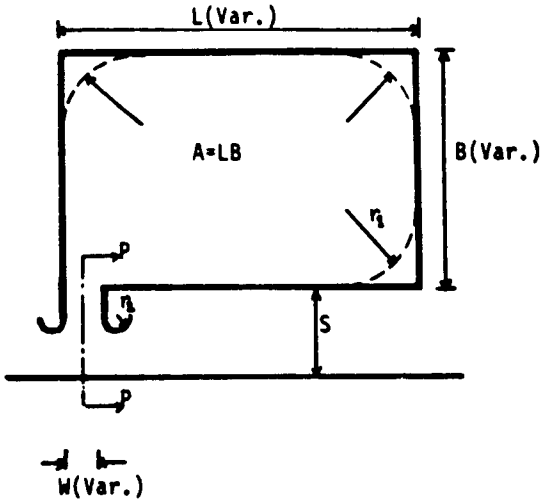

Plan—Single Entrance Basin

(Note: r_1 =250', all cases, Rounded Corner
r_2 =75', all cases)

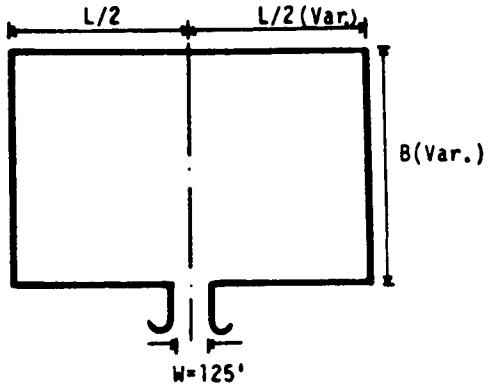

Plan—Center Entrance Basin

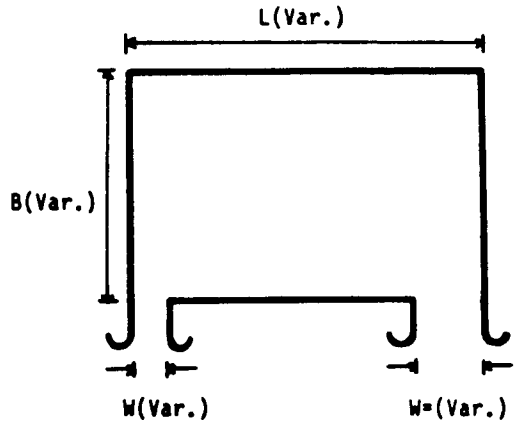

Plan—Double Entrance Basin

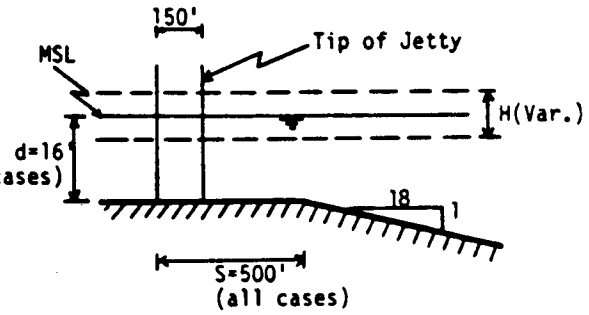

Sect. P-P

Figure 2. Definition and Notation Diagram

Concentratration ratios used to determine basin average $\bar{R}$: $\bar{E}=1-\bar{R}$				
Entrance Width		12-point average $1-\left(\frac{C_{q,L}}{C_{o,L}}\right)^{1/4}$	Mixed $1-\left(\frac{C_{q,L,m}}{C_{o,L}}\right)^{1/4}$	120-point average $1-\left(\frac{C_{q,L,n}}{C_{o,L}}\right)^{1/4}$
W=125'	———	⊡	⊙	△
W=250'	— — —	◧	◑	◭
W=500'	- - - - - - -	■	●	▲

Figure 3. Data Plot Symbol Identification

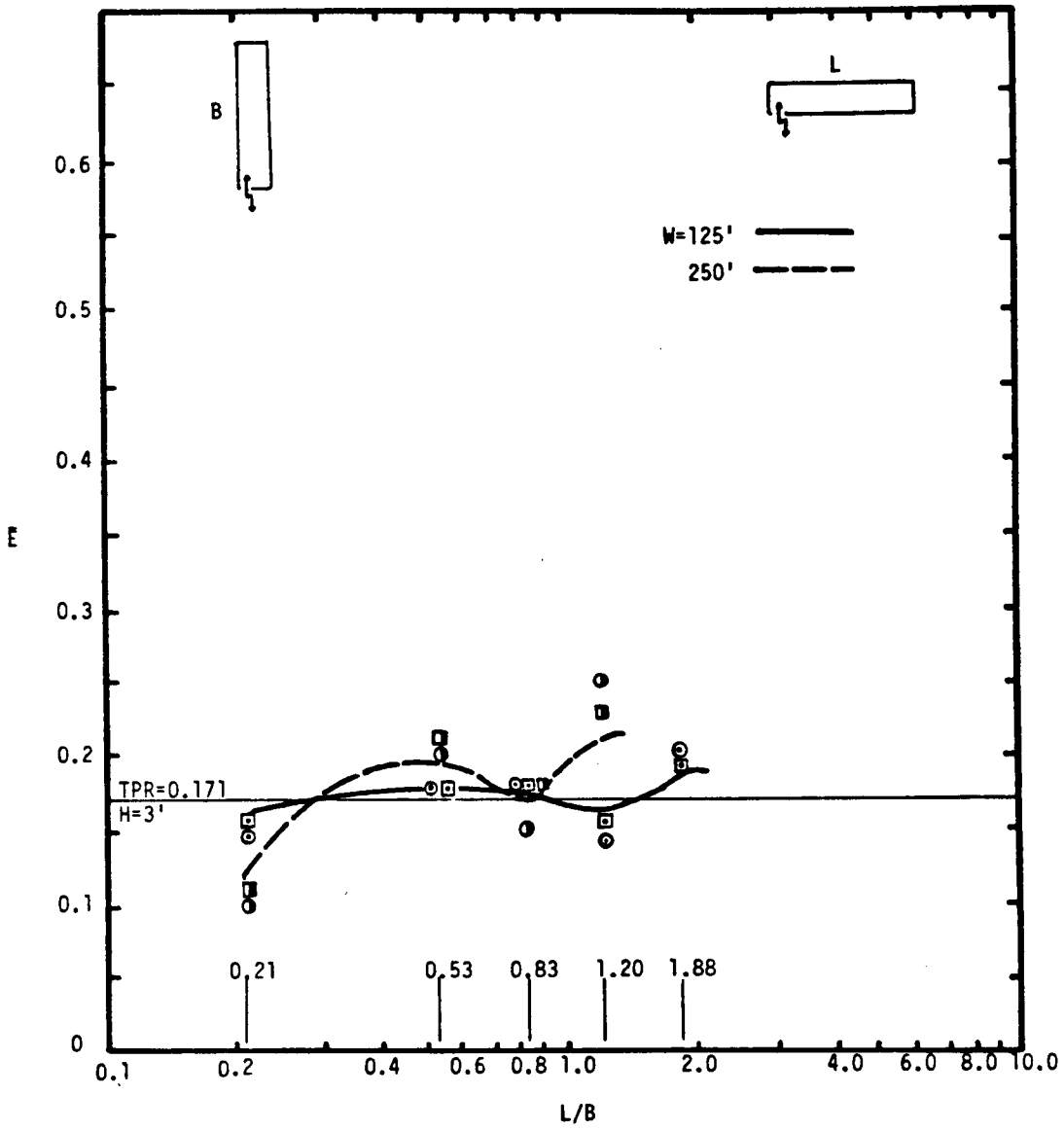

Figure 4. Average Exchange Coefficients, Single Asymmetric Entrance, H = 3 feet.

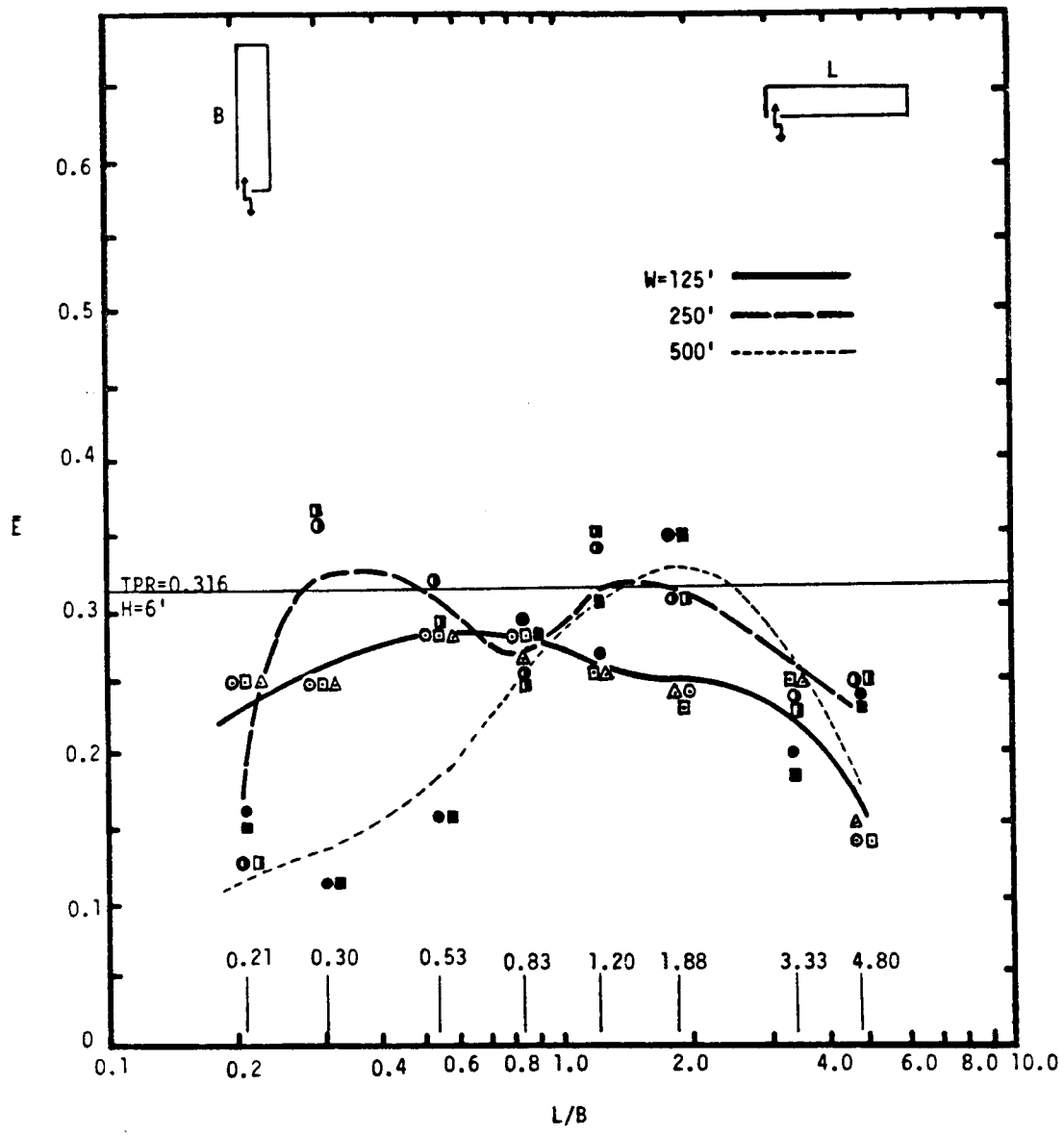

Figure 5. Average Exchange Coefficients, Single Asymmetric Entrance, H = 6 feet.

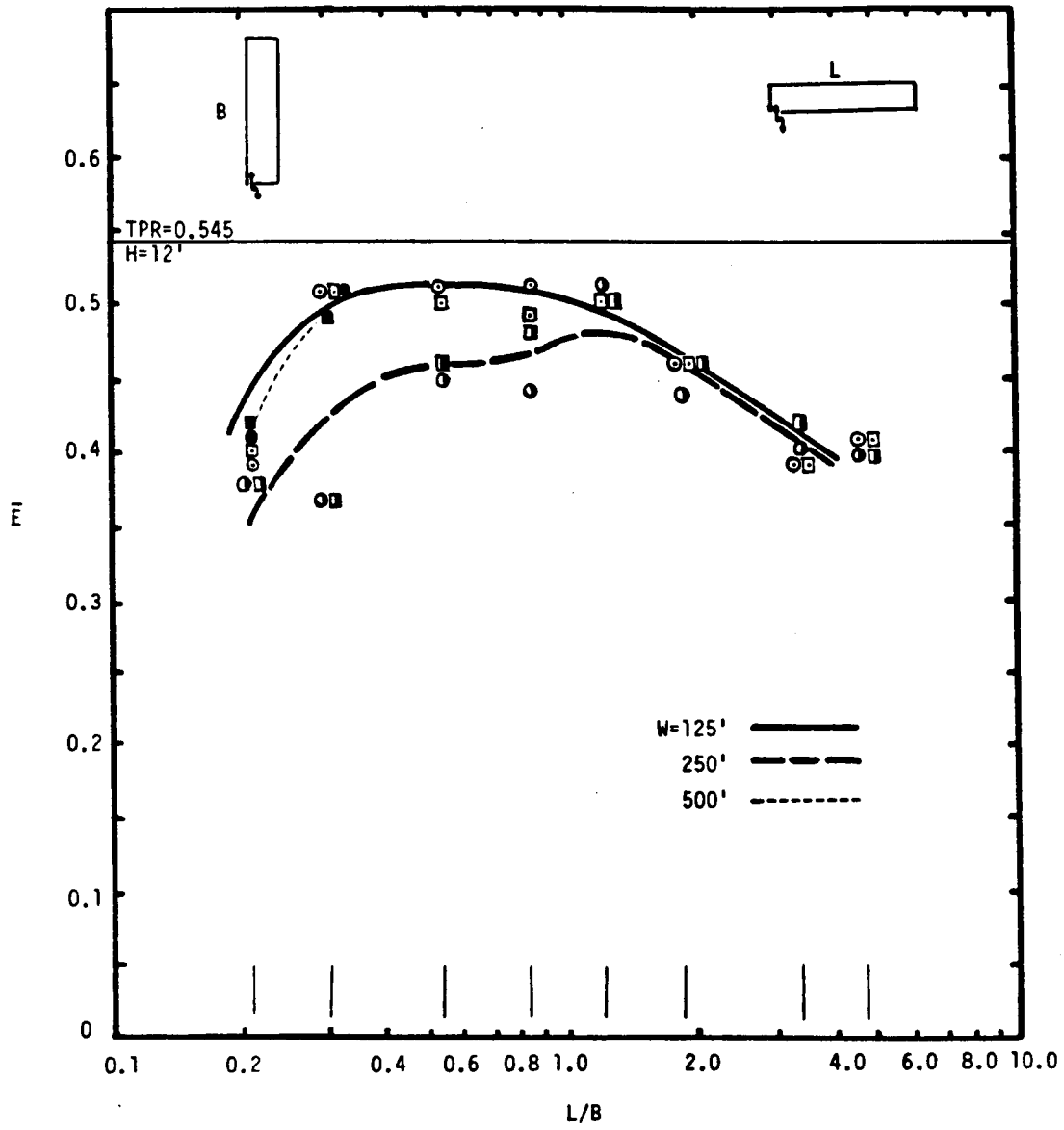

Figure 6. Average Exchange Coefficients, Single Asymmetric Entrance, H = 12 feet.

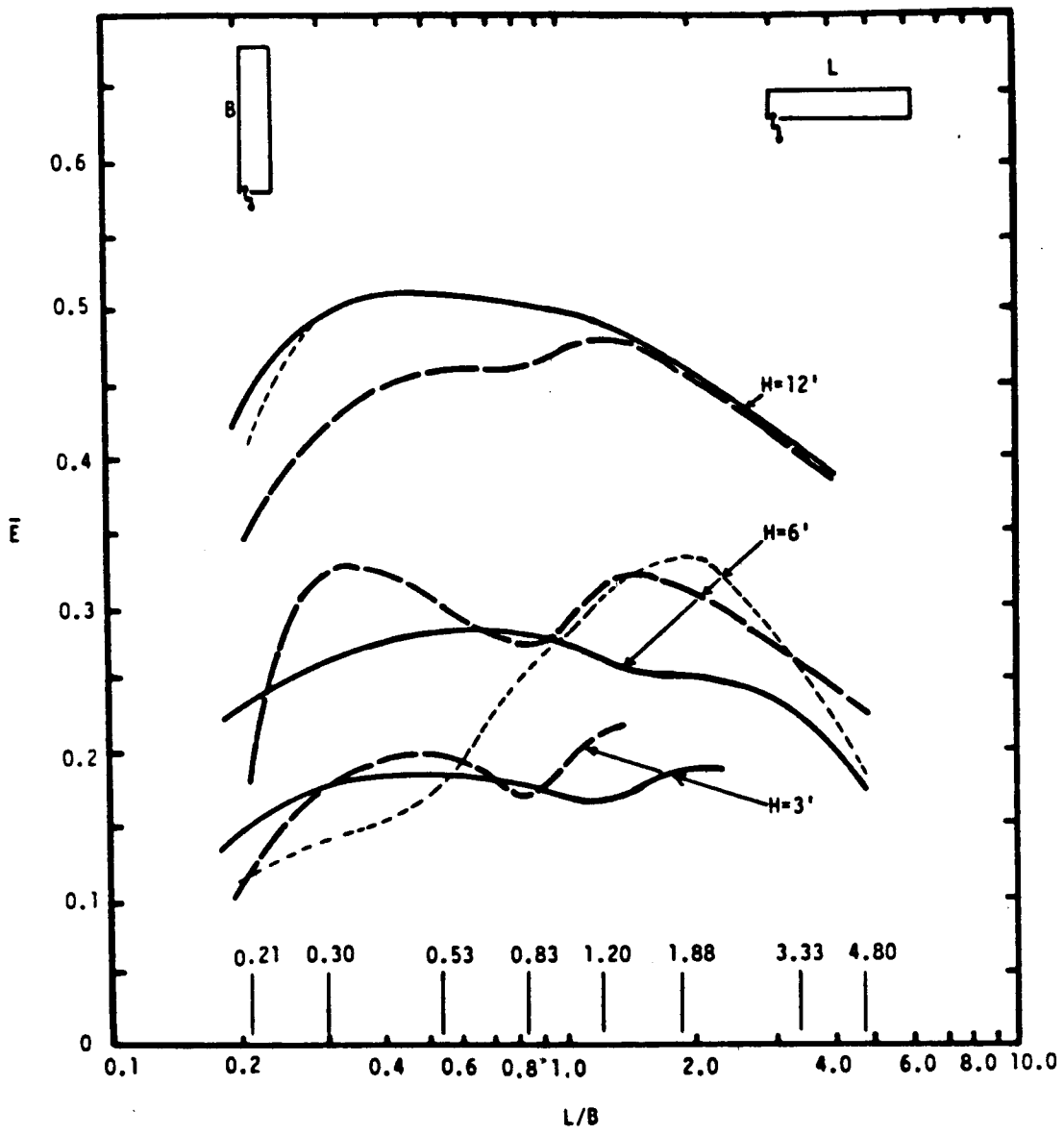

Figure 7. Average Exchange Coefficients, Single Asymmetric Entrance, Summary Plot.

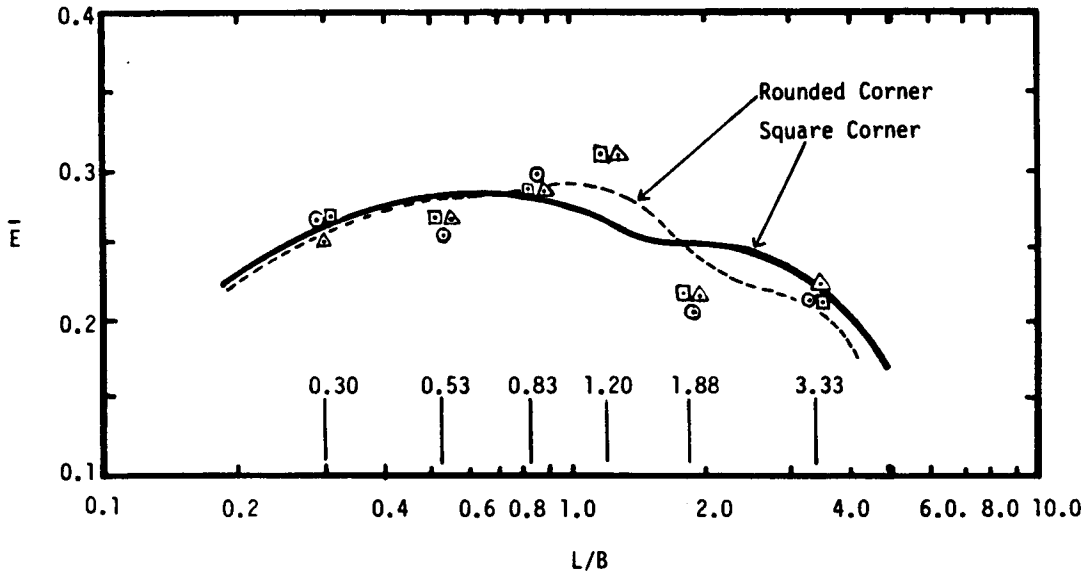

Figure 8. Comparison of Average Exchange Coefficients, Single Asymmetric Entrance, Square Corners vs. Rounded Corners; H = 6 feet.

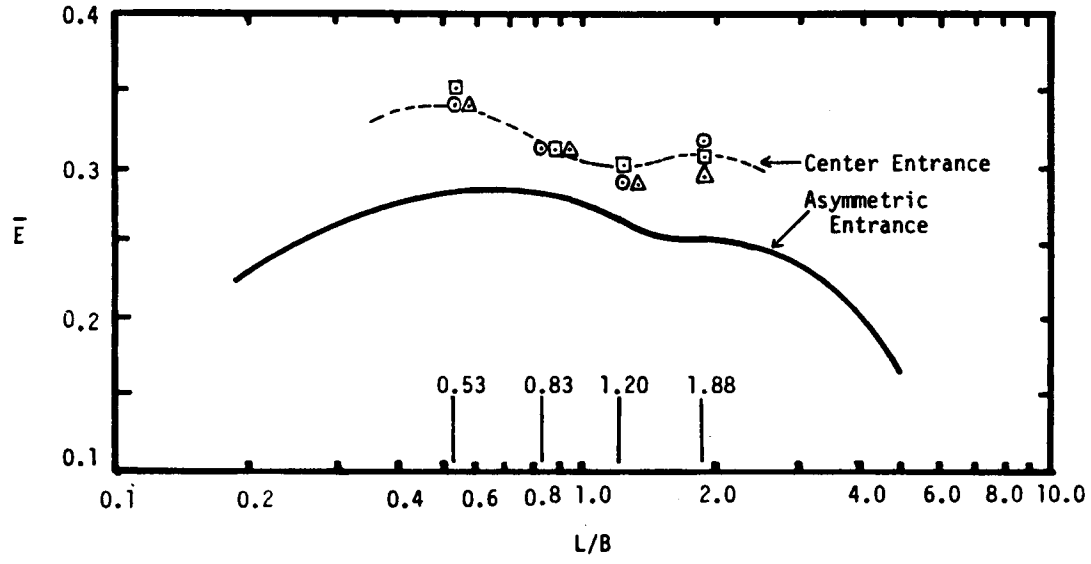

Figure 9. Comparison of Average Exchange Coefficients, Square-Corner Basin, Asymmetric Entrance vs. Center Entrance; H = 6 feet.

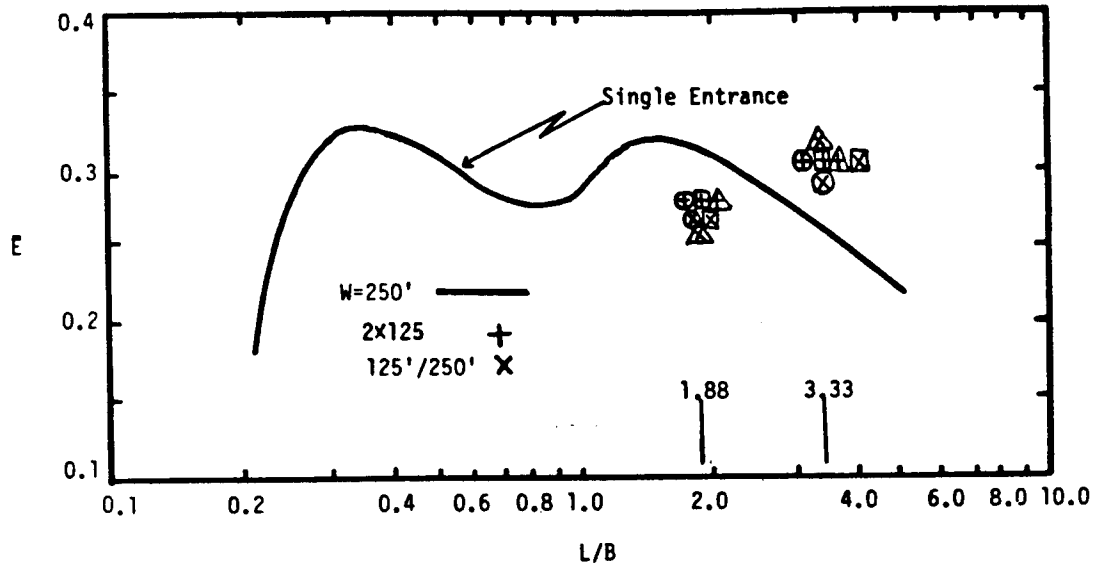

Figure 10. Comparison of Average Exchange Coefficients, Rectangular Basin, Single 250-foot Entrance vs. Two Entrances; H = 6 feet.

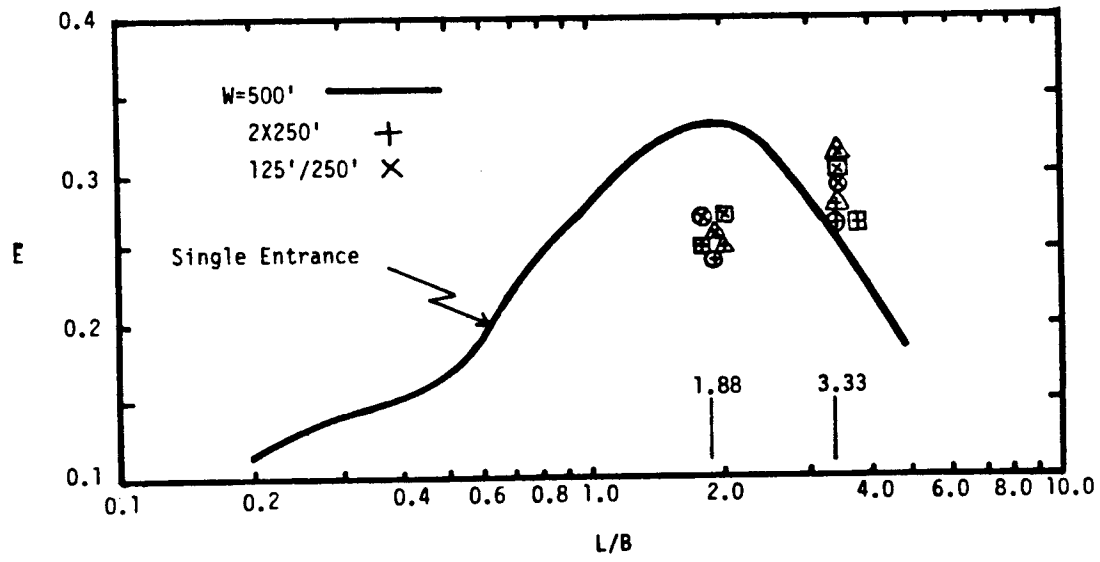

Figure 11. Comparison of Average Exchange Coefficients, Rectangular Basin, Single 500-foot Entrance vs. Two Entrances; H = 6 feet.

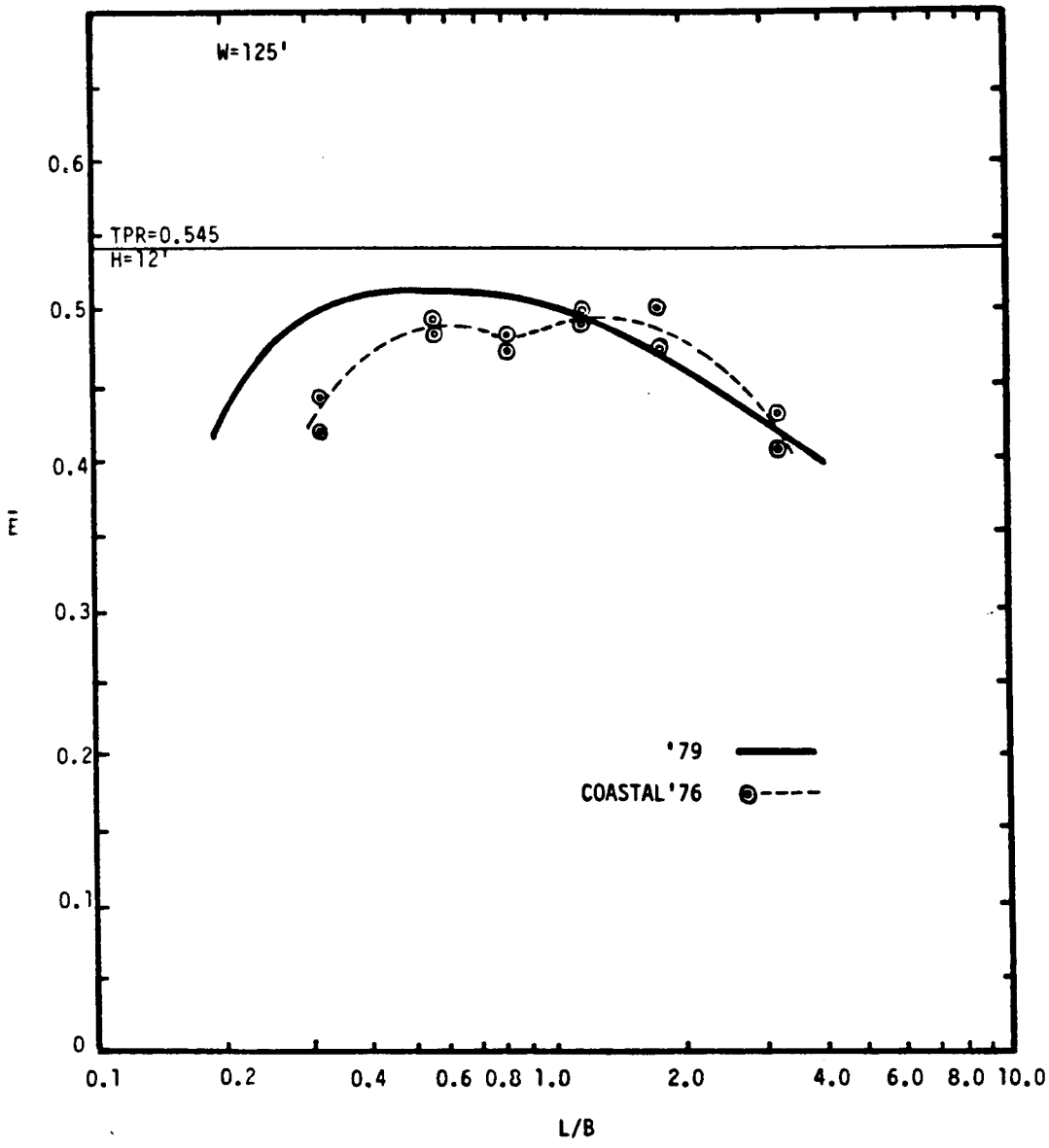

Figure 12. Comparison of Average Exchange Coefficients, Single Asymmetric Entrance, Fluorescent Dye Method (1976) vs. Photodensitometer Method (1979), H = 12 feet.

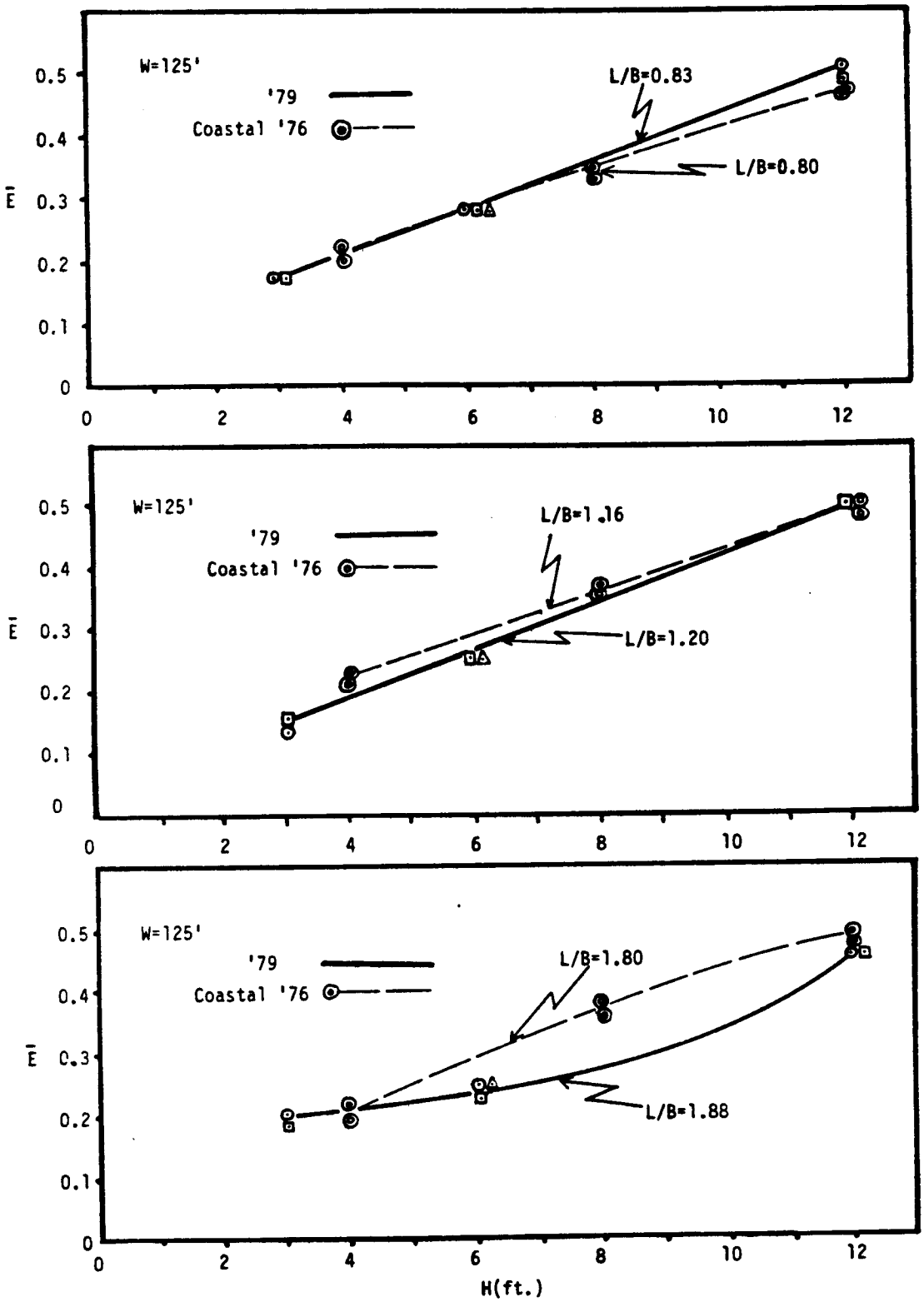

Figure 13. Comparison of Average Exchange Coefficients, Single Asymmetric Entrance, Fluorescent Dye Method (1976) vs. Photodensitometer Method (1979).

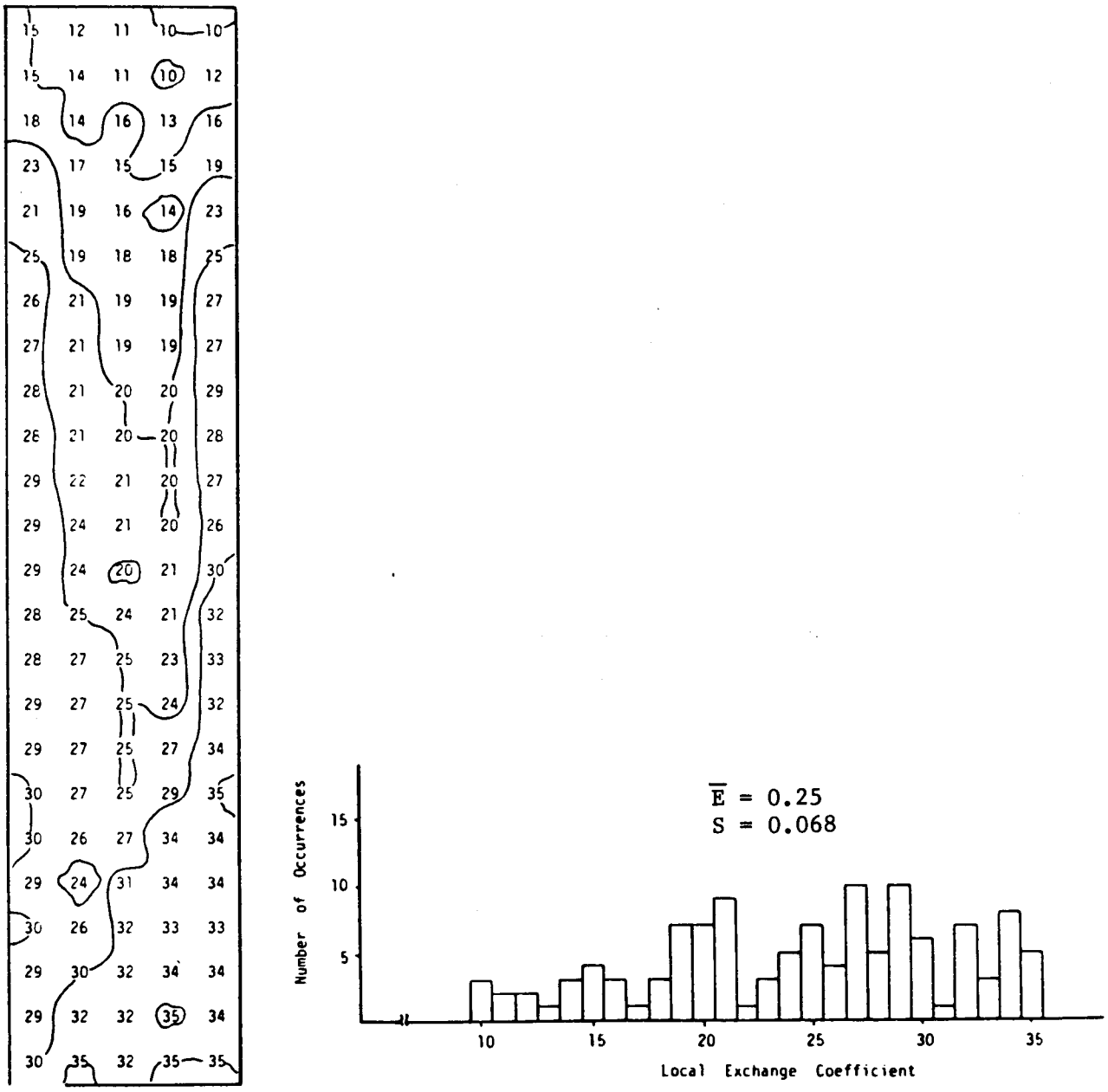

Figure 14. Square Corners, Single Entrance, H = 6 feet, w = 125 feet, L/B = 0.21.

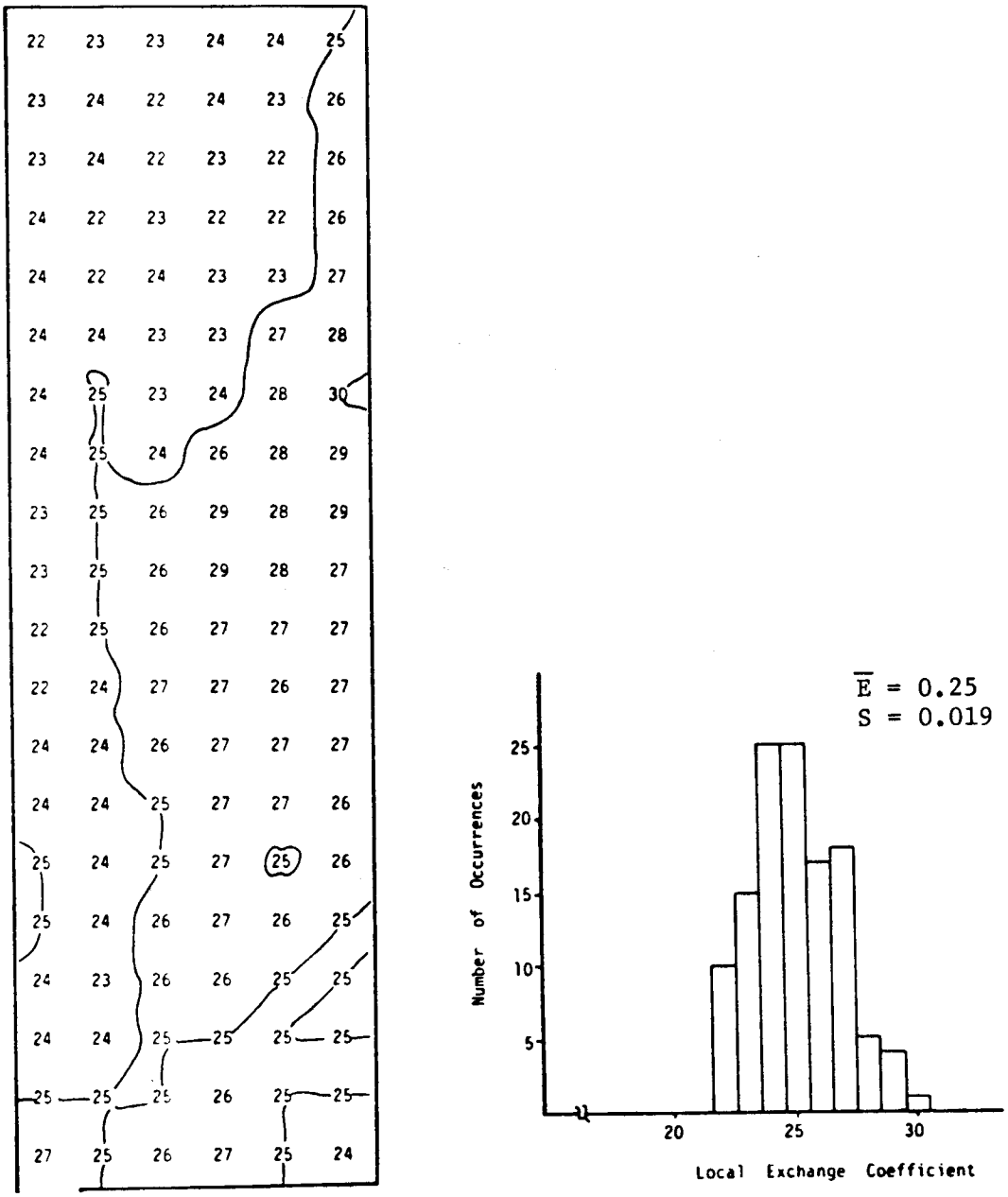

Figure 15. Square Corners, Single Entrance, H = 6 feet, w = 125 feet, L/B = 0.30.

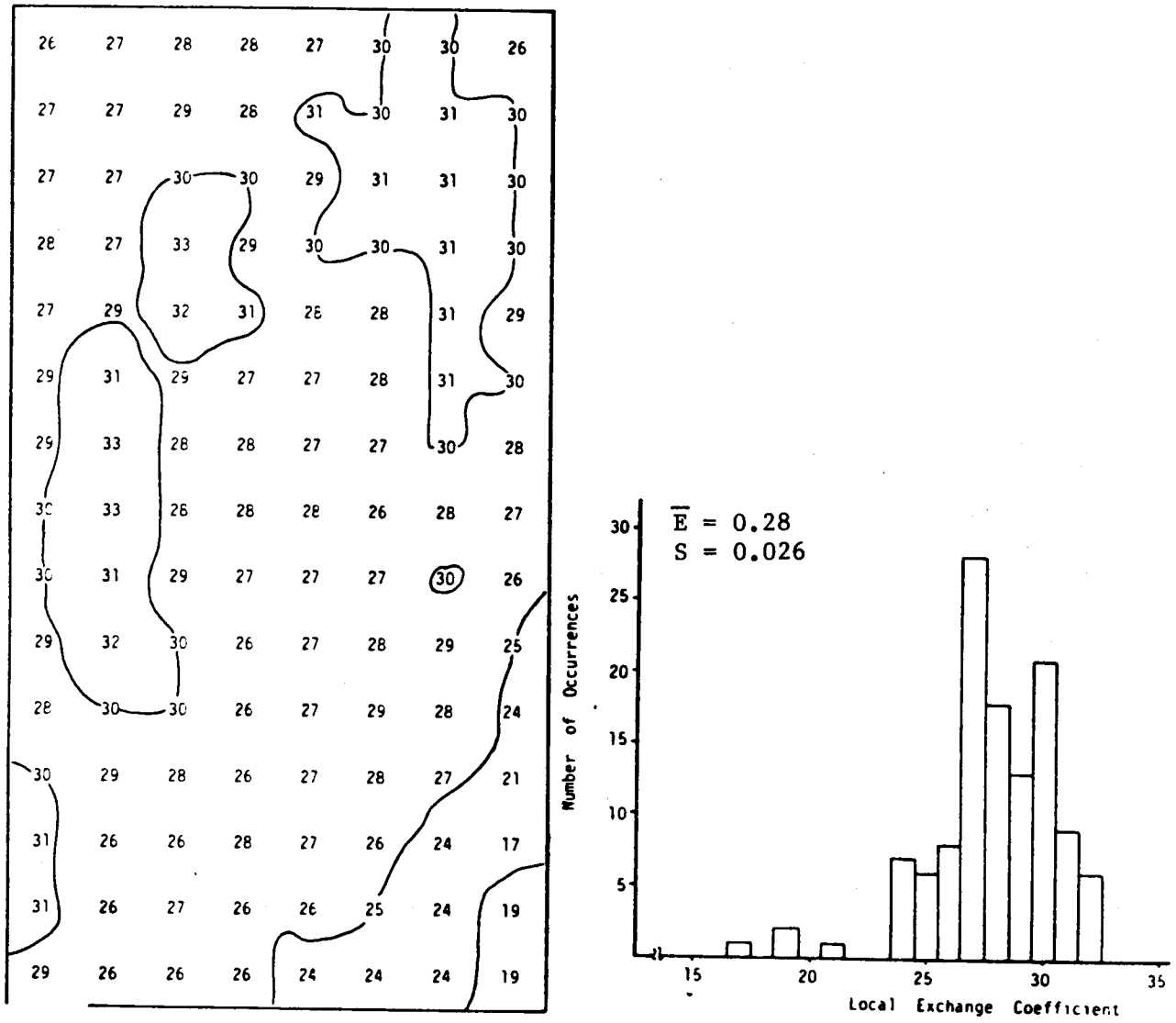

Figure 16. Square Corners, Single Entrance, H = 6 feet, w = 125 feet, L/B = 0.53.

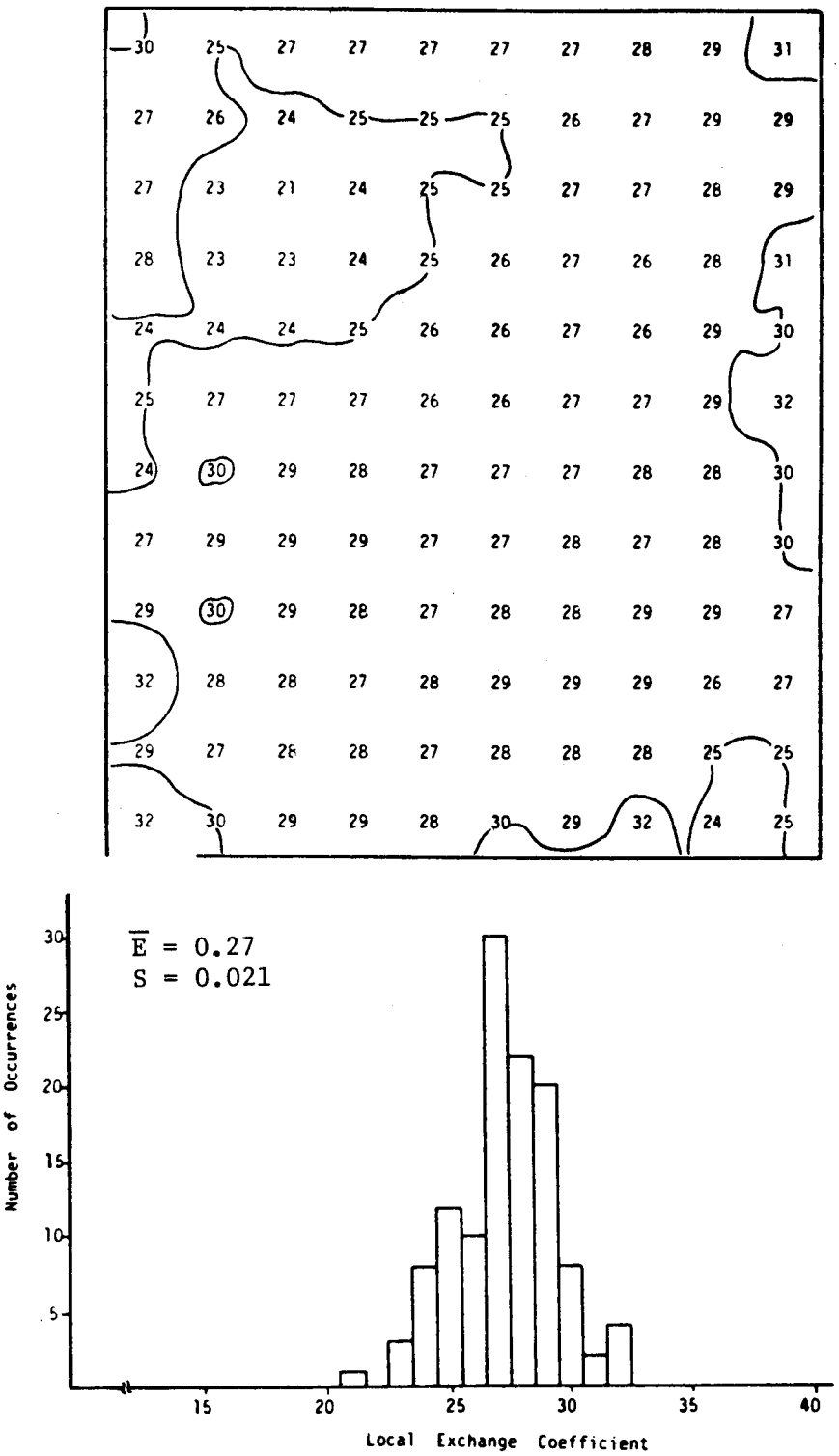

Figure 17. Square Corners, Single Entrance, H = 6 feet, w = 125 feet, L/B = 0.83.

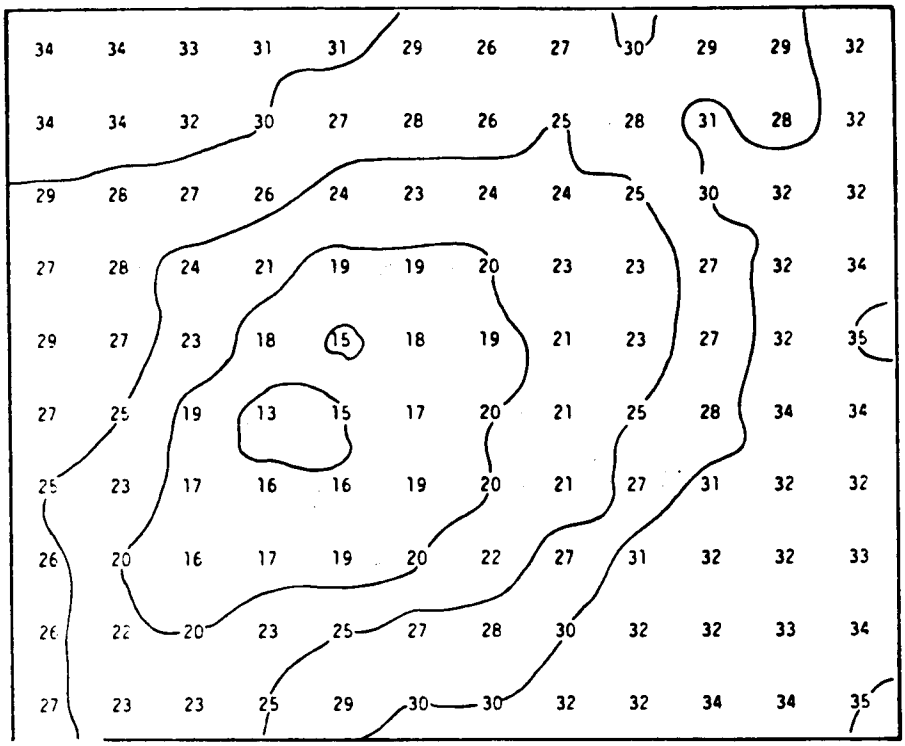

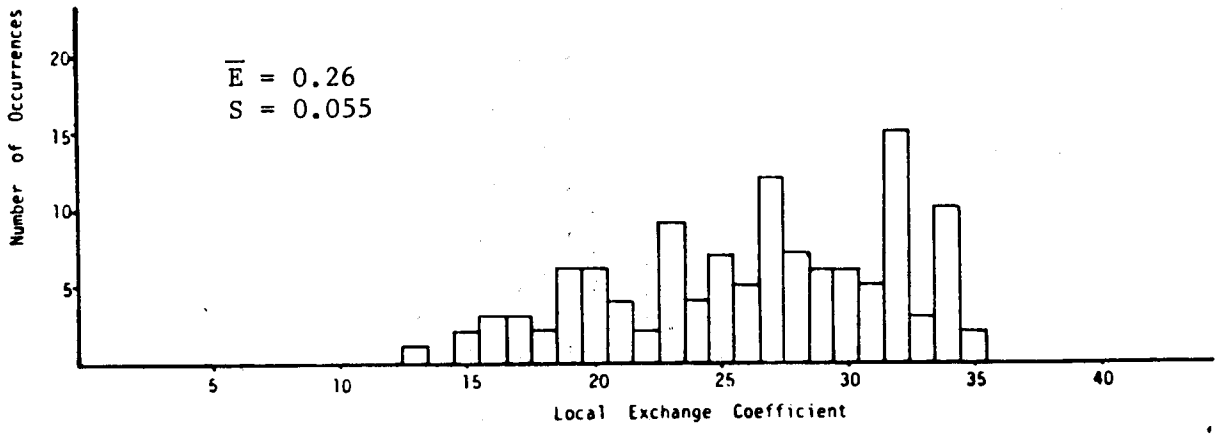

Figure 18. Square Corners, Single Entrance, H = 6 feet, w = 125 feet, L/B = 1.20.

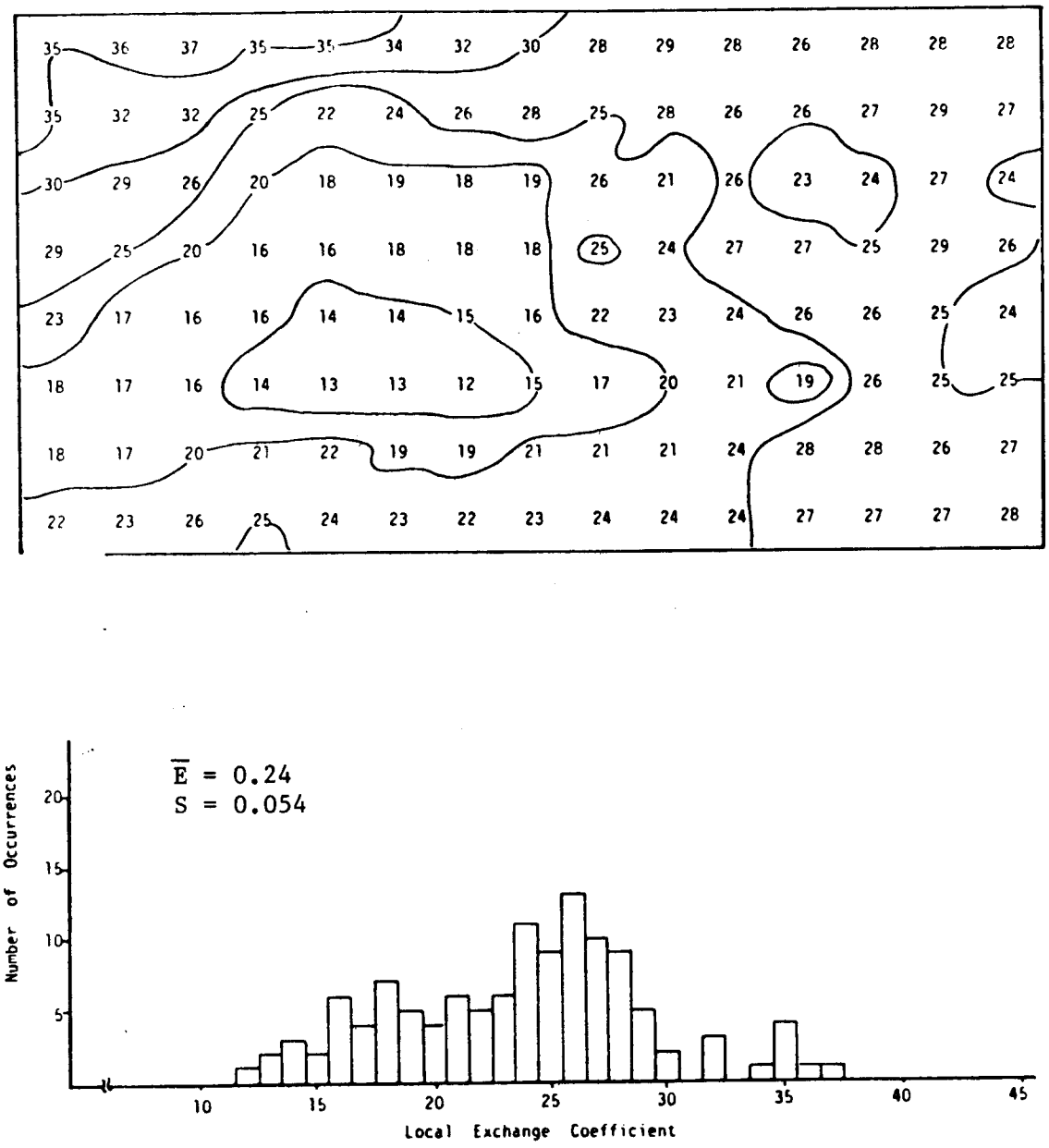

Figure 19. Square Corners, Single Entrance, H = 6 feet, w = 125 feet, L/B = 1.88.

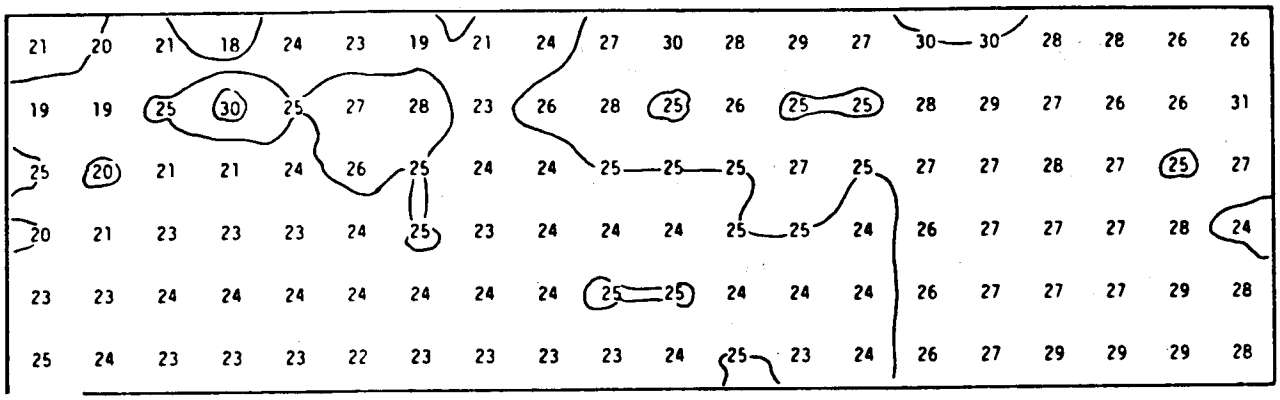

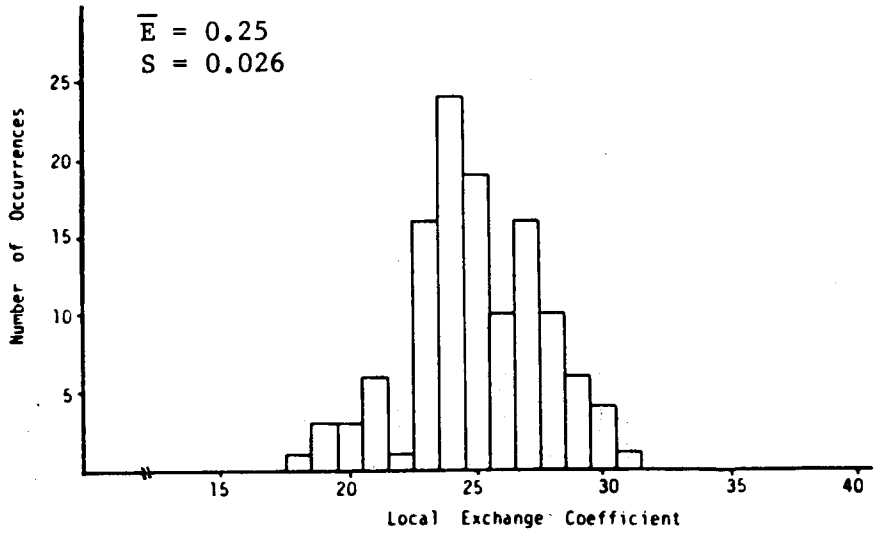

Figure 20. Square Corners, Single Entrance, H = 6 feet, w = 125 feet, L/B = 3.33.

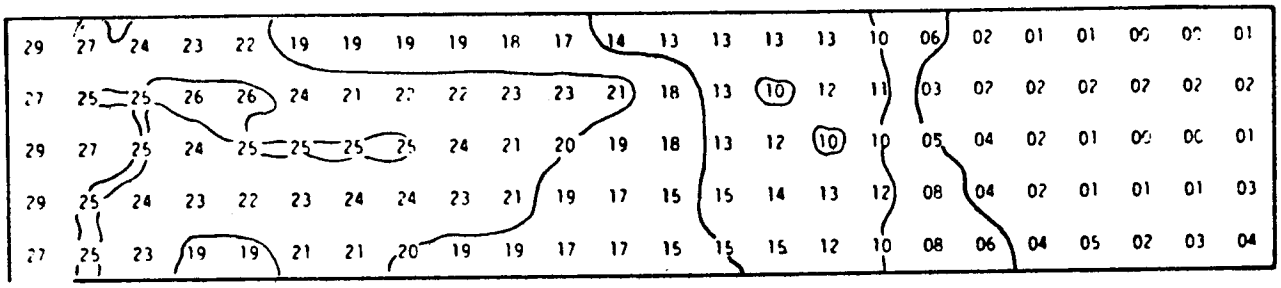

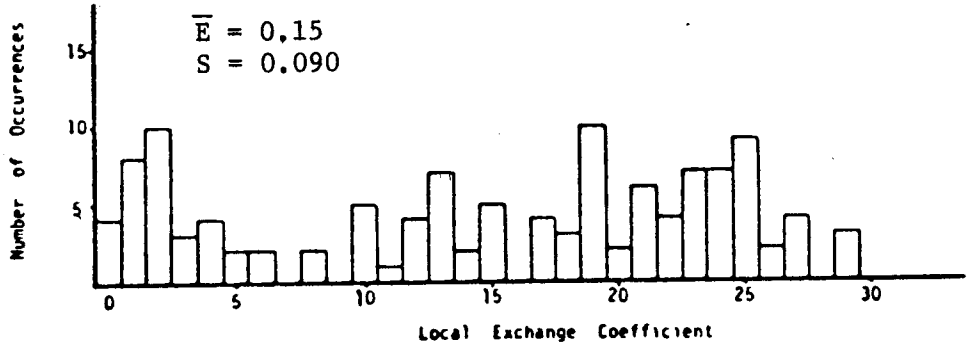

Figure 21. Square Corners, Single Entrance, H = 6 feet, w = 125 feet, L/B = 4.80.

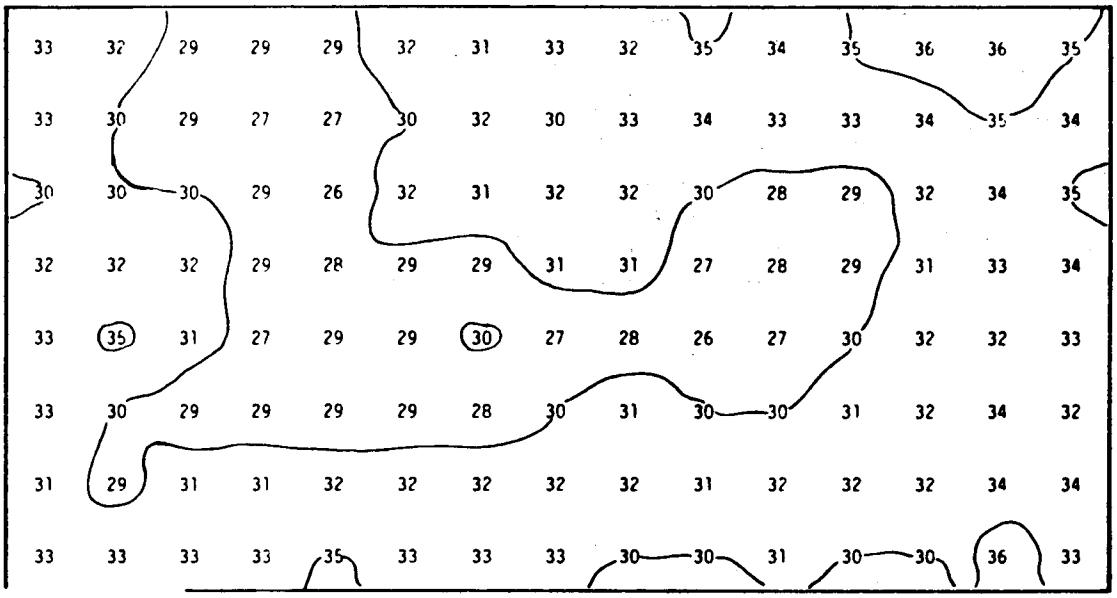

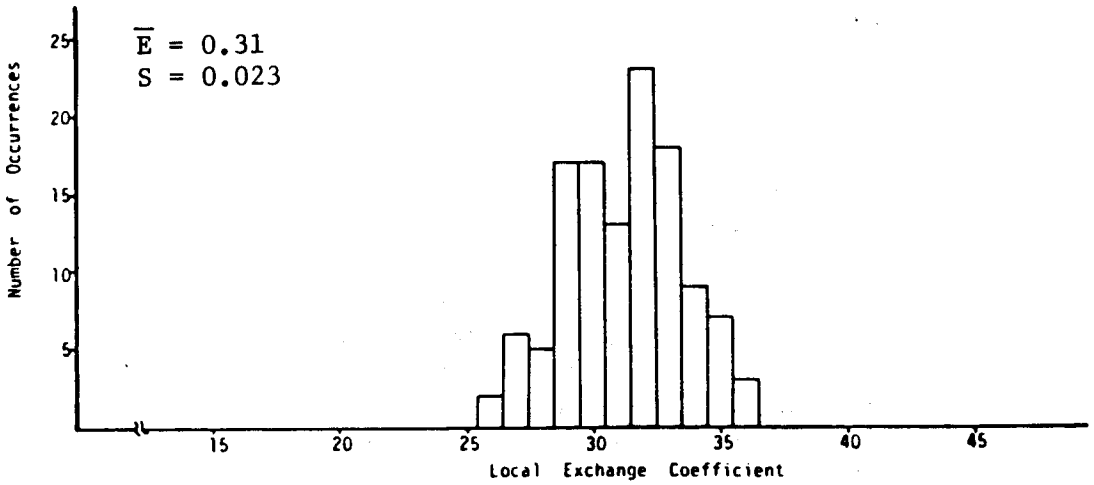

Figure 22. Square Corners, Single Entrance, H = 6 feet, w = 250 feet, L/B = 1.88.

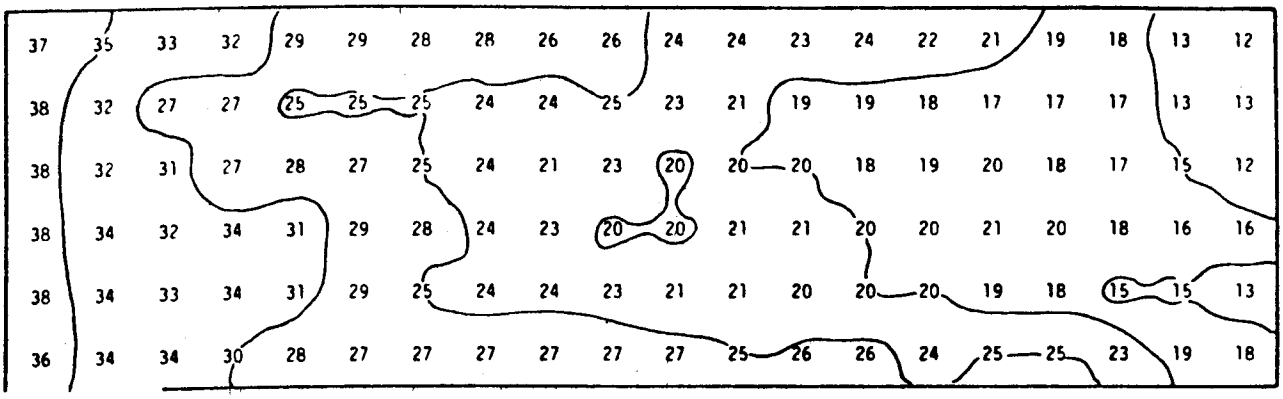

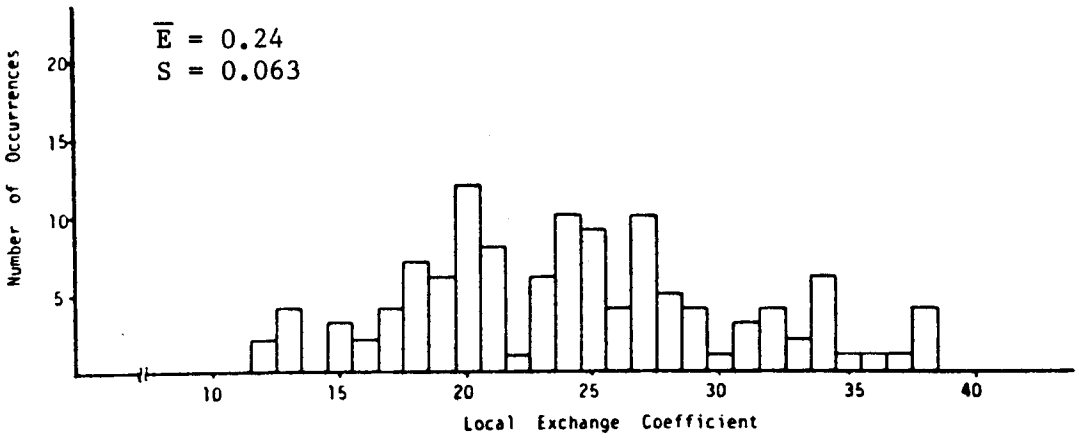

Figure 23. Square Corners, Single Entrance, H = 6 feet, w = 250 feet, L/B = 3.33.

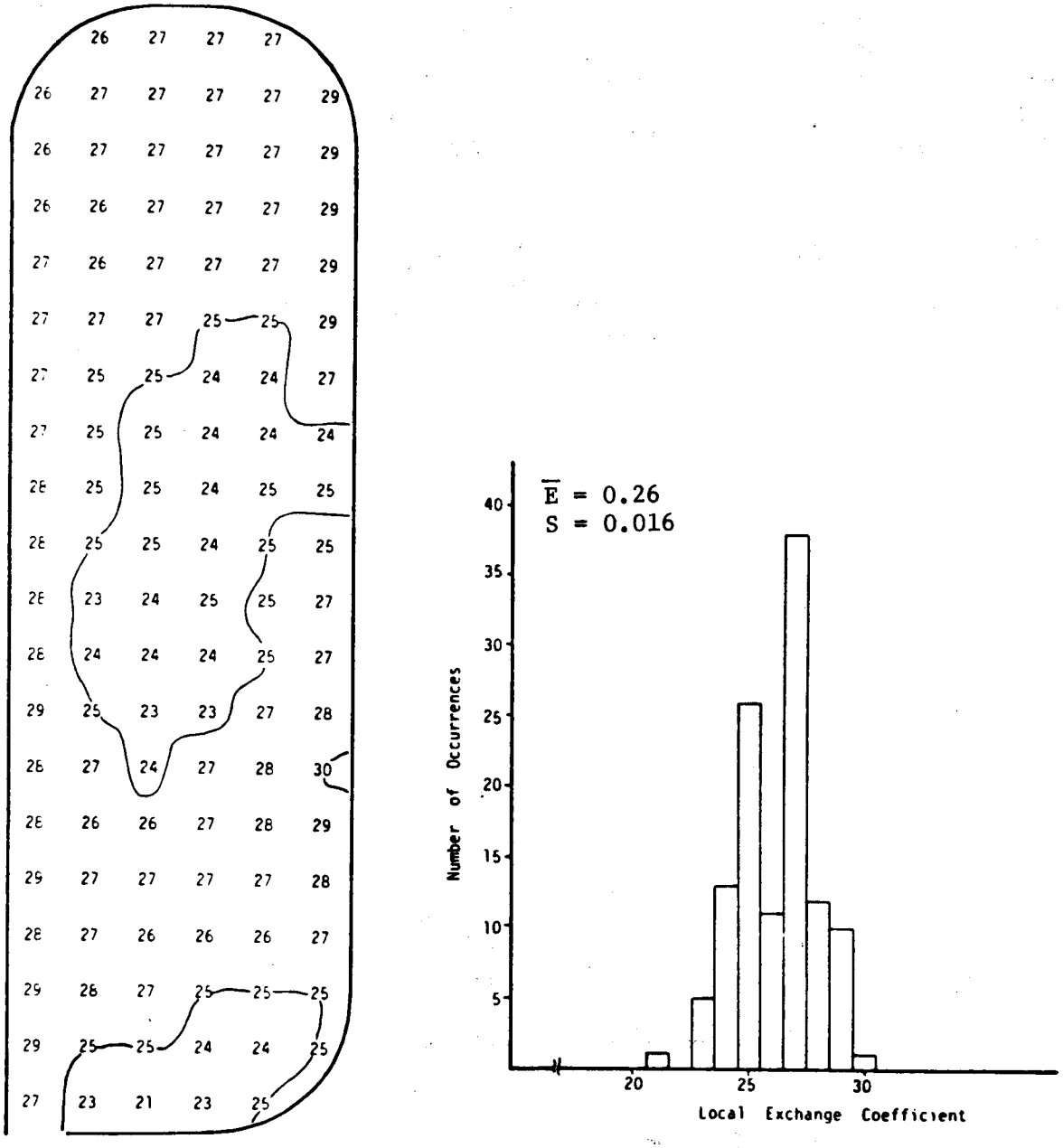

Figure 24. Rounded Corners, Single Entrance, H = 6 feet, w = 125 feet, L/B = 0.30.

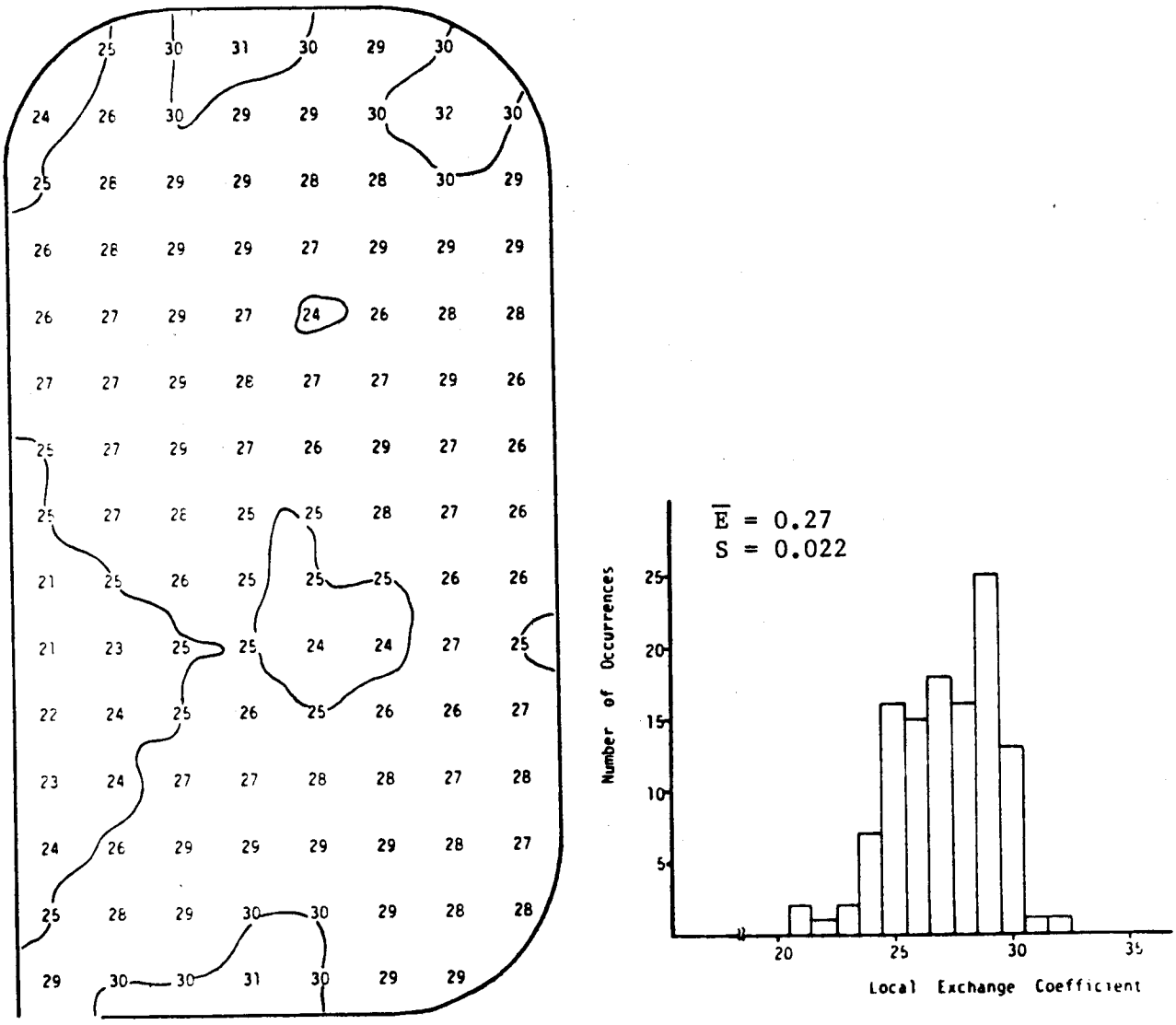

Figure 25. Rounded Corners, Single Entrance, H = 6 feet, w = 125 feet, L/B = 0.53.

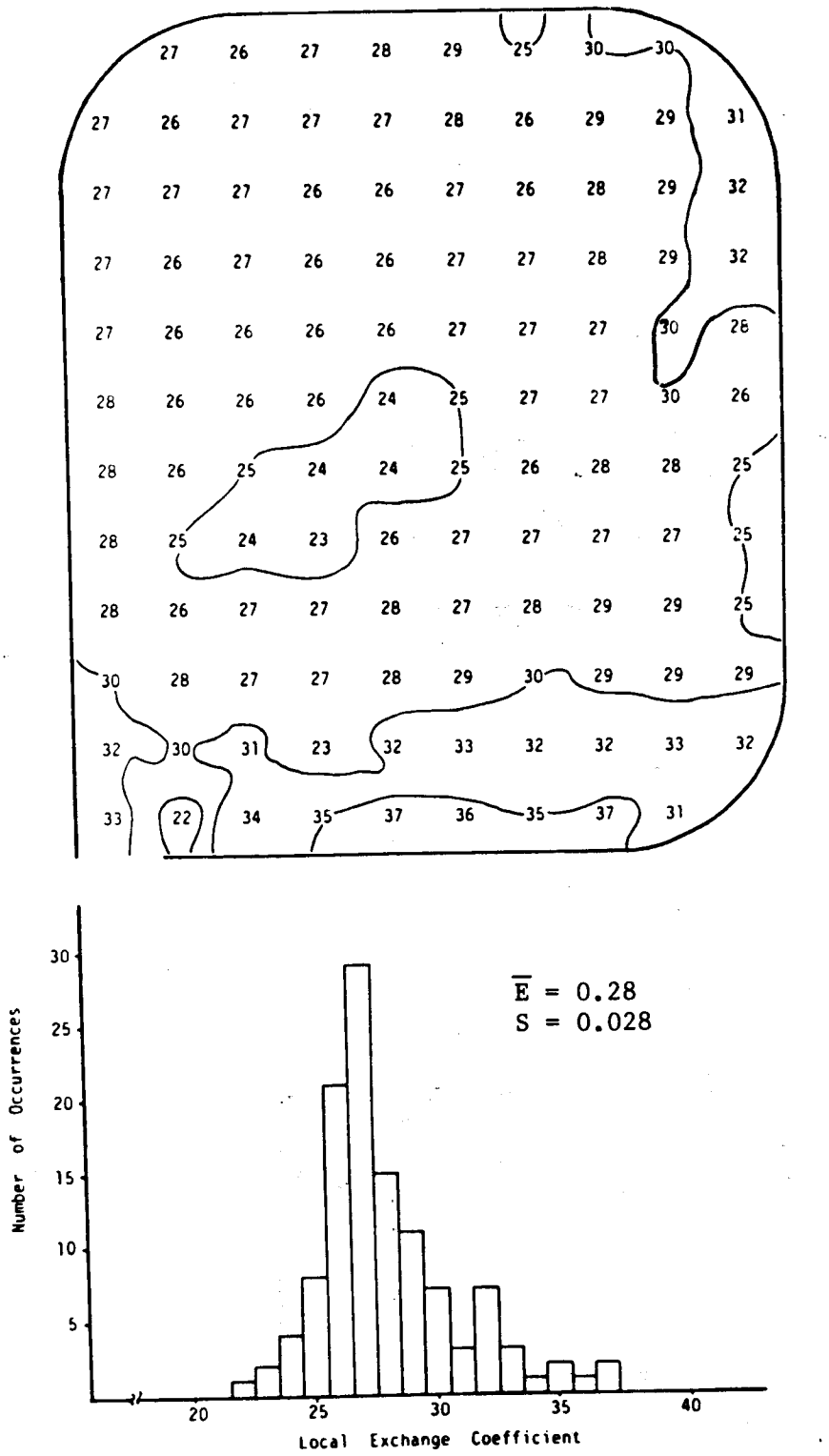

Figure 26. Rounded Corners, Single Entrance, H = 6 feet, w = 125 feet, L/B = 0.83.

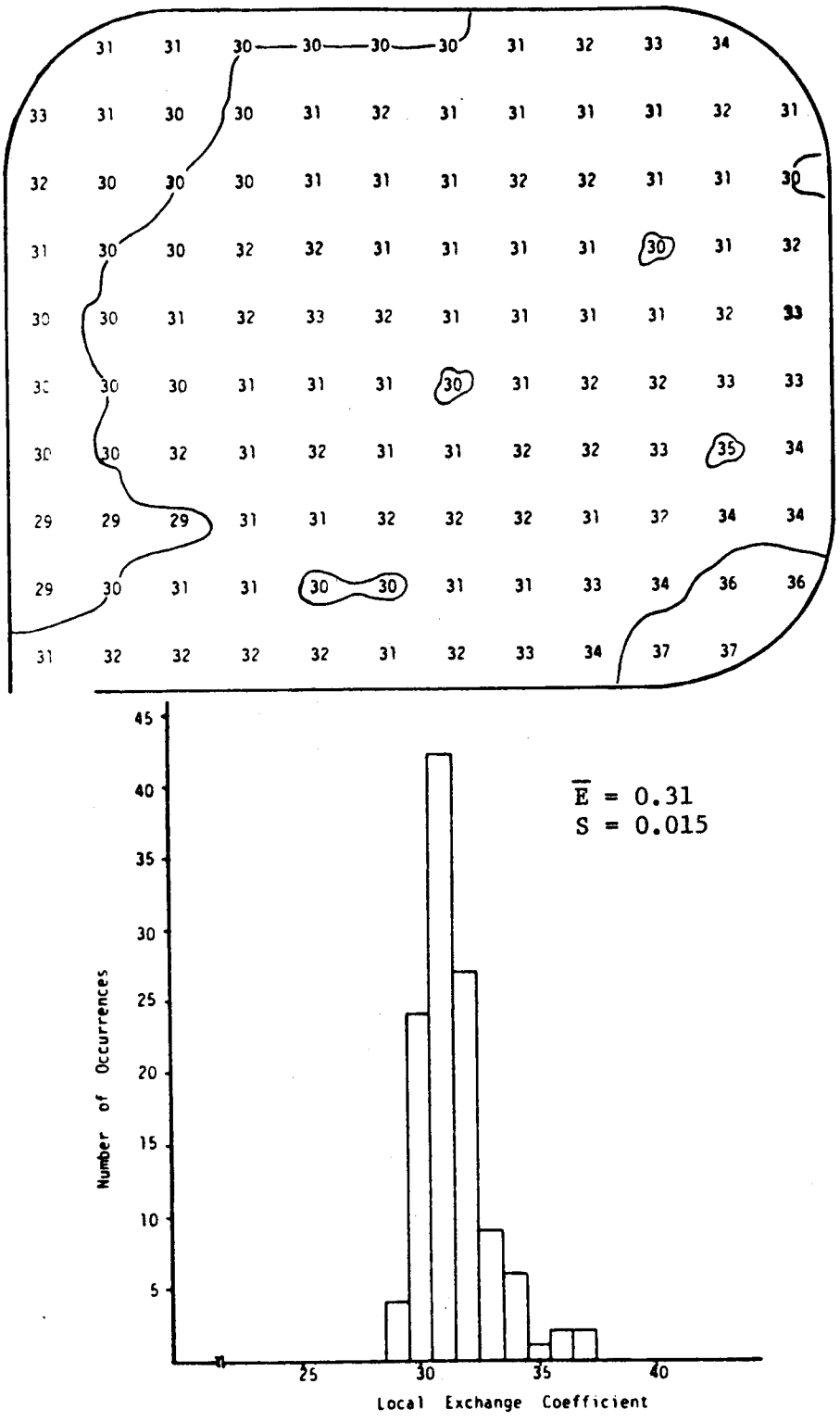

Figure 27. Rounded Corners, Single Entrance, H = 6 feet, w = 125 feet, L/B = 1.20.

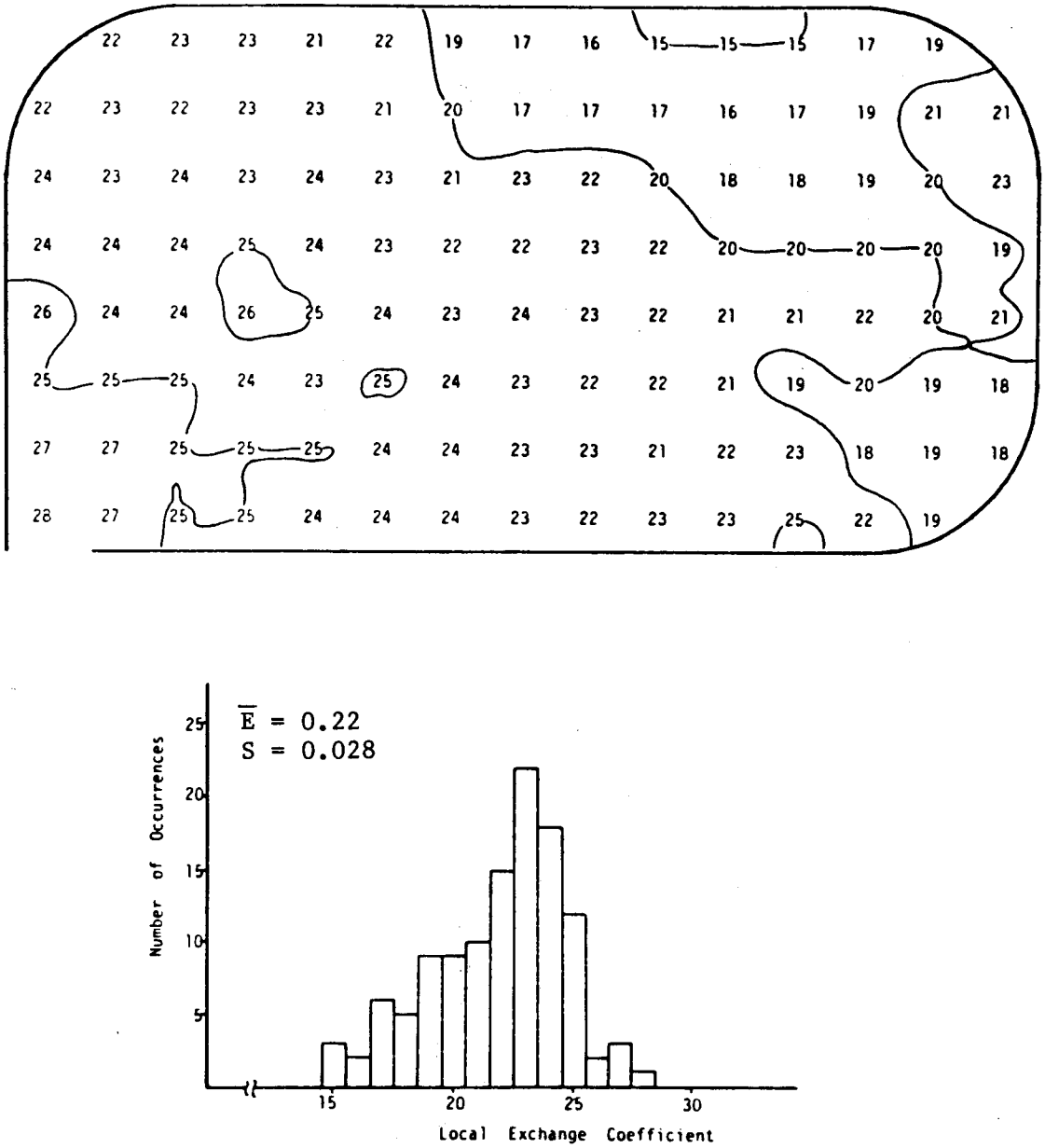

Figure 28. Rounded Corners, Single Entrance, H = 6 feet, w = 125 feet, L/B = 1.88.

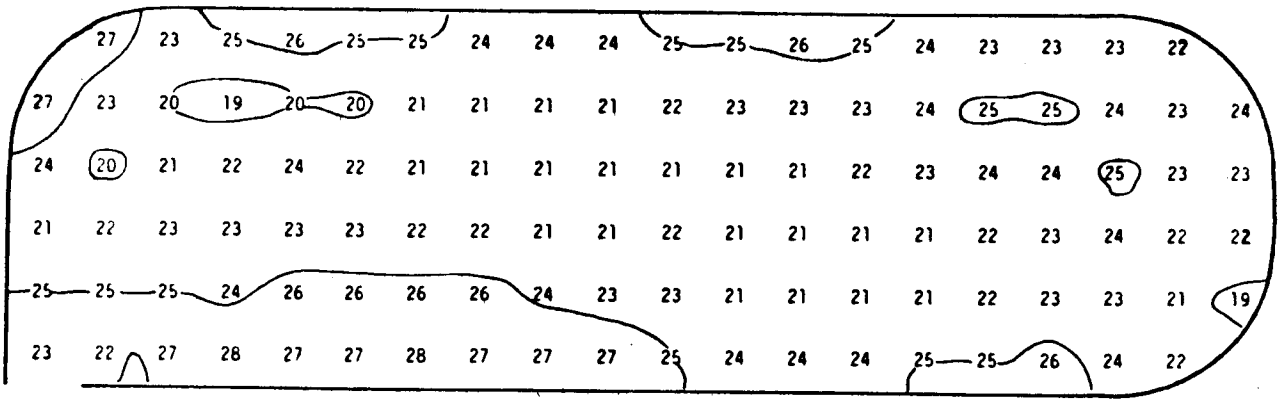

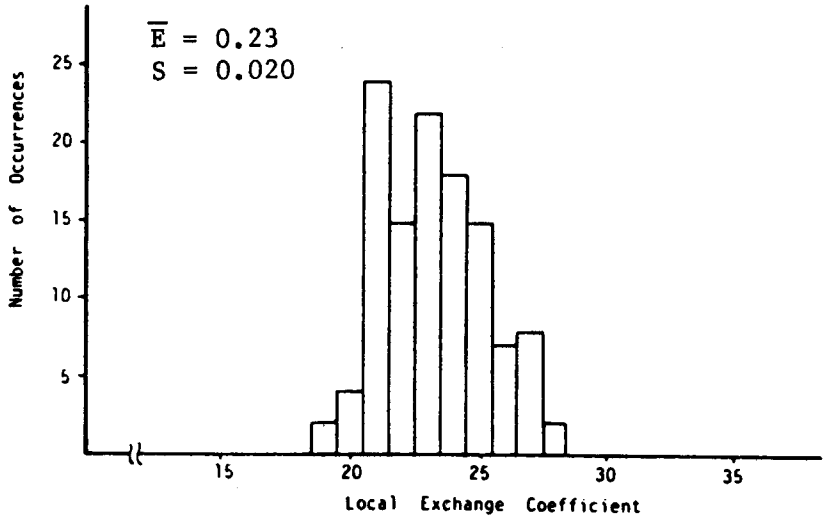

Figure 29. Rounded Corners, Single Entrance, H = 6 feet, w = 125 feet, L/B = 3.33.

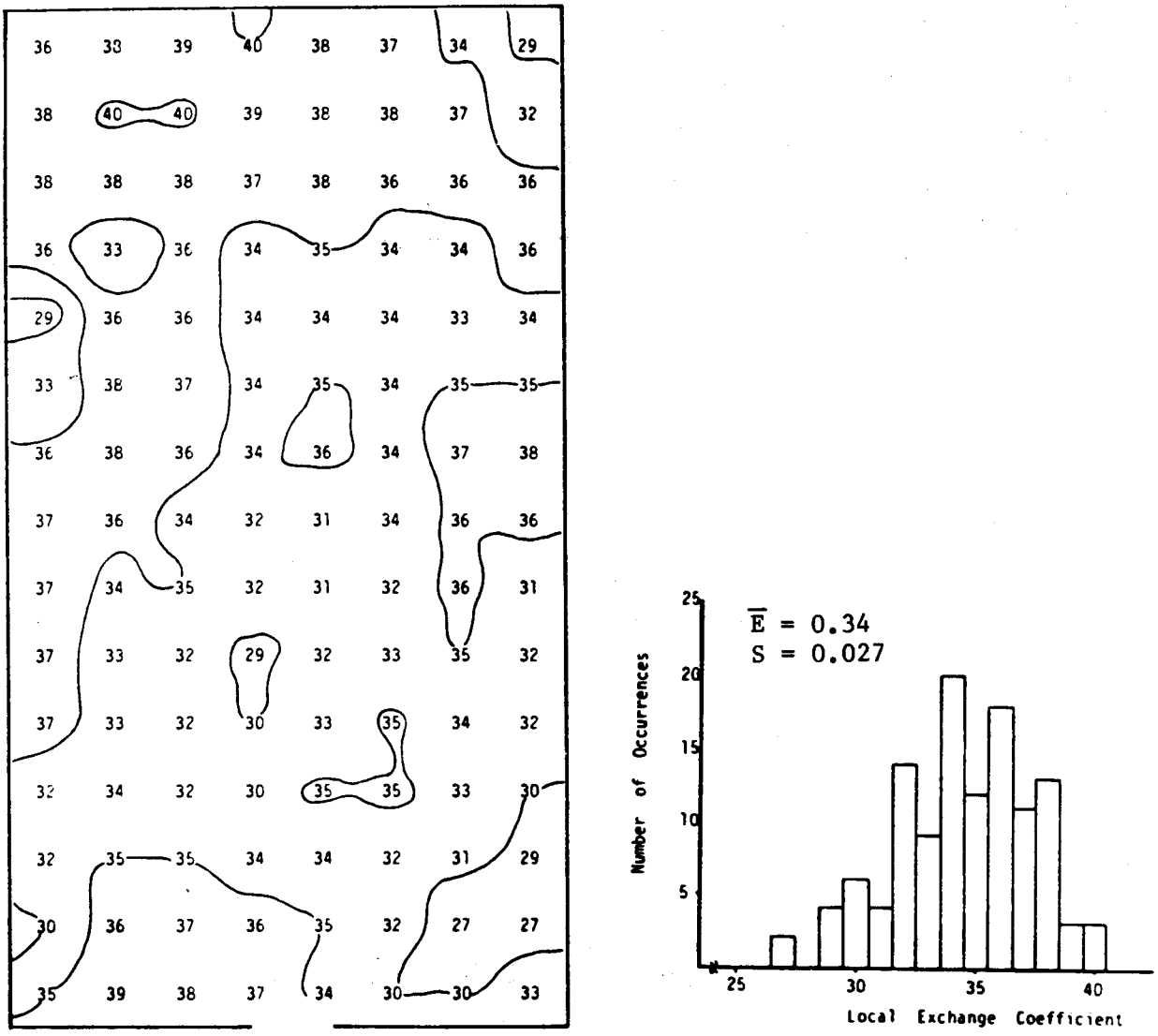

Figure 30. Square Corners, Center Entrance, H = 6 feet, w = 125 feet, L/B = 0.53.

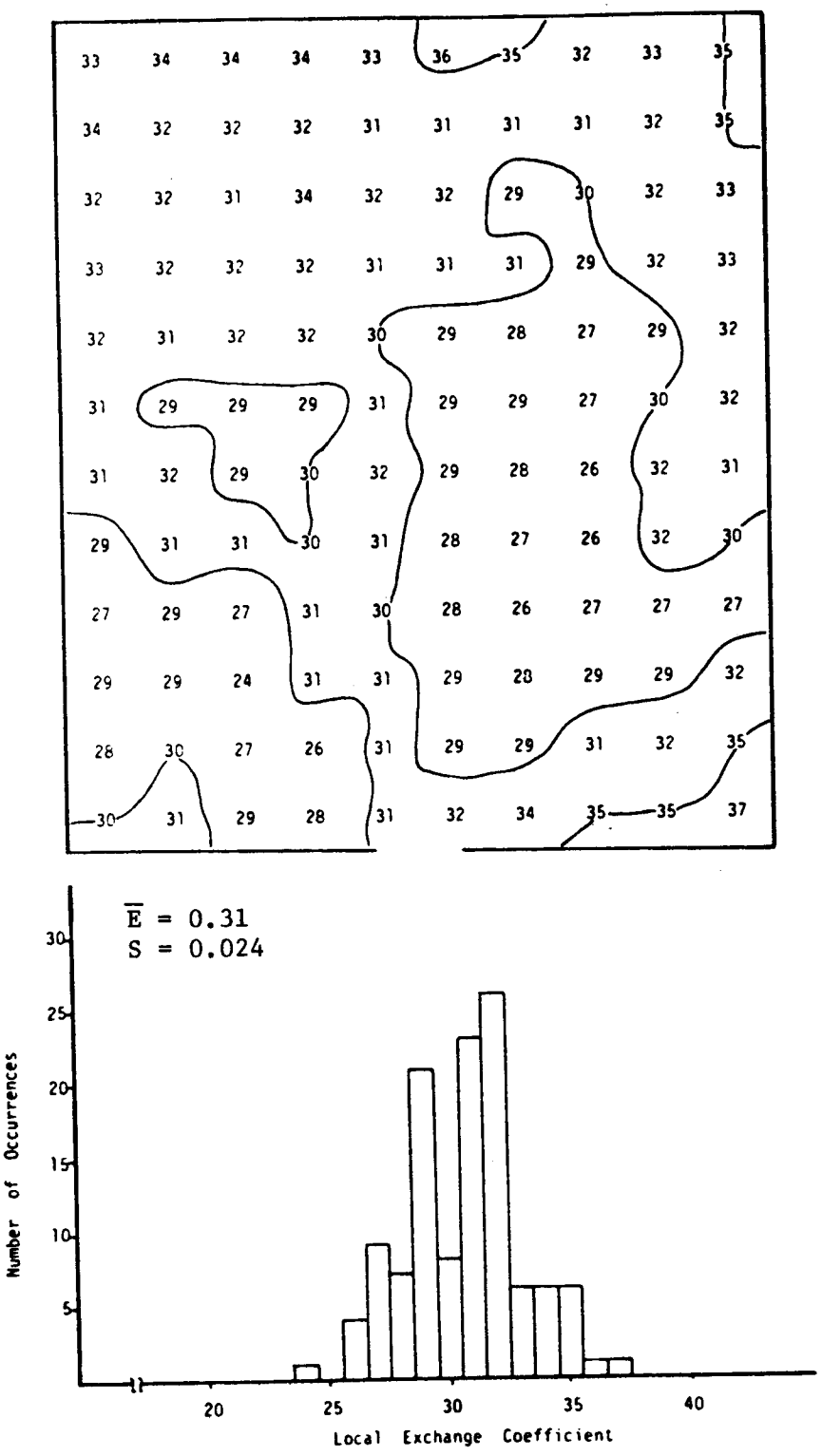

Figure 31. Square Corners, Center Entrance, H = 6 feet, w = 125 feet, L/B = 0.83.

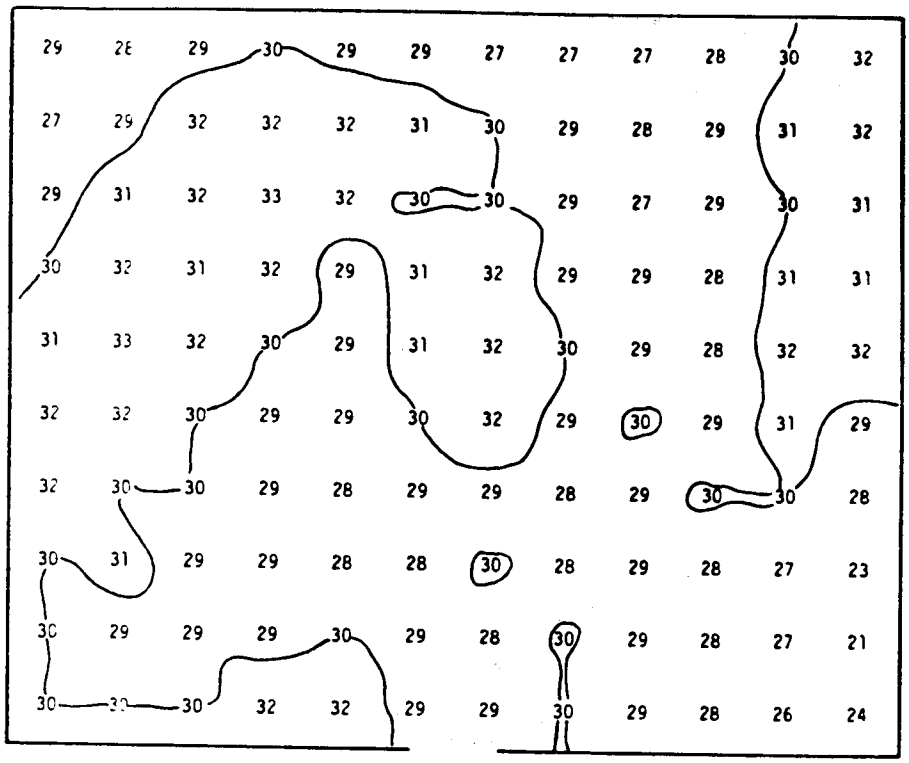

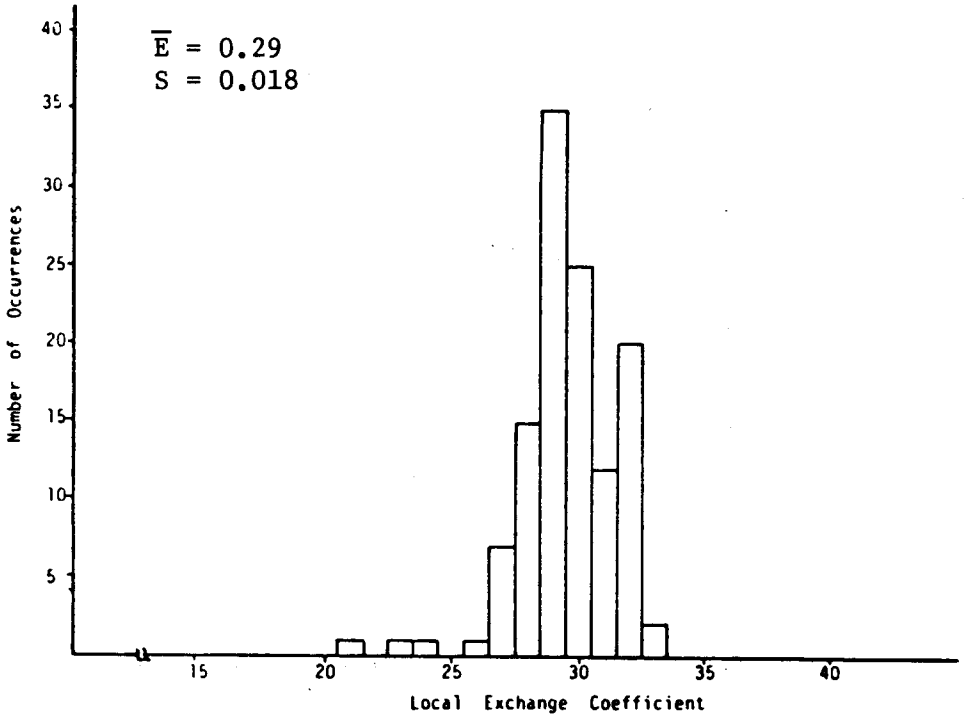

Figure 32. Square Corners, Center Entrance, H = 6 feet, w = 125 feet, L/B = 1.20.

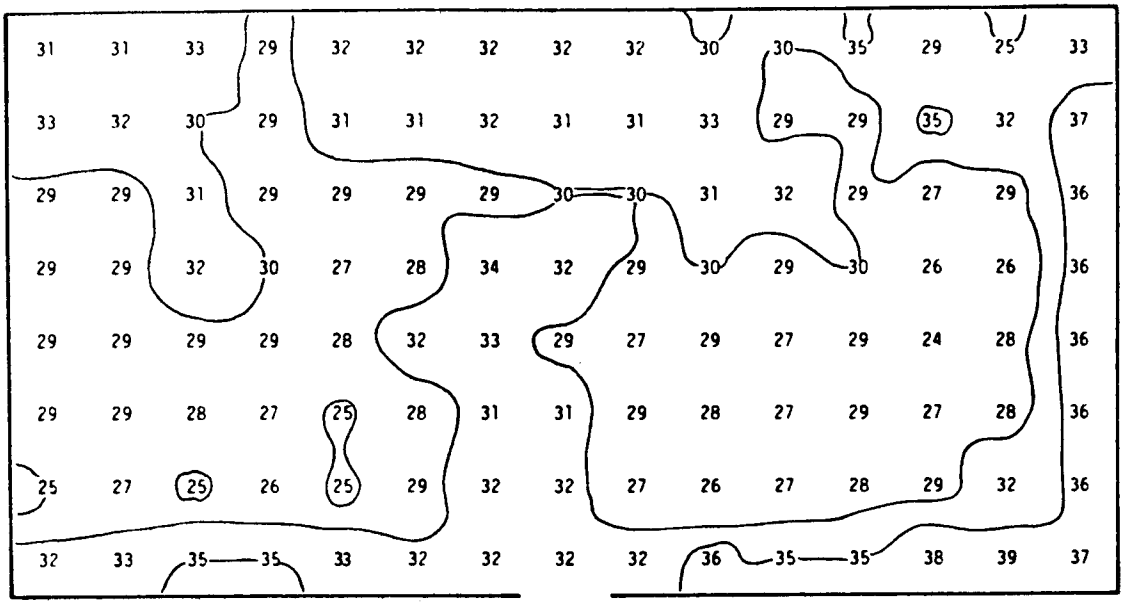

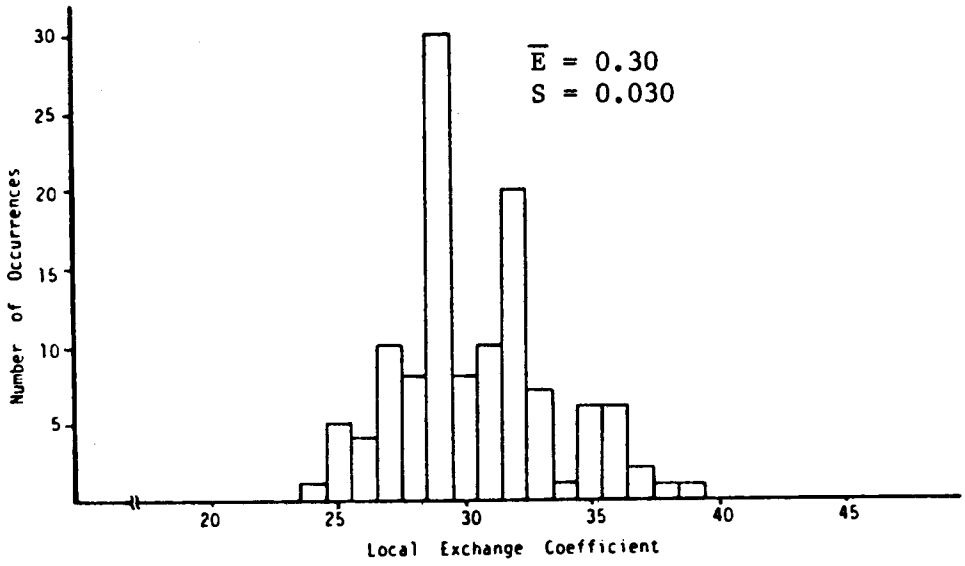

Figure 33. Square Corners, Center Entrance, H = 6 feet, w = 125 feet, L/B = 1.88.

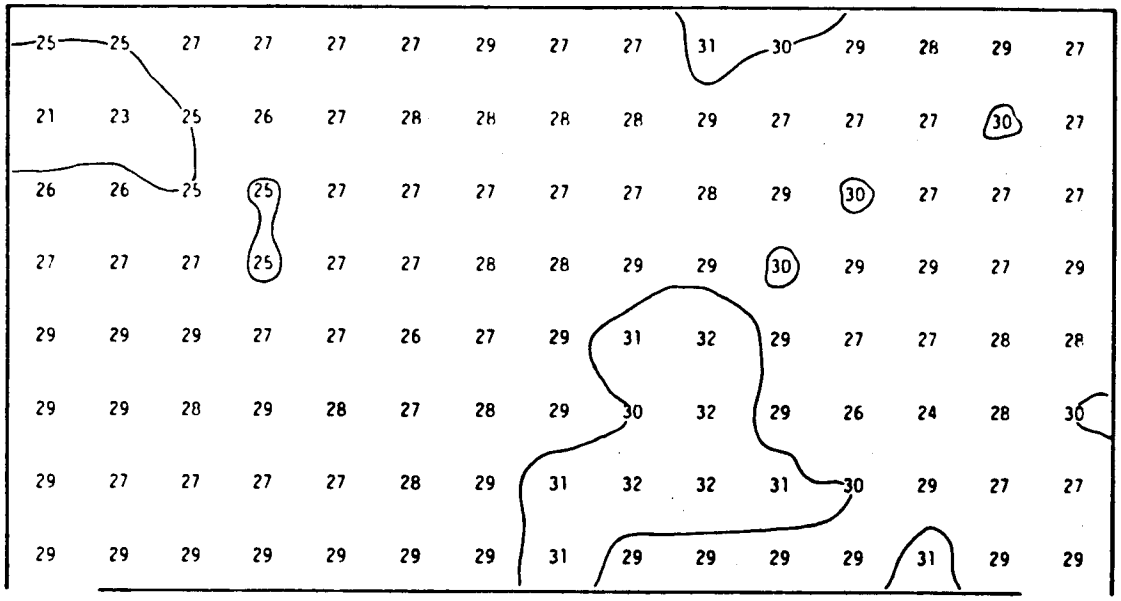

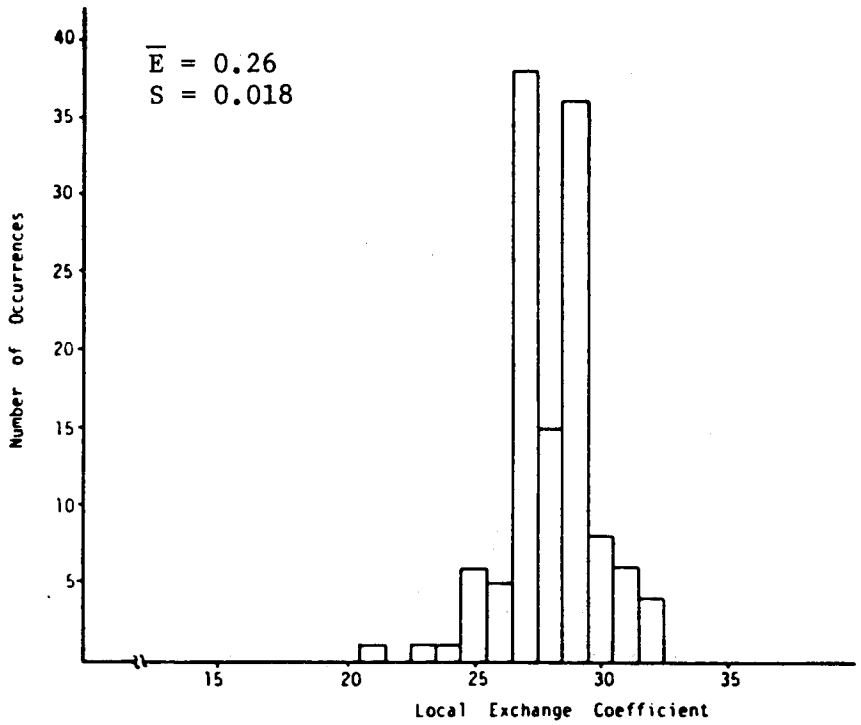

Figure 34. Square Corners, Double Entrance, H = 6 feet, w = 125, 125, L/B = 1.88.

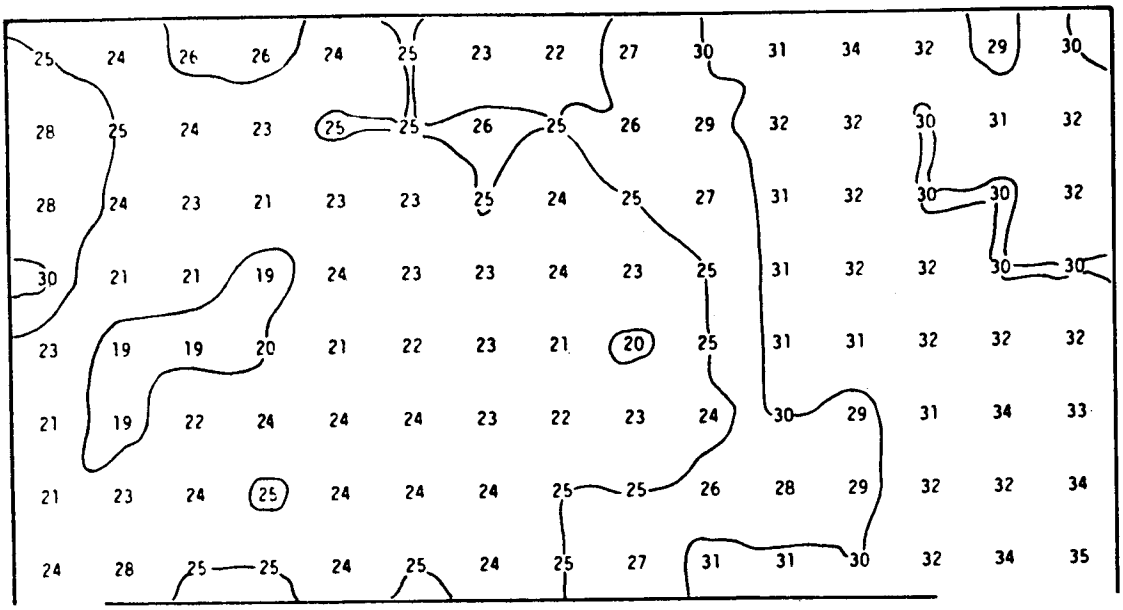

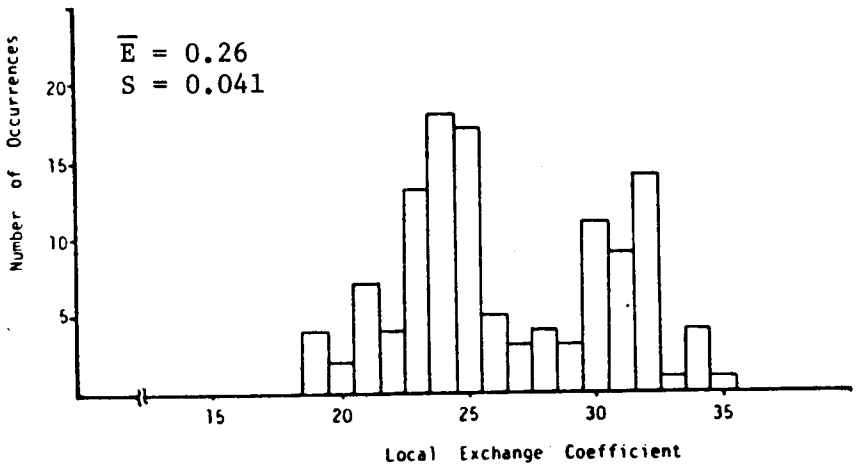

Figure 35. Square Corners, Double Entrance, H = 6 feet, w = 125, 250, L/B = 1.88.

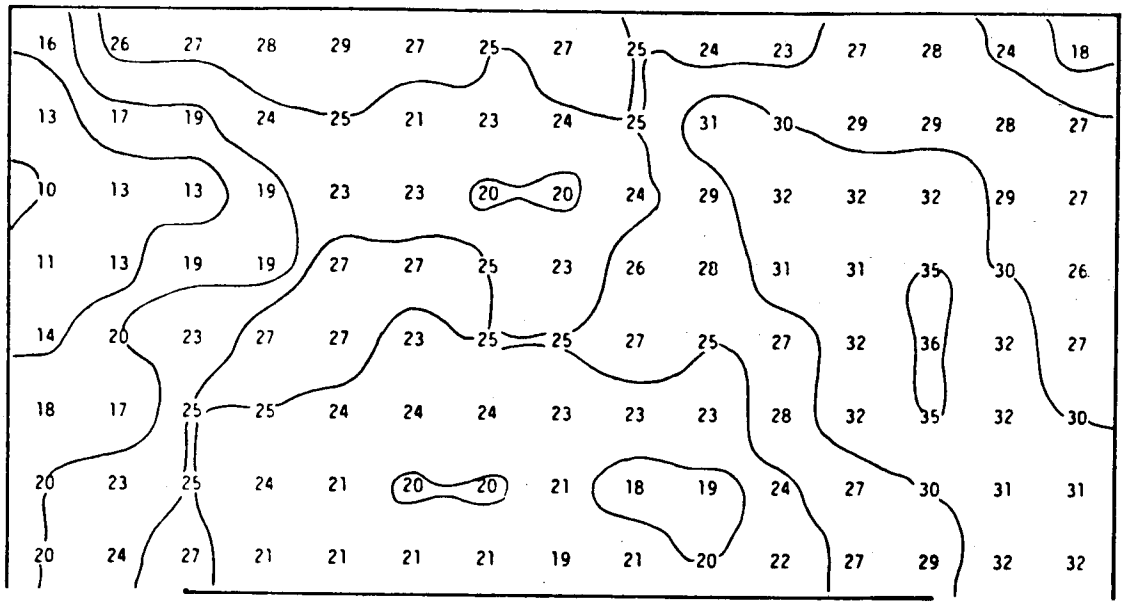

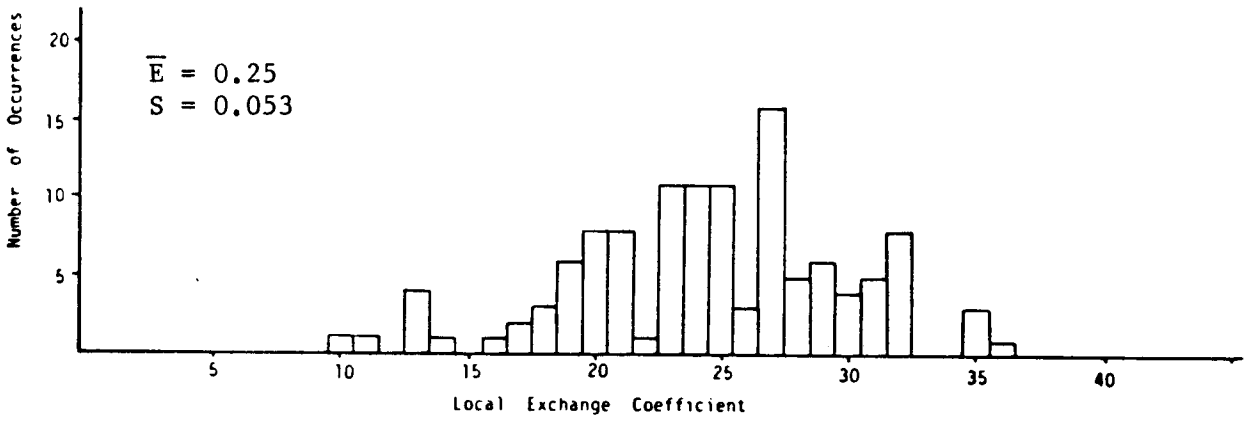

Figure 36. Square Corners, Double Entrance, H = 6 feet, w = 250, 250, L/B = 1.88.

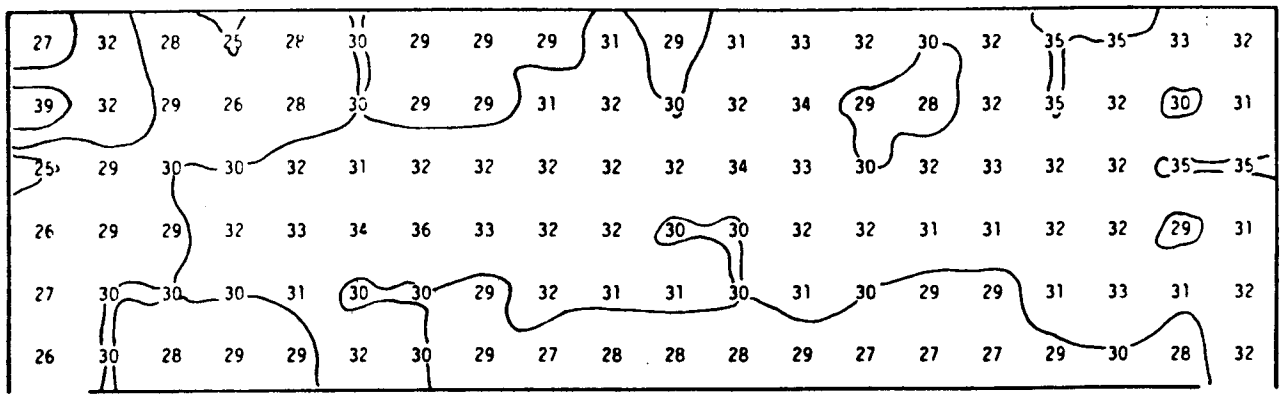

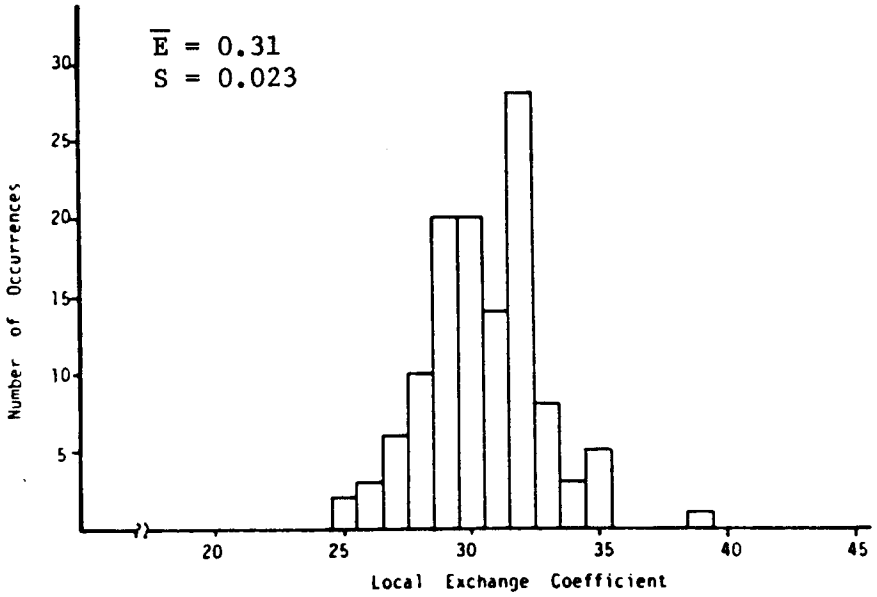

Figure 37. Square Corners, Double Entrance, H = 6 feet, w = 125, 125, L/B = 3.33.

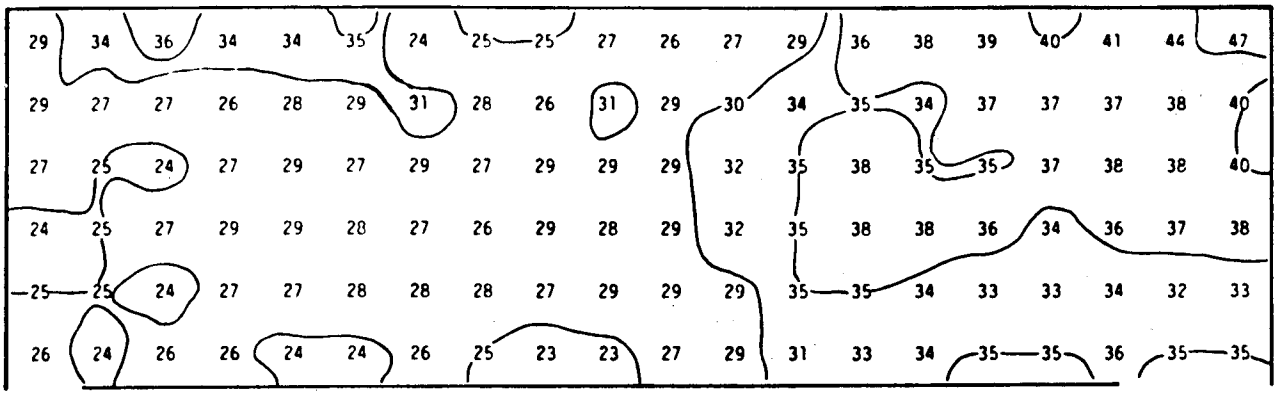

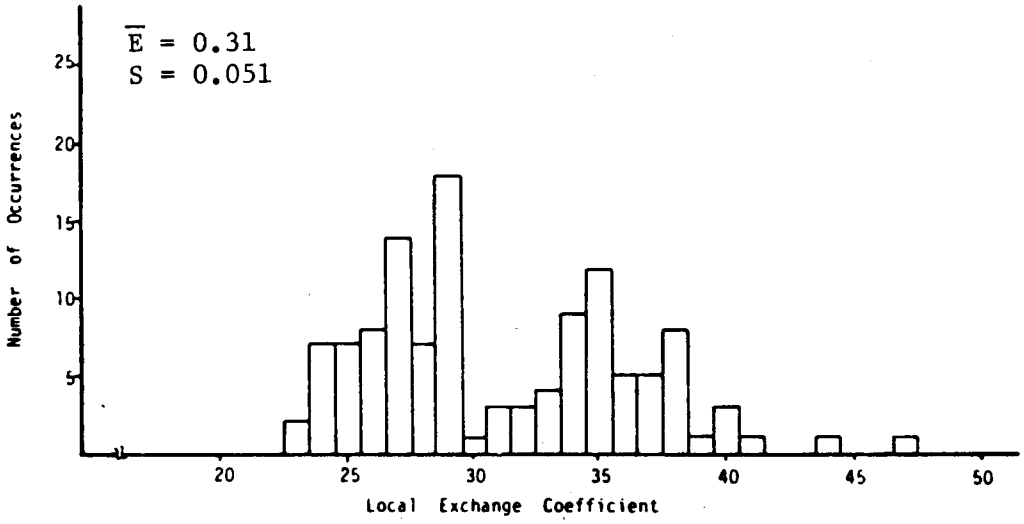

Figure 38. Square Corners, Double Entrance, H = 6 feet, w = 125, 250, L/B = 3.33.

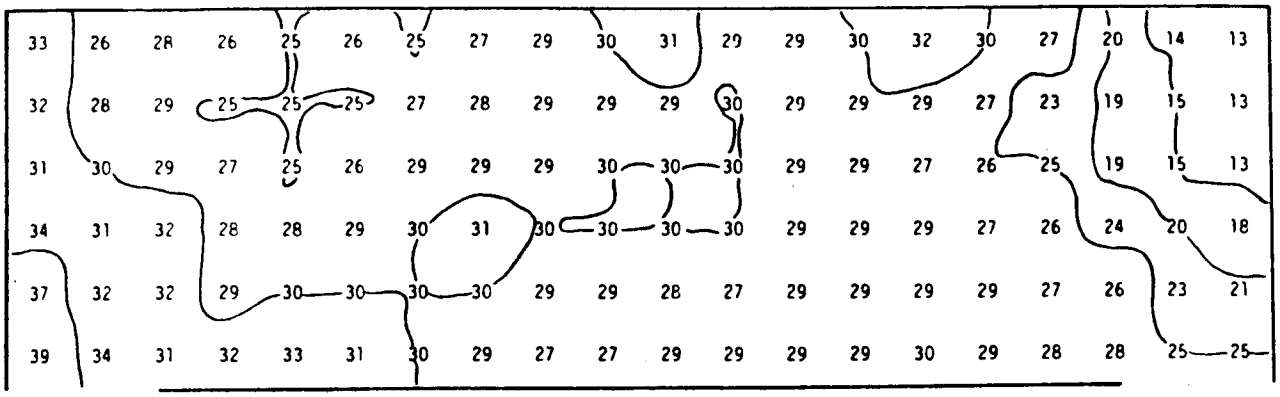

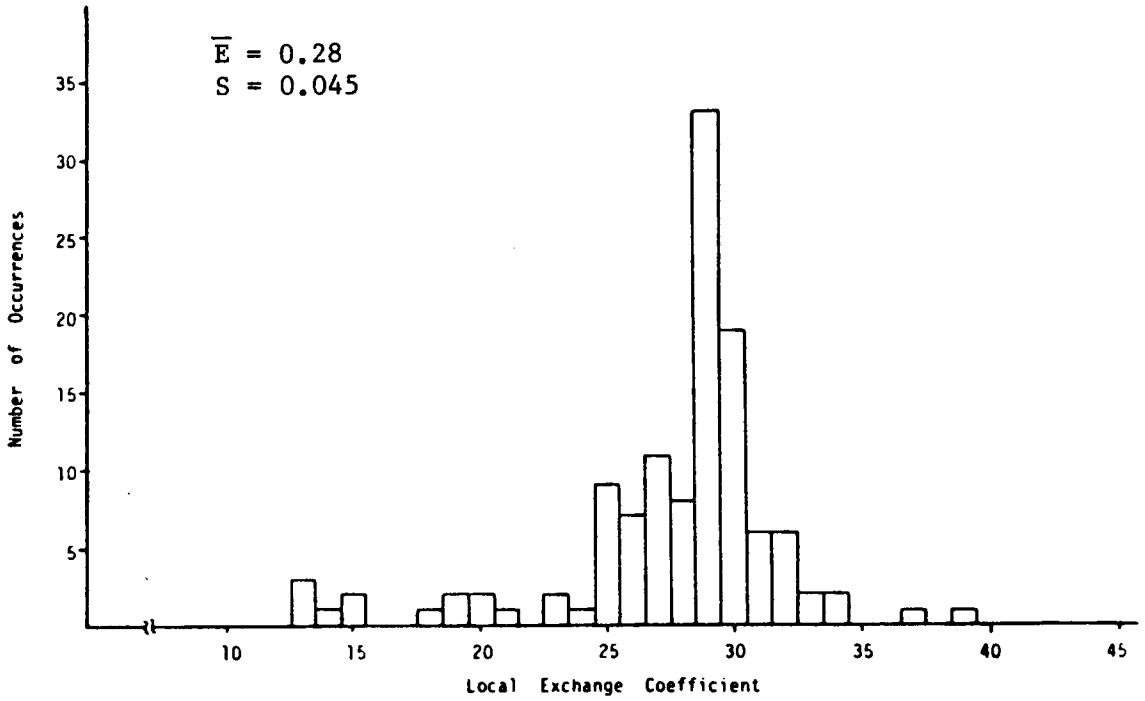

Figure 39. Square Corners, Double Entrance, H = 6 feet, w = 250, 250, L/B = 3.33.

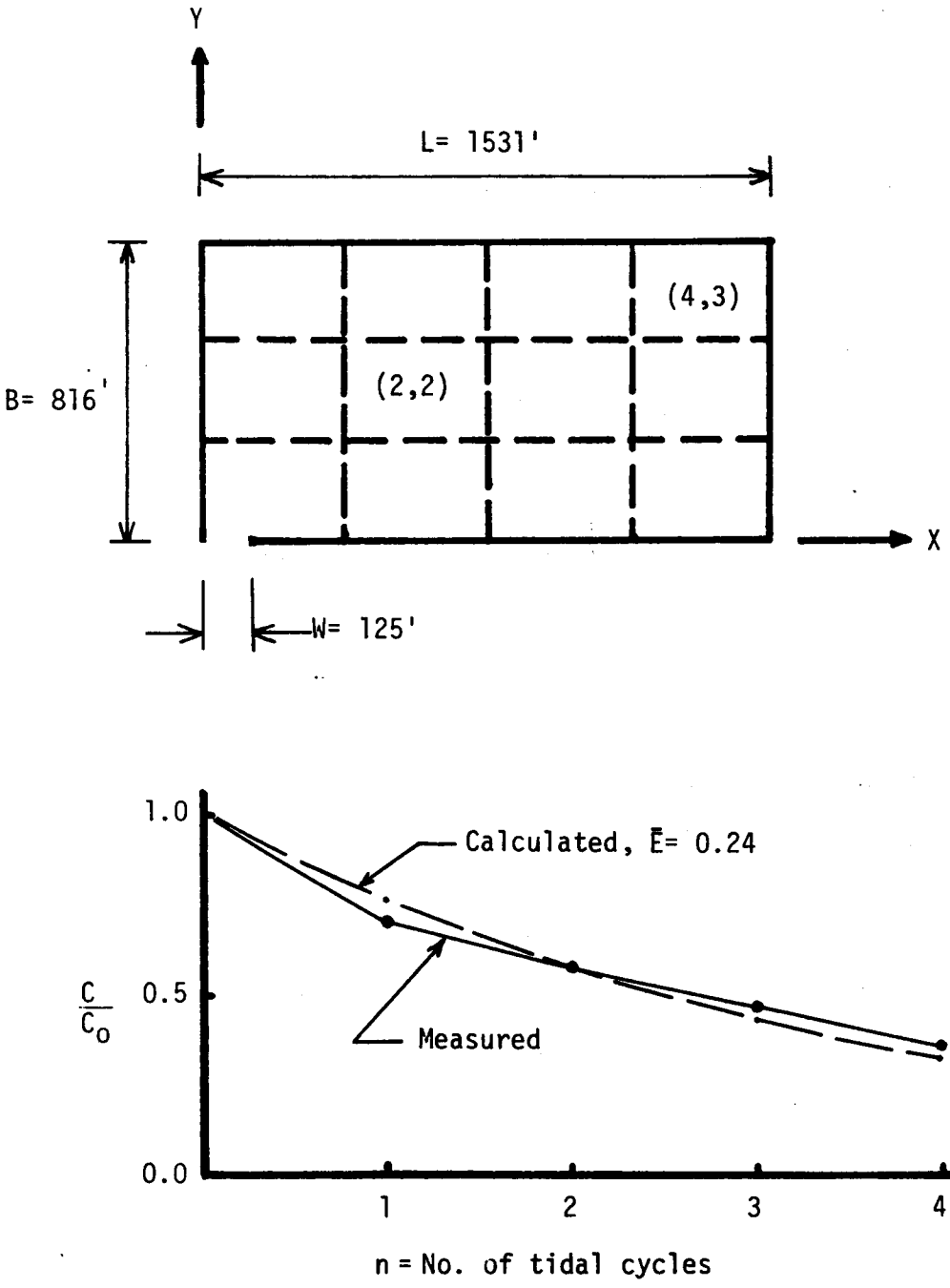

Figure 40. C/C_o vs. Number of Tidal Cycles, Square Corners, Single Entrance, H = 6 feet, w = 125 feet, L/B = 1.88.

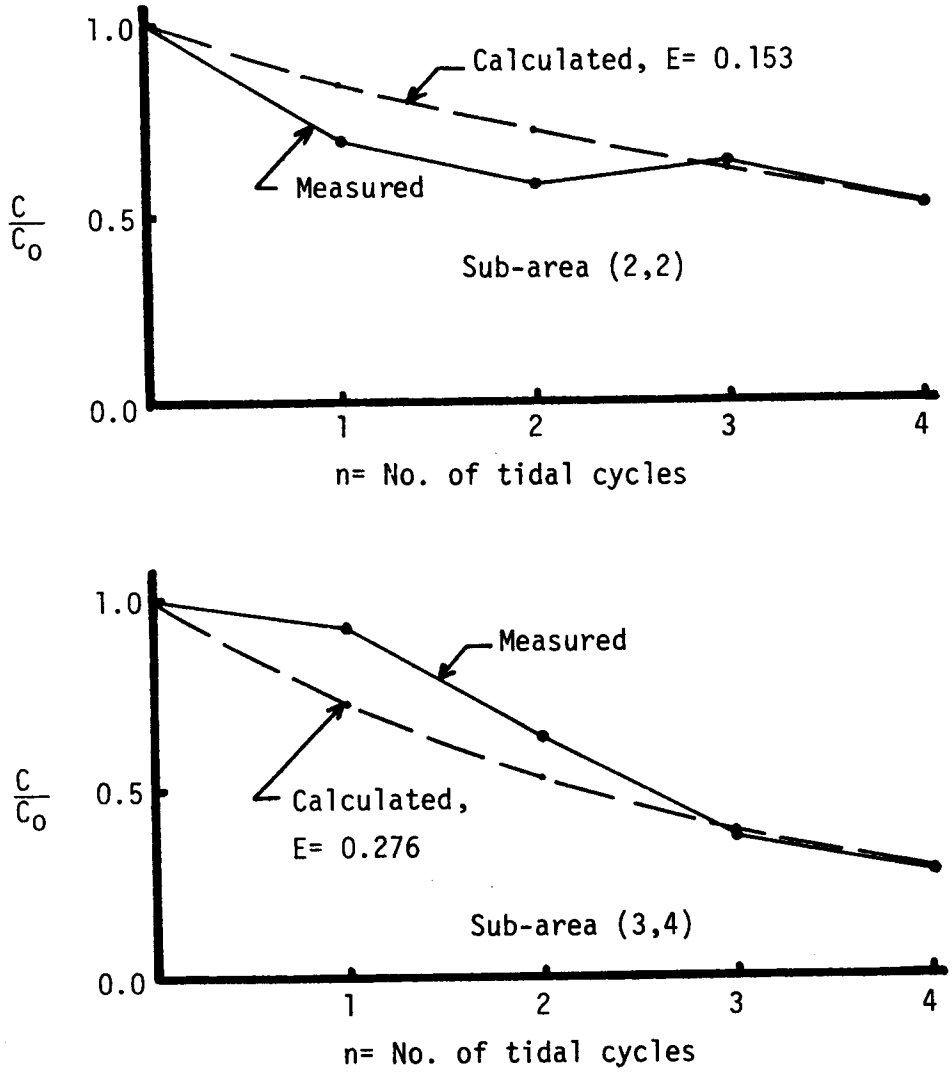

Figure 41. C/C_o in Sub-Areas (2,2) and (4,3) vs. Number of Tidal Cycles, H = 6 feet, w = 125 feet, L/B = 1.88.

Table 1

Metric Equivalents

Lengths

1 foot = 0.305 meter
3 feet = 0.91 meter
6 feet = 1.83 meters
12 feet = 3.66 meters
16 feet = 4.88 meters
125 feet = 38.1 meters
250 feet = 76.2 meters
500 feet = 152.4 meters

Areas

10.76 sq ft = 1.00 sq meter
1.25×10^6 sq ft = 116,200 sq meters
2.471 acres = 1.00 hectare = 10,000 sq meters
28.7 acres = 11.62 hectares

Table 2

Data Summary

Configuration Identification

I. Square Corners, Single Asymmetric Entrance

II. Rounded Corners, Single Asymmetric Entrance

III. Square Corners, Central Entrance

IV. Square Corners, Double Entrance

			Average Exchange Coefficient $\overline{E}$ (by method indicated)					Spatial Var. (120-pt rdgs)	
Config.	H-ft	w-ft	L/B	12-pt Avg.	Mixed	Avg. R_i	120-pt Avg.	S	$S/\overline{E}$
I	3	125	0.21	0.16	0.15	0.16			
			0.53	0.18	0.18	0.17			
			0.83	0.18	0.18	0.17			
			1.20	0.16	0.14	0.15			
			1.88	0.19	0.20	0.17			
		250	0.21	0.12	0.10	0.12			
			0.53	0.21	0.20	0.21			
			0.83	0.18	0.15	0.17			
			1.20	0.23	0.25	0.23			
I	6	125	0.21	0.25	0.25	0.24	0.25	0.068	0.27
			0.30	0.25	0.25	0.24	0.25	0.019	0.08
			0.53	0.28	0.28	0.28	0.28	0.026	0.09
			0.83	0.28	0.28	0.27	0.27	0.021	0.08
			1.20	0.26			0.26	0.055	0.21
			1.88	0.23	0.24	0.23	0.24	0.054	0.23
			3.33	0.25			0.25	0.026	0.10
			4.80	0.14	0.14	0.14	0.15	0.090	0.60
		250	0.21	0.13	0.13	0.13			
			0.30	0.37	0.36	0.36			
			0.53	0.28	0.32	0.28			
			0.83	0.25	0.26	0.25			
			1.20	0.35	0.34	0.34			
			1.88	0.31	0.31	0.31	0.31	0.023	0.07
			3.33	0.23	0.24	0.23	0.24	0.063	0.26
			4.80	0.25	0.25				
		500	0.21	0.15	0.17	0.14			
			0.30	0.12	0.12	0.12			
			0.53	0.16	0.16	0.16			
			0.83	0.28	0.29	0.27			
			1.20	0.31	0.27	0.26			
			1.88	0.35	0.35	0.34			
			3.33	0.18	0.20	0.18			
			4.80	0.23	0.24	0.22			

Table 2
(continued)

Config.	H-ft	w-ft	Average Exchange Coefficient $\bar{E}$ (by method indicated) L/B	12-pt Avg.	Mixed	Avg. R_i	120-pt Avg.	Spatial Var. (120-pt rdgs) S	$S/\bar{E}$
I	12	125	0.21	0.40	0.39	0.40			
			0.30	0.51	0.51				
			0.53	0.50	0.51	0.50			
			0.83	0.49	0.51	0.48			
			1.20	0.50		0.49			
			1.88	0.46	0.46	0.44			
			3.33	0.39	0.39	0.39			
			4.80	0.41	0.41	0.40			
		250	0.21	0.38	0.38	0.37			
			0.30	0.37	0.37	0.36			
			0.53	0.46	0.45	0.44			
			0.83	0.48	0.44	0.47			
			1.20	0.50	0.51	0.50			
			1.88	0.46	0.44	0.45			
			3.33	0.42	0.40	0.42			
			4.80	0.40	0.40	0.40			
		500	0.21	0.42	0.41	0.41			
			0.30	0.49	0.51	0.48			
II	6	125	0.30	0.27	0.27	0.26	0.26	0.016	0.06
			0.53	0.27	0.26	0.26	0.27	0.022	0.08
			0.83	0.28	0.29	0.28	0.28	0.028	0.10
			1.20	0.31		0.30	0.31	0.015	0.05
			1.88	0.22	0.21	0.21	0.22	0.028	0.13
			3.33	0.22	0.22		0.23	0.020	0.09
III	6	125	0.53	0.35	0.34	0.34	0.34	0.027	0.08
			0.83	0.31	0.31	0.31	0.31	0.024	0.08
			1.20	0.30	0.29	0.29	0.29	0.018	0.06
			1.88	0.31	0.32	0.29	0.30	0.030	0.10
IV	6	2 x 125	1.88	0.28	0.28	0.27	0.28	0.018	0.06
		125/250	1.88	0.27	0.27	0.26	0.26	0.041	0.16
		2 x 250	1.88	0.25	0.24	0.24	0.25	0.053	0.21
		2 x 125	3.33	0.31	0.31	0.31	0.31	0.023	0.07
		125/250	3.33	0.30	0.29	0.29	0.31	0.051	0.16
		2 x 250	3.33	0.27	0.27	0.26	0.28	0.045	0.16